NAVAL POSTGRADUATE SCHOOL

MONTEREY, CALIFORNIA

THESIS

CLOUD CLIMATOLOGIES FOR ROCKET TRIGGERED LIGHTNING FROM LAUNCHES AT CAPE CANAVERAL AIR FORCE STATION AND KENNEDY SPACE CENTER

by

Greg J. Strong

March 2012

Thesis Co-Advisors: Tom Murphree
Andrew P. Boerlage

THIS PAGE INTENTIONALLY LEFT BLANK

REPORT DOCUMENTATION PAGE		Form Approved OMB No. 0704-0188

1. AGENCY USE ONLY *(Leave blank)*	2. REPORT DATE	3. REPORT TYPE AND DATES COVERED
	March 2012	Master's Thesis

4. TITLE AND SUBTITLE Cloud Climatologies for Rocket Triggered Lightning from Launches at Cape Canaveral Air Force Station and Kennedy Space Center	5. FUNDING NUMBERS
6. AUTHOR(S) Greg J. Strong	
7. PERFORMING ORGANIZATION NAME(S) AND ADDRESS(ES) Naval Postgraduate School Monterey, CA 93943-5000	8. PERFORMING ORGANIZATION REPORT NUMBER
9. SPONSORING /MONITORING AGENCY NAME(S) AND ADDRESS(ES) N/A	10. SPONSORING/MONITORING AGENCY REPORT NUMBER

11. SUPPLEMENTARY NOTES The views expressed in this thesis are those of the author and do not reflect the official policy or position of the Department of Defense or the U.S. Government.

12a. DISTRIBUTION / AVAILABILITY STATEMENT	12b. DISTRIBUTION CODE
Approved for public release; distribution is unlimited	A

13. ABSTRACT

We have conducted a study on the development of detailed climatological probabilities of violating cloud related Lightning Launch Commit Criteria (LLCC) used by Cape Canaveral Air Force Station and Kennedy Space Center (CCAFS and KSC). This study was conducted to provide the 45th Weather Squadron with improved capabilities for operational forecasting for launches from CCAFS and KSC. Our focus was on developing methods to produce climatological probabilities of violating one of the LLCC, the thick cloud layer rule. We developed a hybrid process of blending data from the Climate Forecast System Reanalysis (CFSR), meteorological aerodrome reports (METARs), radiosonde observations (RAOBs), and expert meteorologist data sets to create a merged data set for determining the probability of violating the thick cloud layer rule.

Using our blended hybrid process, we computed cloud thicknesses, and probabilities of violating the thick cloud LLCC for each day of the year at 00Z and 12Z. Additionally, we conducted a sensitivity analysis to identify the potential for modifying the thick cloud LLCC. A primary result from our study is a sub-daily data set of the climatological probabilities of violating the thick cloud layer rule. We conducted eight validation case studies that demonstrated our calculated violations match well with observed violations. The development of a merged data set that provides more useful information than any one of the individual data sets is a technique that is likely to be useful in solving many other climatological problems

14. SUBJECT TERMS	15. NUMBER OF PAGES
Cape Canaveral Air Force Station, Climate Forecast System Reanalysis, Cloud Climatolgies, Kennedy Space Center, Lightning Launch Commit Criteria, Rocket Triggered Lightning, Thick Cloud	159
	16. PRICE CODE

17. SECURITY CLASSIFICATION OF REPORT	18. SECURITY CLASSIFICATION OF THIS PAGE	19. SECURITY CLASSIFICATION OF ABSTRACT	20. LIMITATION OF ABSTRACT
Unclassified	Unclassified	Unclassified	UU

NSN 7540-01-280-5500

Standard Form 298 (Rev. 8-98)
Prescribed by ANSI Std. Z39.18

THIS PAGE INTENTIONALLY LEFT BLANK

Approved for public release; distribution is unlimited

CLOUD CLIMATOLOGIES FOR ROCKET TRIGGERED LIGHTNING FROM LAUNCHES AT CAPE CANAVERAL AIR FORCE STATION AND KENNEDY SPACE CENTER

Greg J. Strong
Captain, United States Air Force
B.S., University of South Alabama, 2006

Submitted in partial fulfillment of the
requirements for the degree of

MASTER OF SCIENCE IN METEOROLOGY

from the

NAVAL POSTGRADUATE SCHOOL
March 2012

Author: Greg J. Strong

Approved by: Tom Murphree
Thesis Co-Advisor

Andrew P. Boerlage
Thesis Co-Advisor

Wendell Nuss
Chair, Department of Meteorology

THIS PAGE INTENTIONALLY LEFT BLANK

ABSTRACT

We have conducted a study on the development of detailed climatological probabilities of violating cloud related Lightning Launch Commit Criteria (LLCC) used by Cape Canaveral Air Force Station and Kennedy Space Center (CCAFS and KSC). This study was conducted to provide the 45th Weather Squadron with improved capabilities for operational forecasting for launches from CCAFS and KSC. Our focus was on developing methods to produce climatological probabilities of violating one of the LLCC, the thick cloud layer rule. We developed a hybrid process of blending data from the Climate Forecast System Reanalysis (CFSR), meteorological aerodrome reports (METARs), radiosonde observations (RAOBs), and expert meteorologist data sets to create a merged data set for determining the probability of violating the thick cloud layer rule.

Using our blended hybrid process, we computed cloud thicknesses, and probabilities of violating the thick cloud LLCC for each day of the year at 00Z and 12Z. Additionally, we conducted a sensitivity analysis to identify the potential for modifying the thick cloud LLCC. A primary result from our study is a sub-daily data set of the climatological probabilities of violating the thick cloud layer rule. We conducted eight validation case studies that demonstrated our calculated violations match well with observed violations. The development of a merged data set that provides more useful information than any one of the individual data sets is a technique that is likely to be useful in solving many other climatological problems.

THIS PAGE INTENTIONALLY LEFT BLANK

TABLE OF CONTENTS

LIST OF FIGURES

LIST OF TABLES

LIST OF ACRONYMS AND ABBREVIATIONS

14 WS	14th Weather Squadron
45 WS	45th Weather Squadron
AC-67	Atlas-Centaur-67 rocket
AFSPC	Air Force Space Command
AMU	Applied Meteorology Unit
CCAFS	Cape Canaveral Air Force Station
CFSR	Climate Forecast System Reanalysis
FAA	Federal Aviation Administration
KSC	Kennedy Space Center
LAP	Lightning Advisory Panel
LWO	Launch Weather Officer
LLCC	Lightning Launch Commit Criteria
METAR	Meteorological Aerodrome Report
NARR	North American Regional Reanalysis
NASA	National Aeronautics and Space Administration
NPS	Naval Postgraduate School
NCAR	National Center for Atmospheric Research
NCEP	National Centers for Environmental Prediction
RAOB	Rawinsonde Observation
RRA	Range Reference Atmosphere

THIS PAGE INTENTIONALLY LEFT BLANK

ACKNOWLEDGMENTS

This thesis is a compilation of the efforts and contributions from several key individuals. I would like to first thank my advisors, Dr. Tom Murphree and Col (USAF Ret) Andrew P. Boerlage for their continuous guidance, motivation, and wisdom through the entire process. Thanks to Mr. William Roeder, and Mr. Todd McNamara from the 45th Weather Squadron for continually providing their top-notch expertise and direction for the focus of our research. This research project was supported by funding from the USAF 45th Operations Group. Additionally, thanks to Mr. Bruce Ford, Ms. Mary Jordan, and Mr. Bob Creasey for their crucial computer programming and coding knowledge essential to our research process.

My home away from home was with my Naval Postgraduate School classmates, thanks to them for being my “brothers” along the way. I would also like to thank my mom and dad for being there from the very beginning and always pushing me to do my best. Finally, my wonderful wife and three children are what kept me inspired and motivated to achieve success along this journey. Thank you, Jennifer, Jonathan, Brandon, and Camdyn, for being the most understanding, patient, and loving family a husband and dad could ask for.

THIS PAGE INTENTIONALLY LEFT BLANK

I. INTRODUCTION

A. BACKGROUND

One of man's greatest scientific accomplishments is successfully launching a rocket from Earth into space. U.S military operations around the world are dependent upon these rockets to deliver critical payloads, such as navigation, communication, and weather satellites. Along with this incredible feat, there are obvious dangers and hazards. This places safety at the absolute forefront of space flight. Many of the potentially unsafe conditions are based upon varying meteorological parameters. These can range from something as simple as a temperature constraint, a wind direction and speed limitation, to potential for lightning occurrence, or a specific cloud formation surrounding the launch pads. These restrictions are in place to reduce the risk of any adverse effects to the mission, in this case the launch of a space vehicle, manned or unmanned, to space. The 45th Weather Squadron (45 WS) at Patrick Air Force Base, Florida is assigned the task of mitigating the risk of any negative weather impacts to launches from Cape Canaveral Air Force Station (CCAFS), and Kennedy Space Center (KSC). This team of weather professionals works around the clock to provide every launch agency and customer that uses CCAFS and KSC for launch operations with timely and critical weather information. The 45 WS is actively involved in all phases of launch operations: generation, execution, and recovery. All phases are equally important to a successful mission; however, weather impacts during the execution phase present the greatest risk. Any negative impact could potentially lead to a catastrophic launch failure. Mission failure could mean the loss of millions of invested dollars, thousands of preparation hours, a priceless payload, or worse, the lives of those supporting the launch operation.

A study compiled by the 45 WS for CCAFS/KSC from 1988 through 2006 revealed 30 percent of all launch operations from CCAFS/KSC are either delayed or canceled due to weather impacts (Roeder and McNamara 2006). Weather is

one of the key factors launch decision makers inquire about in weeks and days leading up to a launch. Launch operations are time sensitive, and many decisions made are based in large part on weather forecasts provided by the 45 WS. The 45 WS assigns a specific weather professional to each launch platform (e.g., Delta, Atlas, Falcon, etc.). These squadron members are identified as launch weather officers (LWOs). Each LWO is in direct communication with the launch customer or agency on a daily basis. The team at the 45 WS begins their official forecast process as far out as seven days prior to launch, but they also receive requests weeks to months in advance to provide climatological planning information. This information may steer mission planners to alter their mission schedule.

The 45 WS members have numerous criteria or thresholds they must consider when making their forecasts. They range from user-defined constraints, such as wind or temperature limitations during fueling, or range safety defined constraints, which include a complex set of Lightning Launch Commit Criteria (LLCC). The LLCC are a set of rules that outline meteorological conditions that could potentially lead to a lightning related hazardous situation during launch. Violations of these LLCC are the largest source of negative weather impacts to space launches (Roeder and McNamara 2006, FAA 2003). Accurately predicting these conditions can potentially save up to millions of dollars, and more importantly save lives by mitigating a potential catastrophic loss of mission or personnel (Roeder et al. 1999).

B. LIGHTNING LAUNCH COMMIT CRITERIA

1. History

Early in the spaceflight era, rules were in place prohibiting any vehicle from launching through a thunderstorm (Merceret et al. 2010). This was the only official guidance to weather personnel providing support to launch agencies during missions, but this changed after the 1969 launch of Apollo XII. During the Apollo XII countdown, there was no observed natural lightning reported near

CCAFS/KSC, but an approaching cold front with numerous cumuliform clouds was approaching the area. These clouds were extremely large, with tops exceeding the freezing level height. Understanding the relationship between clouds and freezing level heights will prove to be an important concept in later discoveries, as it will lead to re-defining the set of evaluated LLCC. Note in Figure 1 that while there was a large cumulus cloud observed immediately over the launch pad, it was not a thunderstorm. Therefore, it was not considered a threat to the launch.

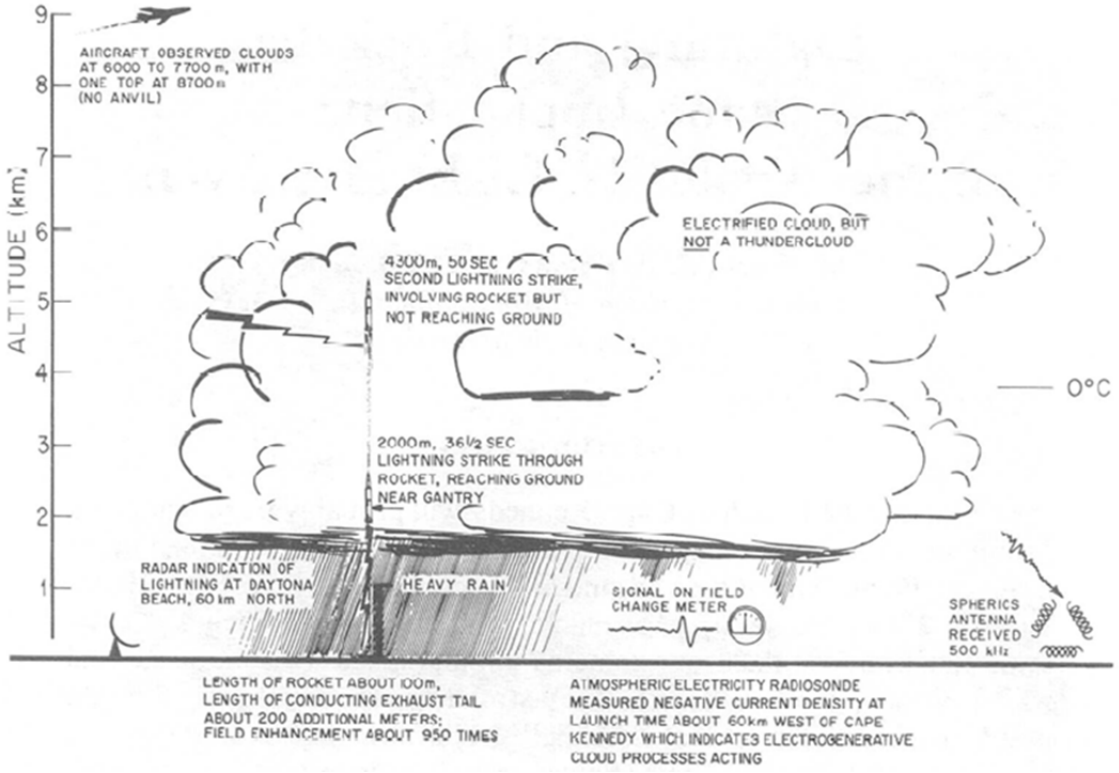

Figure 1. Depiction of meteorological conditions near the site of the Apollo XII incident (From: Merceret et al. 2010)

As the Saturn V rocket with the manned space capsule ascended, it experienced two lighting strikes in a span of 52 seconds (Merceret et al. 2010). The jolt severed communication between the vehicle's command module navigation system, and the mission's control center. Apollo XII avoided potential

catastrophe by regaining communication and successfully completed its objective of landing on the moon. However, this event would permanently alter weather support to spaceflight operations by generating more restrictive rules for LWOs to monitor during launches (Merceret et al. 2010).

Immediately following the Apollo XII incident, scientists in the meteorology and spaceflight fields recognized the Apollo XII events were significant, and began taking precautions to protect space vehicles, and explore better capabilities for predicting when a similar incident could occur (NASA Facts 1998). The outcome was a new set of LLCC for the weather teams to monitor during launches.

By 1987, scientists had created a more restrictive set of LLCC. The newest rules directed that a space vehicle could not launch:

1) Through a thunderstorm/cumulonimbus cloud
2) Within 5 miles of a thunderstorm/cumulonimbus cloud or 3 miles of the associated anvil top
3) Through a cold front or squall line associated clouds with tops 10,000 feet or higher
4) Through middle cloud layers, 6000 feet or greater in depth, where the freezing level is in the clouds
5) Through cumulus clouds where the freezing level is in the clouds

Despite these newly modified LLCC, Atlas/Centaur 67 (AC 67) experienced a similar situation as Apollo XII, but with greatly different results. As the AC 67 vehicle began its ascent, it also experienced a lightning strike in conditions where no natural lightning was observed. Only a few seconds after this strike, the vehicle showed signs of steering off the nominal course, and began breaking apart. The range safety officer sent the self-destruct signal, destroying the vehicle and its Fleet SatCom satellite payload, but protecting lives. The destruction of the AC 67 vehicle generated a large inquiry into the cause of

the event. One of the significant outcomes was the creation of the Lightning Review Committee (LRC), which later became the Lightning Advisory Panel (LAP). This is a group of research scientists in the fields of space flight, meteorology, and atmospheric electricity. Their objective was to come to a consensus, based on their varying expertise, and determine what atmospheric conditions led to the destruction of AC 67 (Merceret et al., 2010).

Figure 2. Triggered lightning strike to AC-67 in 1987. Only seconds after liftoff, the lightning followed the exhaust plume to the ground. (From: Roeder and McNamara 2006)

These two historical events highlight the significance of understanding induced lightning generated from a launched vehicle, versus launching in conditions where natural lightning is observed. This induced, or triggered, lightning is the basis for the majority of the existing LLCC, and represents the initial focus for our research.

2. Triggered Lightning

Discerning between natural and triggered lightning is critically important; eleven of the twelve current LLCC are in place to mitigate the risk of triggered

lightning. Natural lightning is lightning produced by thunderstorms, while triggered lightning results when a rocket is launched into a pre-existing and sufficiently strong electric field (Roeder and McNamara 2006). Additionally, the exhaust plume that extends from the rocket is electrically conductive, and further adds to the potential for a triggered lightning discharge.

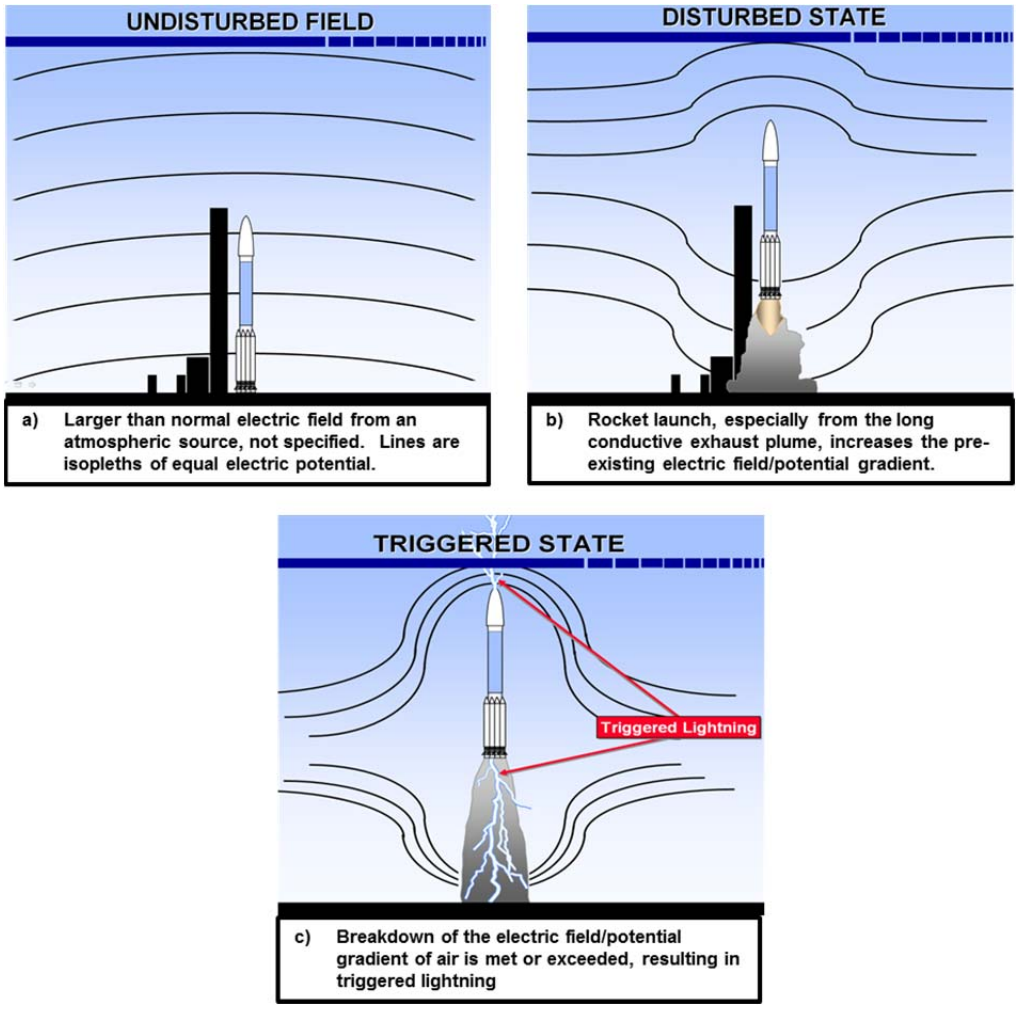

Figure 3. Schematic of the rocket triggered lightning process (From: 45 WS 2009)

In an undisturbed state, the electric field surrounding the launch pad typically exhibits an even spacing of electric potential values (Figure 3a). Once the rocket launches, compression of the electric field can ensue (Figure 3b). If the compression of the electric field continues and reaches or exceeds the existing electric field gradient, a triggered lightning strike can occur (Figure 3c)

(Roeder and McNamara 2006). Rocket triggered lightning can occur in electric fields that are tens to hundreds of times smaller than what is required to produce natural lightning (Merceret et al. 2010). The existing LLCC are in place primarily to protect against electric charge generated because of launching into mixed solid-liquid phase of water (Roeder and McNamara 2006). As seen in previous historical events, launching into non-thunderstorm clouds can still produce lightning if certain meteorological conditions exist. Many of those conditions will deal with clouds that meet specific restrictions, such as proximity, depth, type, and temperatures within the cloud. Accurately measuring these parameters enables the weather team to assess the potential for triggered lightning. Each restriction that is measured provides important information for defining the electric field, or inferring the existence of a mixed phase of water. From 1969–2010, the LLCC have undergone numerous modifications based on new scientific information. A summary of the changes is located in the NASA document, "A History of the Lightning Launch Commit Criteria and the Lightning Advisory Panel for America's Space Program" (Merceret et al. 2010). Since Apollo XII, the LLCCs have evolved from a singularly evaluated LLCC (cannot launch in a thunderstorm), to the present complex set of ten rules.

3. Operational Set of LLCC

When 45 WS LWOs prepare their forecast for upcoming missions, they need to assess the likelihood an LLCC may be violated during the launch countdown. This set of LLCCs is what LWOs actually evaluate and report as "No-Go" (violated), or "Go" (non-violated) to critical mission personnel during countdowns. The latest revision to the LLCC was accepted and put into operational use in 2009. The full set of LLCC evaluated during all launches from CCAFS/KSC is listed below.

1) Surface Electric Field Mill
2) Natural Lightning
3) Cumulus Clouds

4) Attached Anvil Clouds

5) Detached Anvil Clouds

6) Debris Clouds

7) Disturbed Weather

8) Thick Cloud Layer

9) Smoke Plumes

10) Triboelectrification

Each criterion is divided into sub categories based on various parameters, such as temperatures, standoff distances, and time requirements. Some of these rules also have caveats, which allow for relief from violation of the main rule if certain meteorological conditions are met. A complete description and details of all the currently applied LLCC are contained in the Air Force Space Command Manual 91-710 (Air Force Space Command 2004).

C. RESEARCH MOTIVATION/SCOPE

1. Prior Work

Over the years, numerous studies were conducted documenting the natural lighting portions of the LLCC. However, there are relatively few studies assessing the probability of violating, and building climatologies of, the LLCC, especially those dealing with cloud-based criteria. Muller (2010) adequately summarizes much of the previous work done in regards to the natural lightning LLCC.

Goetz (2000) explored the possibility of building hourly and seasonal climatologies of the natural lightning and cumulus cloud LLCC. His work focused on data from 1989–1998, and within a 12 nm radius of the CCAFS/KSC region. The output of his results was an unsmoothed hourly probability of violation for each day of every month and year during the timespan of his study. However, cloud type climatology is relatively difficult to assess given the nature of surface

weather observations, and lack of cloud type input (Taniguchi 2005). This presented some limitations in accurately depicting probabilities of violating the cumulus cloud LLCC. Additionally, his results indicated very large day-to-day variations of the probabilities, possibly due to the relatively short period of record (1989-1998). While this was an early attempt at building LLCC climatology, it did not deliver an operational product the 45 WS could use when preparing their customers for a launch.

Muller (2010) assessed the probabilities of violating the natural lightning LLCC and developed a daily climatology of the probability of violating the natural lightning LLCC. He also conducted a climate analysis of natural lighting around the CCAFS/KSC region and explored interannual and seasonal variations of conditions related to natural lightning using atmospheric reanalysis data. Of note, Muller highlighted the need for a more advanced approach to building climatologies for more of the LLCC.

2. Research Focus

The 45 WS has stressed the importance and significance of assessing the triggered lightning LLCC to develop useful, and usable, operational tools the LWOs can refer to when making their forecasts (Roeder, personal communication). There are millions of dollars invested, thousands of resources used, and countless hours spent in preparation of a CCAFS/KSC launch. Safety is paramount, and mitigating the risk of any catastrophic failure, like AC 67, is paramount when 45 WS personnel are making their predictions of violating the LLCC.

Addressing all of the LLCC would be too difficult for the scope of this research, so we decided to assess several factors to determine where to start. Variables considered in determining our focus were: (a) frequency of violation; (b) false alarm rate; and (c) 45 WS LLCC priority ranking (a ranked set of LLCC based on input from 45 WS members and key operators). All of these factors, coupled with input from the 45 WS directly, led us to focus our research on the

thick cloud layer LLCC. There is no existing complete data base from which the definitive probability of violating one of the LLCC rules can be directly determined. Therefore, in this study, we explored the blending of multiple data sets to develop a merged data set from which the probability of violating the thick cloud layer rule could be directly calculated. We anticipate that future research efforts will be able to apply similar techniques to other LLCC.

Our research was primarily focused on the following topics:

1) Determine the best approach to analyzing and synthesizing multiple data sets to infer cloud thicknesses and the associated applications of the thick cloud layer rule
2) Develop a climatological data base of the thick cloud layer LLCC
3) Build a useful and meaningful metric, such as a probability of violation (POV) for the thick cloud layer rule.
4) Conduct a sensitivity analysis of our resulting POVs for use in determining future applications or modifications of the thick cloud layer rule.

3. Thesis Organization

The topics outlined above are addressed in this thesis through a systematic approach. Chapter II describes our study region, study period, a typical approach the 45 WS employs in evaluating the LLCC during a launch, details of the thick cloud rule, datasets used, and the methodology we applied to our data sets. Chapter III outlines the results from our analyses of the data sets, our blending of the data sets, and our calculations of the climatological probabilities of violating the thick cloud layer LLCC.

Additionally, Chapter III contains the results of our analysis of the sensitivity of the thick cloud layer POVs to variations in the thickness threshold, and a small sample case study of known violations of the thick cloud layer rule. Chapter IV provides a summary of our results, conclusions we have made from them, and suggestions for future research.

THIS PAGE INTENTIONALLY LEFT BLANK

II. DATA AND METHODS

A. STUDY REGION AND PERIOD

The CCAFS/KSC region covers nearly 500 square miles along the "Space Coast" of Florida (Figure 4). The launch pads are located along the immediate coast, and are generally separated by approximately 1 nm. Each LLCC is evaluated at the launch complex being used for a particular mission. Additionally, many of the LLCC specify a standoff distance from the launch site within which the rule must also be evaluated. The thick cloud rule specifies that the rule must be evaluated within 5 nm of the launch pad being used for a particular mission (Figure 5).

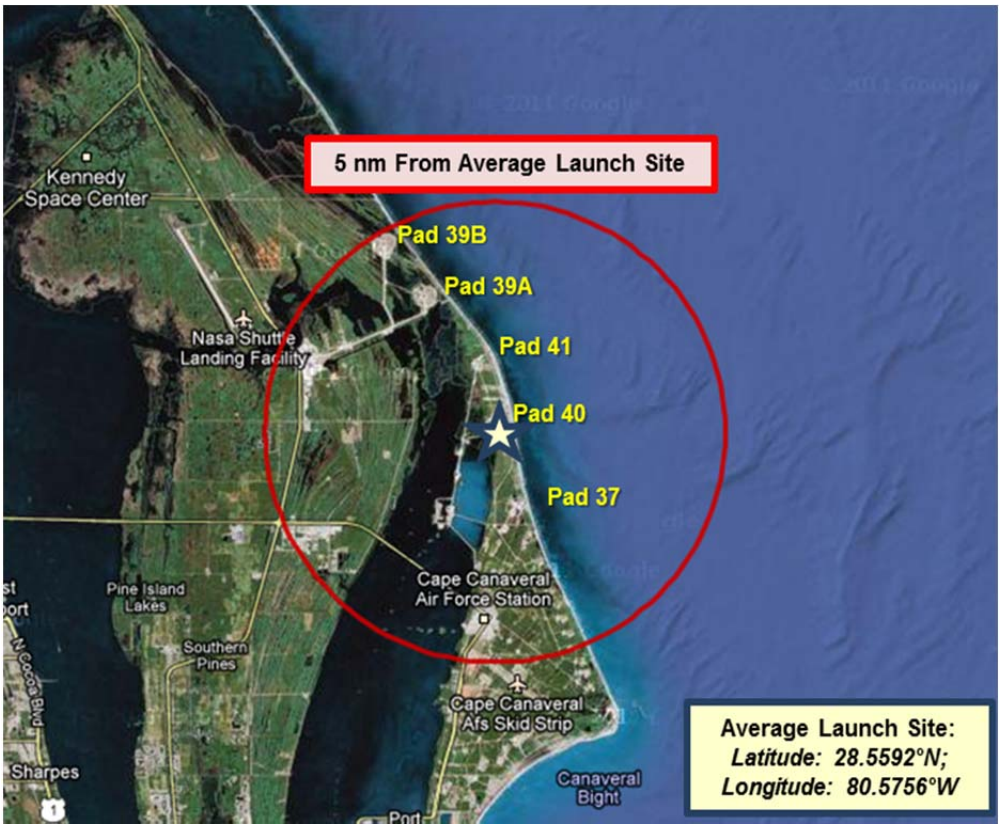

Figure 4. Map indicating five nautical mile ring around the average launch site (light yellow star). The average launch site is the average of the most active launch pads as of September 2011 (Pad 37, Pad 40, and Pad 41). Image created from GPS Visualizer [accessed online at http://www.gpsvisualizer.com/calculators, Sept 2011].

Keeping in mind the spatial limitations of observed and modeled data, we wanted to ensure we captured a large enough sample to allow us to depict the climatology over any of the launch sites at CCAFS or KSC. We determined the best approach was to focus our research on an average launch site location based on the locations of the most active launch pads within CCAFS/KSC. This is similar to the approach Muller (2010) used in his natural lightning LLCC research. We chose the average launch site location based on the most active pads as of September 2011. The location of this average site is 28.5592° north latitude and 80.5756° west longitude. With the launch pads being approximately 1 nm apart, we assumed the meteorological differences between the average launch site and the actual launch sites are minimal, and therefore these differences could be neglected in our study.

To develop a robust climatology, we wanted to evaluate meteorological conditions at a high temporal and spatial resolution, and over a period of 20 years or longer, if possible. Launches have occurred from the CCAFS/KSC region since 1957, and, as described in Chapter I, Apollo XII and AC 67 both resulted in major revisions to the LLCCs. With the addition of the LAP, the first major revision of the LLCC was put into operational use after AC 67 (Merceret et al. 2010). We also needed to consider the availability of the in situ and reanalysis meteorological data needed for our study. Balancing all these factors, we determined a study period of January 1988–December 2010 would provide the optimal combination of data sets.

B. LLCC

1. Launch Day Evaluations

Before identifying what sources of data are available to provide us with necessary meteorological information, it is important to understand the process the weather team follows during a typical launch countdown. The length of a typical launch countdown can vary, but it is typically six hours in duration from clock start to liftoff. It is during this time the LWOs evaluate the complete set of

current LLCCs. This evaluation process includes the use of weather radar, real time satellite data, surface weather observations, weather balloon sounding data, several sources of lightning detection data, weather aircraft reports, and input from other weather personnel and weather equipment. The typical weather team composition on a day of launch is approximately five members, but mission requirements may dictate more or less. Each member has an equally important role: to monitor and report LLCC violations to the lead LWO, who passes that information to launch decision makers. Modern weather instrumentation is extremely accurate; however, certain temporal and spatial limitations set in place during a launch leads to the need for some interpretation of data by LWOs. The published LLCC evaluation documentation states the launch operator must have clear and convincing evidence the evaluated LLCC is *not* violated (Willett et al. 2010).

2. Thick Cloud Layer Rule

As discussed in Chapter I, we determined the focus for our research was the thick cloud layer LLCC. The complete description of the thick cloud layer rule is summarized below.

1) A launch operator must not initiate flight if the flight path will carry the launch vehicle through:
    a) A cloud layer that is greater than or equal to 4,500 feet thick and any part of the cloud layer along the flight path is located at an altitude where the temperature is between 0° Celsius and -20° Celsius, inclusive ; or
    b) Connected to a thick cloud layer that, if within 5 nm from the flight path, is greater than or equal to 4,500 feet thick and has any part located at an altitude where the temperature is between 0°Celsius and -20°Celsius, inclusive.

This rule does not apply if the thick cloud layer is a cirriform cloud layer that has never been associated with convective cloud, is located entirely at altitudes where the temperature is less than or equal to -15° Celsius, and shows no evidence of containing liquid water.

This rule is in place because numerous studies have indicated that launching in these conditions could result in a rocket-triggered lightning strike (Merceret et al. 2010). The sheer complexity of this, or any, LLCC makes it difficult for LWOs to make split second decisions during a launch. To assist LWOs during training and launch countdowns, the 45 WS developed a set of visual aids for each LLCC. Figure 5 depicts a visual representation of part 1.a of the thick cloud rule listed above. It demonstrates that if the cloud layer meets the requirements outlined, the LWO must report it as “red” (or violated). The entire operation becomes “no-go” until the weather team becomes clearly convinced conditions that made this rule “red” no longer exist.

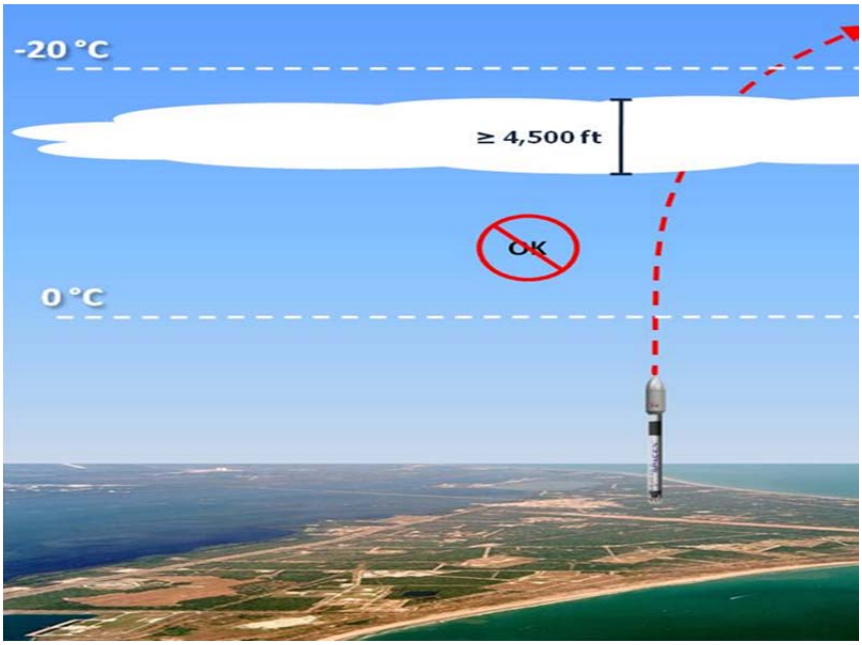

Figure 5. Depiction of an example of a violation of the thick cloud rule (From: 45 WS VA 15-3b 2009)

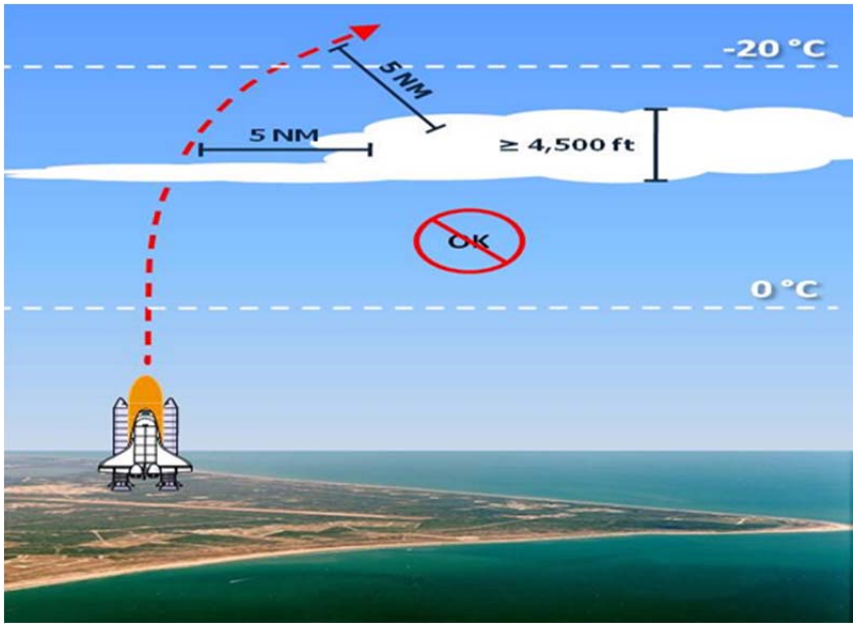

Figure 6. Depiction of an example of a violation of the thick cloud rule (From: 45 WS VA 15-3b 2009)

Similarly, Figure 6 refers to part 1.b of the thick cloud rule. The main difference is in this case the launch vehicle does not actually penetrate a 4,500 foot thick cloud layer that meets the temperature requirements, but into a layer that is attached to that thick cloud layer within 5 nautical miles.

C. METEOROLOGICAL VARIABLE SELECTION

Based on the thick cloud rule definition, we needed to identify key variables for which we could obtain data for a sufficiently long period (e.g., 20 years or longer) and sufficiently high temporal and spatial resolution. There are no adequate data sets that directly describe cloud thickness and the other variables associated with the thick cloud layer rule (e.g., temperature, cloud type). So we needed to obtain data from which we could confidently determine cloud thickness.

A major initial objective in this part of our research was to evaluate the potential data sets for each needed variable and determine its suitability for use in developing the merged data set from which we could directly calculate the POVs. The main variables needed are summarized in the list below and in Figure 7 (all variables are for CCAFS/KSC).

1) Cloud coverage (whether clouds are located over region or not)
2) Height of the cloud top
3) Height of the cloud base
4) Height of the 0° Celsius level (freezing level)
5) Height of the -15° Celsius level
6) Height of the -20° Celsius level

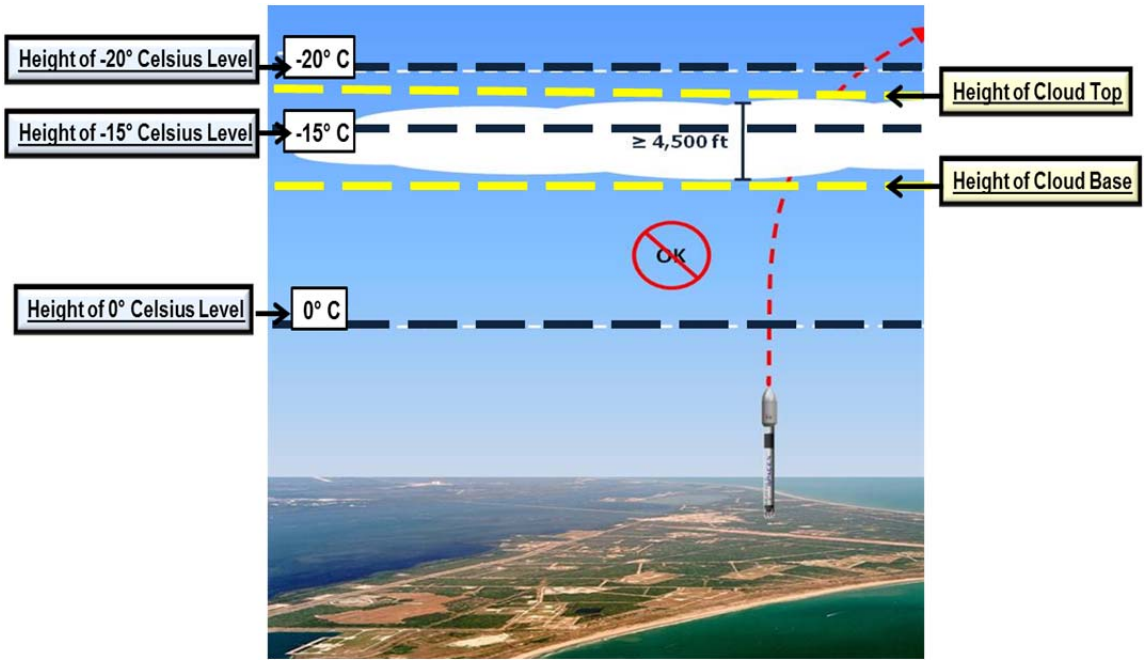

Figure 7. Visual representation of the variables required to calculate thick cloud layer LLCC violations.

Once we determined our set of necessary variables, we began identifying general aspects and characteristics of each individual variable. One area we

needed to evaluate was the average heights of identified temperature levels. Information on the average heights of these temperature levels would enable us to fine-tune our interrogation of the upper and lower boundaries of cloud layers. As the thick cloud LLCC states, the rule is only considered violated if cloud thickness is greater than or equal to 4,500 ft, *and* the temperature stipulations are met as well. To initially evaluate these temperature levels, we applied a tool used by the 45 WS, and developed by the Applied Meteorology Unit (AMU). The AMU is a team of research scientists in the field of meteorology under contract to NASA, who work on a daily basis with the 45 WS. They assist the 45 WS with creating launch operations related weather tools, one of which is the Range Reference Atmosphere (RRA) utility. The RRA ingests twelve years (January 1990–January 2002) of CCAFS radiosonde observations (RAOBs), and calculates monthly and annual climatological averages of specified temperature and height levels. Initially, RAOB data is processed at 0.25 km vertical resolution, and the AMU-created algorithm interpolates this data to the desired temperature or height level. Prior to determining our final set of variable conditions, we used the RRA to determine climatological averages of our needed temperature levels (0°, -15°, and -20° C). The results are shown in Figures 8 and 9.

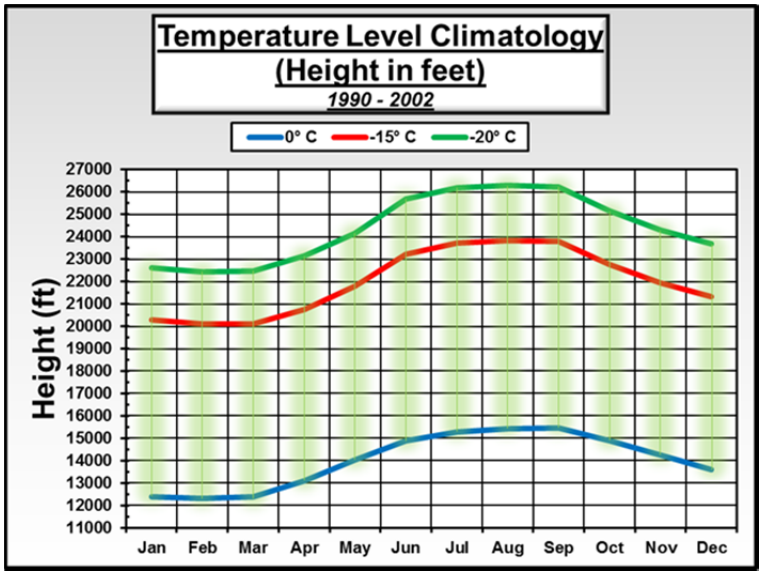

Figure 8. Monthly averages (in feet) of the heights of various temperature levels. Averages were calculated using the AMU RRA utility for RAOBs during Jan 1990–Dec 2002. The green shaded region represents the vertical region in which thick clouds need to exist to lead to a thick cloud rule violation.

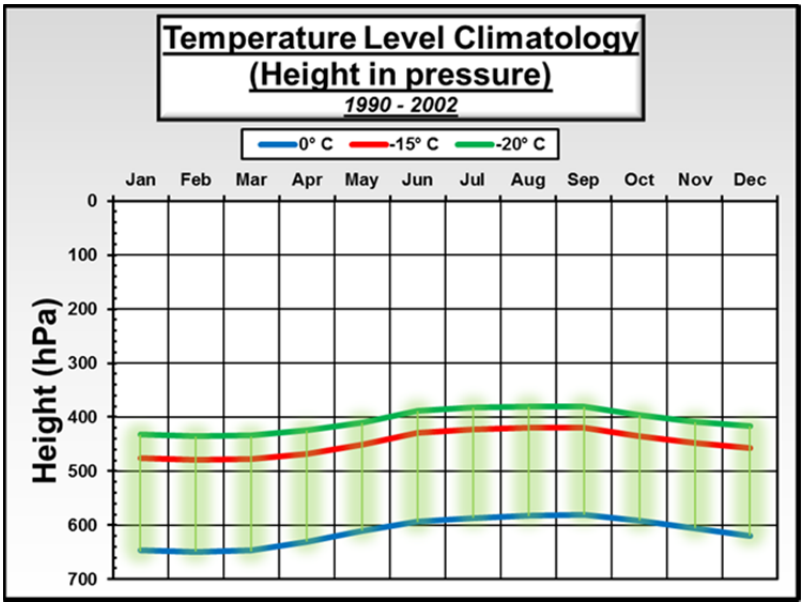

Figure 9. Monthly averages (in pressure) of the heights of various temperature levels. Averages were calculated using the AMU RRA utility for RAOBs during Jan 1990–Dec 2002. The green shaded region represents the vertical region in which thick clouds need to exist to lead to a thick cloud rule violation.

The shaded green regions of Figures 8 and 9 highlight the vertical region within which clouds would need to exist in order to be considered potential violators of the thick cloud LLCC. If any part of a cloud is 4,500 ft thick or greater and located within these regions, it could potentially cause a launch operation to become no-go. We also noted the expected seasonal cycle in the heights: lower in colder winter months and higher in warmer summer months. The tool was used to calculate the average vertical extents measured in feet and hPa. We used this information to evaluate data sets that could potentially provide this information on a long-term daily basis.

The ideal data set for our study would have been one with accurate data for all required variables available in a regularly gridded spatial and temporal array, at high spatial and temporal resolution, and spanning at least 20 years. We realized that such a data set probably did not exist, and we would probably need to develop a method for combining multiple data sets together. Therefore, we needed to develop processes to identify the strengths and weaknesses of various data sets, and determine the best method for combining them into one merged data set.

The four main types of data sets that we used in our study are listed below and described in the following sections:

1. Climate Forecast System Reanalysis (CFSR) data
2. Meteorological aerodrome report (METAR) data
3. Radiosonde observations (RAOBs)
4. Expert meteorologist input data

D. DATA SETS AND SOURCES

1. Climate Forecast System Reanalysis (CFSR)

We considered the many analysis and reanalysis data sets available, and determined that CFSR would offer the best choices for the purposes of our study. The Climate Forecast System Reanalysis (CFSR, Saha et al. 2010) is a

reanalysis data set produced by the National Centers for Environmental Prediction (NCEP), and maintained and distributed by the National Center for Atmospheric Research (NCAR). It is a high-resolution global data set covering the period January 1979–March 2011 (as of March 2012), and provides data for hundreds of atmospheric and oceanic variables at hourly and approximately 0.3 to 0.5 degree horizontal resolution. CFSR uses a coupled atmosphere-ocean-land surface data assimilation and model-based analysis system. The system assimilates in situ observations, satellite radiances, and other observational data. which are then analyzed using a global dynamical coupled atmosphere-ocean-land-ice model. The global atmosphere horizontal resolution is up to ~38km (T382), and up to 64 vertical levels from the surface to .26 hPa. It is initialized four times per day (00Z, 06Z, 12Z, and 18Z), and products are available in up to 1 hour intervals. Details about the CFSR data sets we chose for our research are provided in later sections. Further details of the CFSR data set and processes are provided by Saha et al. (2010).

a. Variables

One of our main tasks early in the process of data set selection was to sort through the hundreds of variables described by CFSR, including the horizontal and vertical locations for which those variables are available. This enabled us to determine which variables at which locations we needed to best describe the cloud and temperature level conditions over CCAFS and KSC. CFSR provided two of our six needed variables directly: cloud coverage and height of the 0° C level. It also provided pressure at cloud tops and bottoms, which we could use to infer a geometric height. However, the heights of the -15° and -20° C levels were not available directly from CFSR. Table 1 summarizes the CFSR variables, or parameters, we selected for evaluation and used in our study.

		Parameter			
		Geopotential Height (m)	Pressure (hPa)	Temperature (K)	Total Cloud Cover (%)
Vertical	Level	700 hPa	Low Cloud Bottom	700 hPa	Entire Atmosphere
		650 hPa	Low Cloud Top	650 hPa	Low Cloud Level
		600 hPa	Middle Cloud Bottom	600 hPa	Middle Cloud Level
		550 hPa	Middle Cloud Top	550 hPa	High Cloud Level
		500 hPa	High Cloud Bottom	500 hPa	
		450 hPa	High Cloud Top	450 hPa	
		400 hPa		400 hPa	
		350 hPa		350 hPa	
		Level of 0° Isotherm		Low Cloud Top	
				Middle Cloud Top	
				High Cloud Top	

Table 1. The CFSR variables we used in our thick cloud LLCC study. The levels listed in each of the four parameter columns indicates the vertical levels for which we obtained and used the CFSR data for that parameter.

We used the AMU RRA results (Figures 8-9) to determine the levels for which to obtain and evaluate CFSR data. These results gave us the climatological means of the heights of the different temperature levels of concern (0°, -15°, and -20°C). We also took into account the variations from these means to ensure we captured the extreme limits of the heights. The lowest climatological height of the 0° C level was 12,311 ft, which equated to a pressure surface of 648 hPa. The highest climatological height of the -20° C level was 26,287 ft, which equated to a pressure surface of 380 hPa. To ensure we completely covered the extreme values, we applied two standard deviations and rounded off to the nearest 50 hPa increment. This provided us with an overall atmospheric boundary of approximately 700–350 hPa for which to obtain and evaluate CFSR data. We assumed that clouds occurring within this vertical region and which violate the 4,500 ft thickness limit would be likely to also violate the thick cloud LLCC because they would also occur within the climatological means of the defined temperature thresholds (0° and -20° C).

b. Spatial and Temporal Resolution

Although CFSR data is available for the entire globe, we were only interested in data at and near CCAFS/KSC. Specifically, we desired data as

close as possible to our average launch site (28.5592° north latitude, 80.5756° west longitude). Many of the analysis and reanalysis data sets available are for large spatial domains, and retrieving information on a smaller scale is sometimes difficult. One of the distinct advantages to using CFSR is the ability to select a spatial subset of the chosen variables. This allowed us to tune our reanalysis data set selection to focus on the Florida Peninsula, and ultimately CCAFS/KSC. Additionally, there were multiple horizontal resolution choices ranging from 0.3° to 2.5°. Our region of interest is located along a coast, so we wanted to ensure we chose a resolution fine enough to capture the coastal conditions as much as possible. We evaluated all choices and determined using the 0.5° horizontal resolution offered the greatest benefits for the purposes of this study. The 0.5° degree mesh places a grid point at 28.5°N latitude, and 80.5°W longitude, very close to the average launch site. In addition, data at this resolution is available on a standard latitude and longitude grid system, whereas the finer 0.3° resolution is placed on a Gaussian grid system. Using the Gaussian grid system was certainly feasible; however, in order to maintain consistency with our other data sets, we chose to use data on the evenly spaced latitude and longitude 0.5° grid system.

In addition to knowing the closest grid point to our average launch site, it was important to have the ability to expand outward to identify differences at other grid points. With CCAFS and KSC being along the coast, there is obvious potential for land water differences to influence the CFSR output, so we wanted to ensure we properly accounted for this. Ultimately, we obtained and evaluated CFSR data for the variables listed in Table 1 at our specified closest grid point, as well as for 1° by 1°, and 3° by 3° regions surrounding our central location (Figure 10).

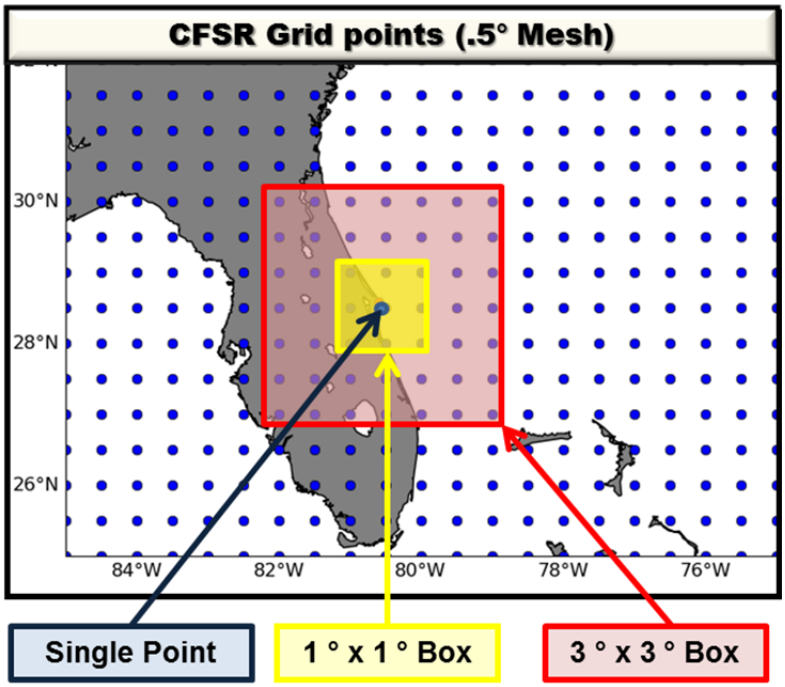

Figure 10. The three regions for which we obtained CFSR data at 0.5° horizontal resolution. The three regions are centered on a CFSR grid point that is very close to the average launch site and span a single grid point, a 1.0° x 1.0° box (yellow), and a 3.0° x 3.0° box (red),

The CFSR data we used was at 37 vertical pressure levels ranging from 1000 hPa to 1 hPa, with a varying vertical separation between the levels. Pressure surfaces in the bottom portion of the troposphere (1000 – 750 hPa) had a separation of 25 hPa, while the middle to upper troposphere (750 – 250 hPa) had a separation of 50 hPa. The separation for pressure surfaces near the top varied from a maximum separation of 25 hPa near the 250 hPa pressure surface, to a minimum separation of 1 hPa for the highest few pressure surfaces.

One other consideration we applied in assessing potential data sets was their spatial and temporal resolution. One of our main goals was to develop sub-daily climatologies for variables that have substantial spatial and temporal variability --- due, in particular, to the significant microscale and mesoscale variability in coastal environments and clouds. Thus, we needed to work with data sets for those variables that have high spatial and temporal resolution, so

the data from any individual point in space would be as representative as possible of our location of interest (e.g., the average launch site).

c. Cloud-Related Variables

As noted in Table 1, CFSR cloud level information is given for constant pressure surfaces. Rather than considering clouds as one entire vertically continuous layer, CFSR breaks the cloud information into layers placed into three categories: low, middle, and high clouds. This is similar to the categorization of clouds used in standard weather observations made by weather personnel around the globe (Saha et al. 2010). The CFSR interfaces between the three layers are 650 hPa and 350 hPa for grid points within the bounds of 45°N and 45°S latitudes. Thus, CFSR low clouds will have bases and tops contained below 650 hPa, mid clouds will have bases and tops between 650 hPa to 350 hPa, and high clouds will have bases and tops above 350 hPa (Figure 11).

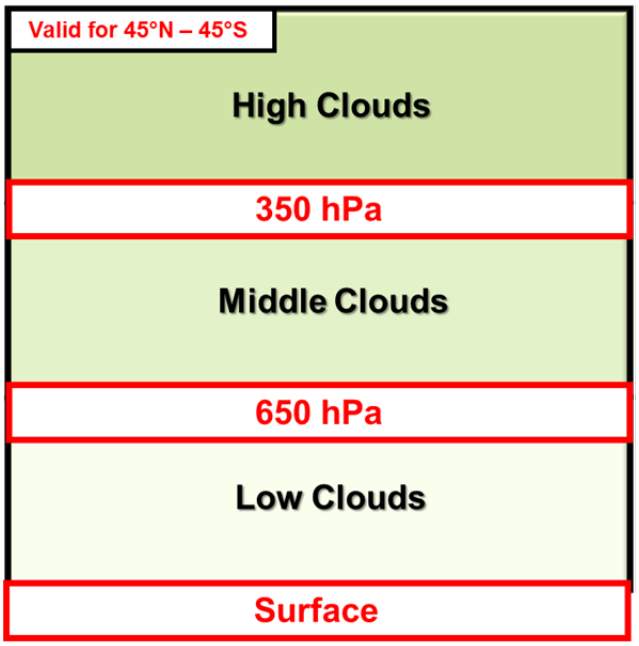

Figure 11. Visual depiction of how the three CFSR cloud layers are defined. This depiction is only valid for locations between 45°N and 45°S latitudes. Pressure levels and red boxed areas represent the interfaces between the layers.

2. Meteorological Aerodrome Report (METAR)

We used METAR data from the KSC Shuttle Landing Facility (SLF), located approximately 2.5 nm from the coastal launch sites in the heart of KSC (Figure 12). Human observations have been made at the SLF location since the inception of the space program. The instrumentation at this site has varied through the years, but, until 2011, a human observer was always a part of the process. Having a human observer is beneficial to ensuring the accuracy and timeliness of meteorological measurements.

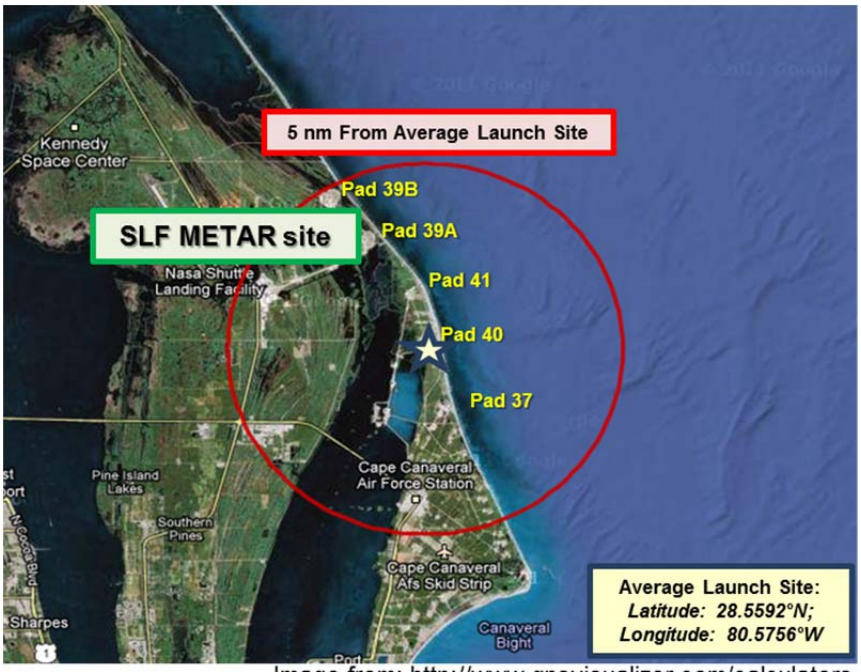

Figure 12. Map indicating location of the official Shuttle Landing Facility (SLF) METAR observing site. This is the location of a human observer and meteorological equipment used to measure cloud conditions. Image created from GPS Visualizer [accessed online at http://www.gpsvisualizer.com/calculators, Sept 2011].

METARs taken in North America follow the World Meteorological Organization (WMO) standards, with only a few modifications for units of measure. A METAR provides many details of a surface weather observation, but for the purposes of this study, the key information needed concerned clouds.

The main cloud data included in a METAR observation is the height of the cloud base, which is reported in feet for the SLF. WMO standards dictate that METARs are taken a minimum of once per hour on the hour, and at other times when certain meteorological conditions are met (known as special observations). We obtained the extensive set of METARs for the SLF from the climate systems division of the 14th Weather Squadron (14 WS) in Ashville, NC.

3. RAOBs

Standard weather balloon launches occur approximately twice per day (00Z and 12Z) from the CCAFS weather balloon facility. Various types of balloons and sounding equipment are released from this location to investigate the atmospheric conditions above the region. The CCAFS weather balloon facility is unique compared to other balloon facilities because the RAOB launch times vary based on meteorological and operational needs. During rocket launch operations, weather balloons are released more frequently; as many as ten within a six hour window. During summer months, sea breeze activity in the region generates a greater threat for severe weather to occur; therefore, balloon release times may vary to accommodate 45 WS members investigating the severe weather potential. As with METARs, RAOBs provide several meteorological parameters, but for this study, we only needed the temperature and dew point data.

The 14 WS provided archives of the RAOB data for CCAFS (WMO identifier KXMR). Additionally, the 14 WS processed the RAOB data through an algorithm based in part on the hypsometric equation to interpolate the data to the nearest 500 ft level, so that the data is provided at 500 ft intervals. The raw RAOB data is available at a vertical interval of approximately .25 km, or approximately 820 ft. Therefore, the 500 ft interpolated RAOB data has a slightly enhanced vertical resolution over the raw sounding data, and therefore increases the ability to describe the vertical structure of the temperature and dew point data.

The interpolated RAOB data also had the advantage for our study of being available in even 500 ft increments, rather than in the uneven increments of the raw sounding data.

4. Expert Meteorologist Input

For our investigation of CFSR, METAR, and ROAB data, we developed a process for comparing the results from these data sets to actual cloud conditions at and near CCAFS/KSC. One way we did this was by comparing satellite imagery to visualizations of the data sets for specific case study. Another method was to survey meteorologists with extensive experience in the CCAFS/KSC region on cloud conditions throughout the year. Our main application of this method was for determining the approximate heights of cloud tops. In particular, we collected information from these meteorologists on cloud top heights for different cloud types and for each month. This was a collaborative effort with a team of expert meteorologists from the 45 WS and the Naval Postgraduate School. Collectively, this included input from a panel of five meteorologists who have an average of 23 years of operational weather forecasting and observing experience. All have first-hand experience with operational weather support to the space program at CCAFS/KSC, including the evaluation of LLCCs during launch countdowns. In developing their inputs to our research project, these meteorologists were able to draw on information not electronically available to other personnel --- for example, weather aircraft reports, weather radar, and weather satellite data related to launch operations that is only maintained in hard copy format. The inputs of these expert meteorologists was crucial to putting together the climatological information we needed to evaluate and supplement the CFSR, METAR, and RAOB data sets, and to develop the probabilities of violations of the thick cloud LLCC.

5. Summary of Data Set Selection

We selected the CFSR, METAR, RAOB, and expert meteorologist inputs as our main potential data sources. However, no one of these data sources had

all the information we needed. But the combination of CFSR, METAR, RAOB, and expert meteorologist input data provided information that came very close to what we needed. For example, these four sources all provided data within approximately 2.5 to 3 nm of the average launch site (Figure 13).

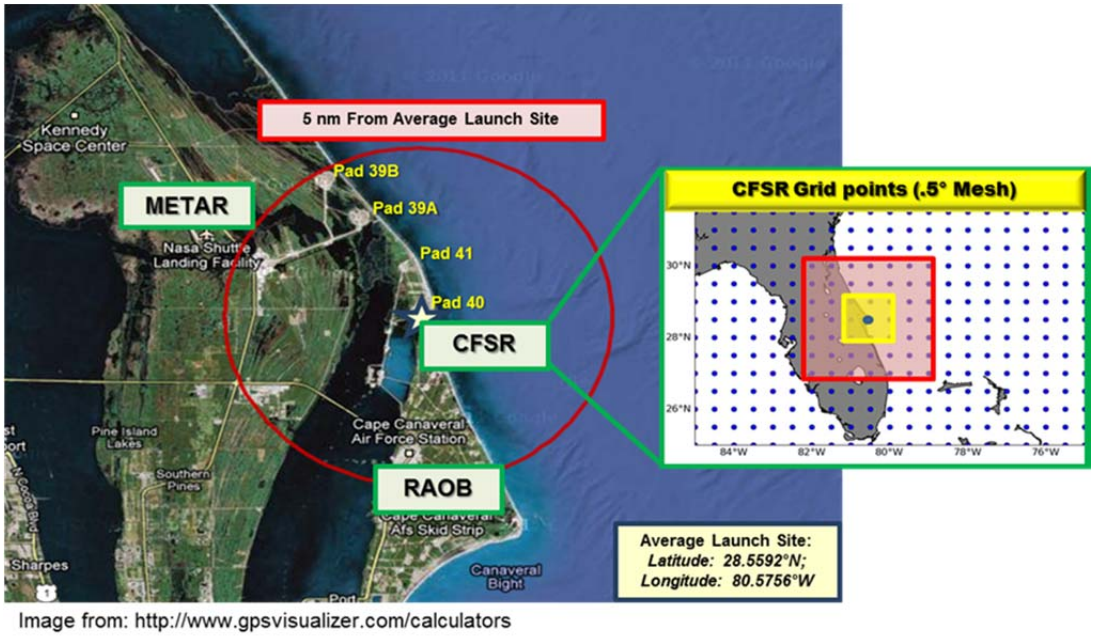

Image from: http://www.gpsvisualizer.com/calculators

Figure 13. Map indicating locations of the CFSR, METAR, and RAOB data sources. Expanded green box represents the details of the grid points for CFSR. Image created from GPS Visualizer [accessed online at http://www.gpsvisualizer.com/calculators, Sept 2011].

Our initial selection of data from the first three sources amounted to hundreds of thousands of lines of data, and required over 2 GB of storage space. To increase the efficiency of our data management and analyses, we determined that condensing the data set inventory would be necessary. In addition, we wanted to condense the data set to help focus our efforts on evaluating the data and determining the confidence we could have in the information provided by each data set. Thus, we developed a reduced data set that is summarized below.

1) CFSR Data

a. Single grid point only: 28.5N ; 80.5W)

b. 00Z and 12Z only

c. 1 Jan 1988–31 Dec 2010

2) METAR

a. 00Z and 12Z only

b. 1 Jan 1988–31 Dec 2010

3) RAOB

a. 00Z and 12Z only

b. 1 Jan 1988–31 Dec 2010

4) Expert Meteorologist Input

a. Monthly averages for 00Z and 12Z only

Note that all the data for this study are from the CFSR, METAR, RAOB, and expert meteorologist data sets, and are for 00Z and 12Z for the period 1 January 1988 through 31 December. Thus, our climatological probabilities of violation and our other results are based on data for these times and dates.

One complication in using these data sets is that there were some temporal inconsistencies between the data sets. For example, CFSR provided data for every variable for 00Z and 12Z for every day during January 1988–2010. However, there were times for which 00Z or 12Z METAR data was not included in the archive. There were also periods in which both a special METAR and standard hourly METAR report made it into the archive and were valid at the same time. As noted previously, RAOB release times from CCAFS varied, which resulted in many of the dates during our study period having no 00Z and/or 12Z observations. To compensate for this, we assumed any RAOB valid from 10Z to 14Z to be representative of 12Z, and counted it as a 12Z observation. Similarly, we assumed any RAOB valid from 22Z to 02Z to be representative of 00Z and counted it as a 00Z observation. Table 2 summarizes the availability of data from the CFSR, METAR, and RAOB data sets.

Total Observations			
	Data Source		
	CFSR	METAR	RAOB
00Z	11680	12076	4370
12Z	11680	12445	9911

Table 2. Total number of times for which data set was available and used in our study from the three data sources shown for 00Z and 12Z of our study period of 1 January 1988–31 Dec 2010.

E. METHODS

1. Overview

We designed our research methods to deliver the following main products:

1. Climatological thick cloud LLCC violation data set
2. Climatological probabilities of violating (POV) thick cloud LLCC data set
3. Data set describing thick cloud POV for a range of thickness thresholds

We generated all three of these products. The second and third products were derived from the first. The third product was the output from our sensitivity analyses.

Our overall approach was to process the data sets described in the prior section to determine the following variables.

1) Determine cloud base height
2) Determine cloud top height
3) Calculate cloud thickness
4) Determine heights of 0°, -15°, and -20° Celsius levels

Once we determined these four variables, we used them to compute the products listed above. Each data set we worked with has its own limitations, and not all of them offered every variable we needed. For example, the METAR data set only gave information about cloud bases. The following sections outline the

how we used each data set individually (CFSR, METAR, RAOB, and Expert Meteorologist), how we used data from one data set to test the data from another data set, and how we combined data from the different data sets to develop a merged data set.

2. CFSR

We investigated CFSR to determine cloud base, top, and thickness information. This included gathering information for both heights and temperatures at the cloud bases and tops. As listed in Table 1, the CFSR data we processed contained cloud base and top information relative to given pressure surfaces. The thick cloud rule is evaluated for a thickness requirement measured in feet. Therefore, we developed a process to convert CFSR cloud bases, tops, and thicknesses from pressure surfaces to feet. To do this, we made use of the hypsometric equation.

$$\boldsymbol{Thickness = Z_2 - Z_1 = \frac{R \cdot T}{g_0} \cdot \ln \frac{P_1}{P_2}}$$

The specific derivations and details of the hypsometric equation can be located in numerous meteorological texts, but we referenced Wallace and Hobbs (1977), and Holton (2004). For the purposes of this study, and based on the format of the CFSR data, we needed to make some assumptions and modifications to the use of the hypsometric equation. Listed below are the details on our use of the hypsometric equation for determining the thickness of a cloud layer.

- $\boldsymbol{Z_2 - Z_1}$ is the thickness of the layer (in meters), where $\boldsymbol{Z_2}$is the highest point in altitude of the layer, and $\boldsymbol{Z_1}$is the lowest point in altitude of the layer.
- $\boldsymbol{R}$ is the gas constant for dry air (287 $\frac{J}{Kg\ K}$)
- $\boldsymbol{T}$ is the average temperature (in Kelvin) of the layer

- is the global average gravitational acceleration at mean sea level (9.80665 ─)
- is the pressure (in hPa) of the layer's lower surface
- is the pressure (in hPa) of the layer's upper surface

Table 3 summarizes the variables, or parameters, we used calculate cloud layer thickness using the hypsometric equation. Note that CFSR provided data for all the variables needed for this calculation, except ***T*** at the cloud base. However, CFSR does contain temperature values at the 700-350 hPa pressure levels in 50 hPa increments. We used this information to make several modifications and assumptions to our application of the hypsometric equation, so that we could calculate cloud layer thicknesses.

		Parameter			
		Geopotential Height (m)	**Pressure (hPa)**	**Temperature (K)**	**Total Cloud Cover (%)**
Vertical	**Level**	700 hPa	Low Cloud Bottom	700 hPa	Entire Atmosphere
		650 hPa	Low Cloud Top	650 hPa	Low Cloud Level
		600 hPa	Middle Cloud Bottom	600 hPa	Middle Cloud Level
		550 hPa	Middle Cloud Top	550 hPa	High Cloud Level
		500 hPa	High Cloud Bottom	500 hPa	
		450 hPa	High Cloud Top	450 hPa	
		400 hPa		400 hPa	
		350 hPa		350 hPa	
		Level of 0° Isotherm		Low Cloud Top	
				Middle Cloud Top	
				High Cloud Top	

Table 3. The CFSR variables we used in our thick cloud LLCC study. The levels listed in each of the four parameter columns indicates the vertical levels for which we obtained and used the CFSR data for that parameter. The yellow highlighting indicates the parameters and the levels for which CFSR data was used to calculate cloud layer thickness using the hypsometric equation.

a. Average Temperature (T) Calculations

To calculate the average temperature, ***T***, we used two temperature levels; cloud base, and cloud top. For purposes of this section only, T_b is the temperature at cloud base, T_t is the temperature at cloud top, and T_p is the

temperature at the indicated pressure surface, where p is the pressure surface in hPa. The average temperature was calculated as:

$$\boldsymbol{T = \frac{T_t + T_b}{2}}$$

As previously noted, anytime the model indicated a cloud, the CFSR output would contain the temperature at cloud top. However, the temperature at cloud base was not a given value. To calculate the temperature at cloud base, we made the assumptions and modifications summarized below. Additionally, some of the calculations below were dictated by the fact that our CFSR data set contained information between 700 and 350 hPa only. The process we used to determine these temperatures is summarized in the equations below and in Figure 14.

1) For clouds with bases and tops below (at an altitude lower than) the 700 hPa level:

$$\boldsymbol{T_b = T_t}$$

2) For clouds with bases below, but tops above (at an altitude higher than) 700 hPa:

$$\boldsymbol{T_b = T_{700}}$$

3) For clouds with bases and tops above 700 hPa, but below 350 hPa:

$$\boldsymbol{T_b = T_{p\ below\ cloud\ bottom} + \frac{(P_{below\ cloud\ bottom} - P_{cloud\ bottom})}{50} \cdot (T_{p\ above\ cloud\ base} - T_{p\ below\ cloud\ base})}$$

4) For clouds with bases and tops above 350 hPa:

$$\boldsymbol{T_b = T_{350}}$$

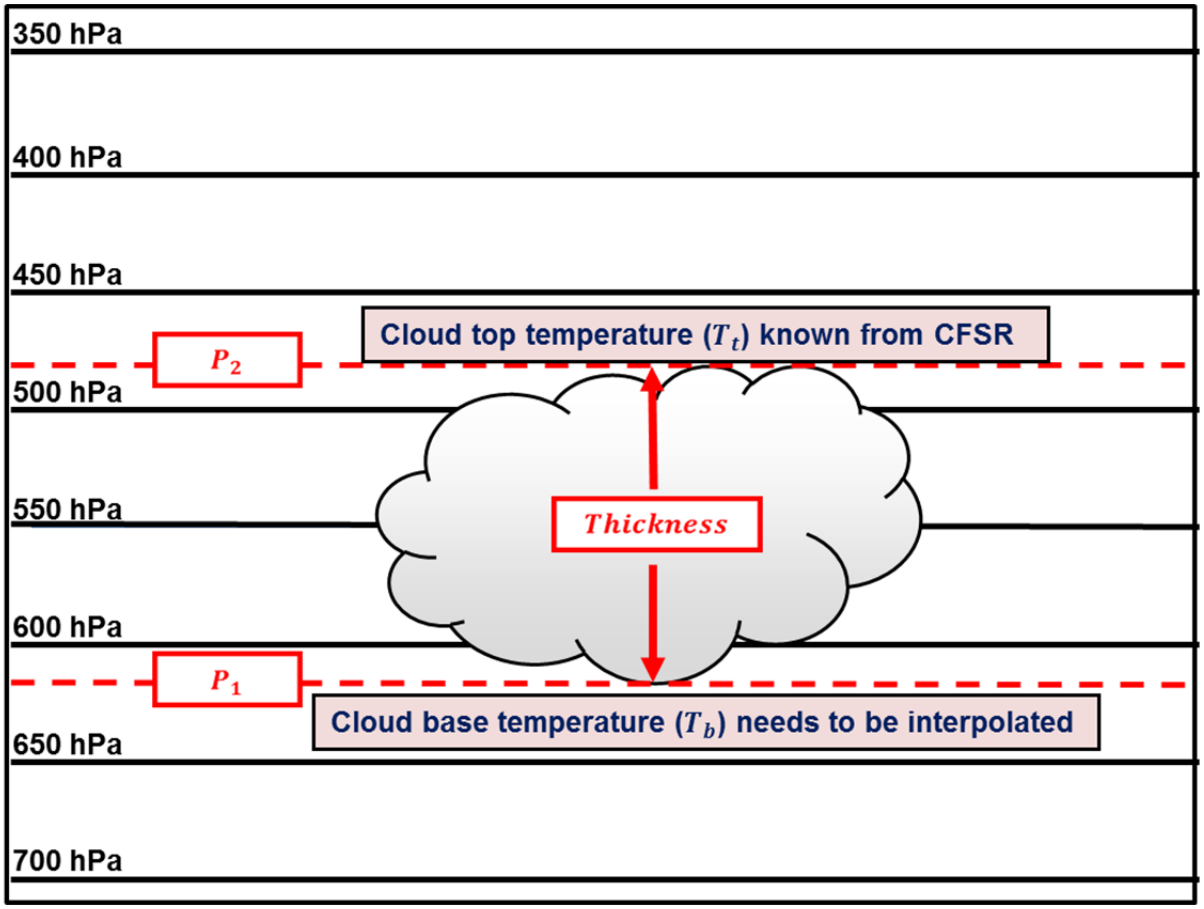

Figure 14. Visual representation of an example of how the P_1, P_2, T_t, and T_b surfaces were evaluated and applied to the hypsometric equation to calculate the cloud thickness.

In the example from Figure 14, the cloud base was located somewhere between the 650 and 600 hPa pressure surfaces. CFSR provided a pressure value in hPa for the cloud base. The estimated cloud base temperature was computed based on using the temperatures at the pressure surfaces above and below the cloud base in the manner described below.

_____)

($P_{cloud\ base}$ is the CFSR given pressure at cloud base)

Recall that the CFSR cloud data is allocated in 50 hPa increments, which is why we chose to divide our pressure surfaces into 50 hPa increments in the equation above.

b. Cloud Thickness Calculations

Once we were able to calculate the average temperature of the cloud layer, we could then apply the full use of the hypsometric equation. The thickness of any given cloud layer in CFSR was computed with the set of variables listed in Table 1, and using the average temperature calculations listed in the previous section of this study. Using the hypsometric equation yielded a thickness measurement in meters, so we also needed to apply a final conversion from meters to feet. We used the standard conversion of 1 meter = 3.2808399 feet. Therefore, our final CFSR cloud thickness equation was calculated as:

$$\boldsymbol{Thickness\ (ft) = Z_2 - Z_1 = \left(\frac{R \cdot T}{g_0} \cdot \ln\frac{P_1}{P_2}\right) \cdot 3.2808399}$$

c. Cloud Base Height and Cloud Top Height Calculations

After calculating cloud thicknesses, we then solved the hypsometric equation for the estimated heights of the cloud tops (Z_2), and cloud bases (Z_1). Recall that the initial CFSR data set included heights of pressure surfaces in 50 hPa increments between 700 and 350 hPa. We used this information to define the cloud base and cloud top heights in meters, and then converted to feet. The CFSR cloud base pressure was located between two of the defined pressure surfaces. For example, if CFSR gave a cloud base pressure of 610 hPa, the cloud base pressure would be located between the 650 and 600 hPa pressure surfaces (Figure 15). Using the hypsometric equation, we calculated the thickness of the layer between the pressure surface below the cloud base and the pressure at the cloud base.

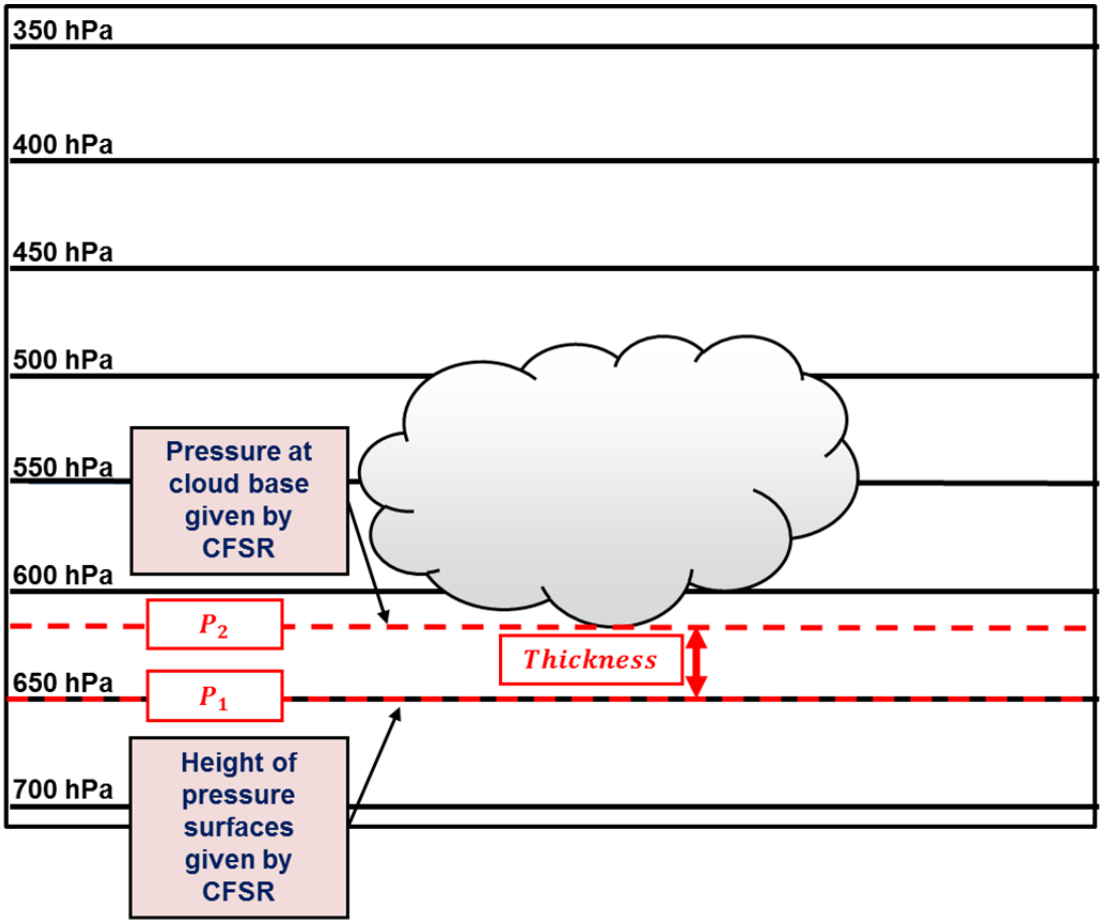

Figure 15. Visual representation of an example of how the P_1, and P_2 surfaces were used in calculating the height of the cloud base. P_2 is the pressure given by CFSR at the base of the cloud, and P_1 is the height of the first CFSR given pressure surface located below the base of the indicated cloud.

Once the thickness of this layer was determined, we applied the known height of the pressure surface located below the cloud base to solve the hypsometric equation for the cloud base.

- Original hypsometric equation: — —
- Re-arranged for the cloud base: — —

This method was applied using a similar definition of the variables similar to that in the previous application of the hypsometric equation, but with the modifications listed below.

- $\boldsymbol{Z_2}$ is the height of the cloud base
- $\boldsymbol{Z_1}$is the height of the closest pressure surface below the cloud base given by CFSR
- $\boldsymbol{P_1}$ is the closest pressure surface below the cloud base
- $\boldsymbol{P_2}$ is the pressure at the cloud base
- $\boldsymbol{T}$ is calculated as $\frac{\boldsymbol{Temperature\ at\ P_2 + Temperature\ at\ P_1}}{\boldsymbol{2}}$

To calculate the cloud top heights, we simply added the cloud thickness to the cloud base height. Since both the cloud base height, and thickness were already converted to feet, no further conversion was necessary.

d. Height of 0° Isotherm

The only temperature level directly output via CFSR was the height of the 0° isotherm, in meters above Earth's surface. The only modification we needed to make was to re-calculate the values to be expressed in feet. Again, we used the standard conversion of 1 meter = 3.2808399 feet. Multiplying every CFSR output of the 0° isotherm height by this value satisfied the requirement.

3. METAR

As previously stated, only the METAR cloud base information was used for this study. For every observation in our data set, we simply extracted the cloud base height and set every other part of the METAR observation aside in a separate file. Cloud base information is reported in a METAR as the amount of sky they are estimated to cover, with the cloud base heights measured in feet. Coverage is estimated in 1/8ths of the sky (oktas), and is based on summing upward from the surface to the highest layer of cloud observed. Therefore, a weather observer, or cloud measuring equipment, detects and reports clouds

from the ground up. This indicates the potential for an overcast layer of lower clouds to obscure a higher layer of clouds from the view of the observer or equipment. WMO standards dictate cloud heights be reported by level. There are three cloud layer groups, or what WMO calls *genera*: low, mid, and high cloud layers (WMO 2008). The average base height of low, mid, and high clouds varies by latitude, but our study region fell within the WMO standards for temperate regions. Tables 4 and 5 summarize the cloud layer height ranges, as well as reporting increments. We assigned this cloud layer definition to all data sets.

Cloud Layer Base Height Ranges (ft)					
Low Cloud		**Mid Cloud**		**High Cloud**	
Surface	6,500	6,500	20,000	20,000	40,000

Table 4. Summary of defined cloud base heights for temperate regions. Data taken from World Meteorological Organization Chapter 15 “Observation of Clouds” (accessed online at http://library.wmo.int)

Increments of Reportable Values of Cloud Base Height	
Range of Height Values (ft)	**Reportable Increment (ft)**
≤ 5,000	To nearest 100
> 5,000 but ≤ 10,000	To nearest 500
> 10,000	To nearset 1,000

Table 5. Summary of reportable cloud base height values. Data taken from Federal Meteorological Handout—1 Chapter 9 “Sky Condition”.

For the purposes of this study, we primarily needed to work with METAR information on cloud base heights and whether clouds were reported or not. For this reason, we separated the cloud coverage amount from the base height, which resulted in a data set containing only METAR cloud base heights for all 00Z and 12Z times.

3. RAOB

a. Cloud Bases and Tops

RAOB data yields information relative to the vertical structure of the atmosphere. There is no definitive way to extract cloud layer information from RAOB data; however, there are empirical rules that are widely accepted for basic applications. The basic principle involves using the RAOB temperatures and dew point depressions to calculate relative humidities. The Air Force Weather Agency (AFWA) document, "Meteorological Techniques"(AFWA/TN-98/002, 2006) contains information to aid operational forecasters with techniques to improve forecasting skills. For this study, we used the cloud layer temperature and dew point depression rules set in "Meteorological Techniques" to identify cloud layers from RAOB data.

Cloud Base Temperature / Dew Point Depression Relationship	
Cloud Base Temperature (°C)	**Dew Point Depression (°C)**
$\geq 0°$	$\leq 2°$
Between 0°and -10°	$\leq 3°$
Between -10° and -20°	$\leq 4°$

Table 6. Summary of RAOB temperature and dew point depression relations and how they were applied in thick cloud LLCC study.

RAOB data was given in 500 ft increments from the surface up to sounding completion, which can vary for every RAOB. However, based on the thick cloud LLCC temperature thresholds, we only used RAOB data from the surface up to the -20° C level. Therefore, we did not calculate RAOB cloud data at temperatures colder than -20°C. Each line of RAOB data contained temperature and dew point values at the specified time. To compute the dew point depression, we simply subtracted the dew point from the temperature. We evaluated RAOB data for clouds by beginning at the lowest level, and worked up in the vertical to sounding completion, or -20° C level, whichever occurred first. As we followed the RAOB in the vertical, the first level in which one of the requirements defined in Table 6 was met was classified as the cloud base.

Continuing in the vertical, we continued to identify a cloud layer until we reached a level at which the requirements defined in Table 6 were no longer met, which we defined as the cloud top.

As soon as a weather balloon is released, it will ascend and drift horizontally, based on the ambient atmospheric conditions. However, for most applications in our study, we assumed the entire sounding was representative of the vertical profile of temperature and dew point information directly over the study region.

b. Height of 0°C, -15°C, and -20°C Levels

The heights of the 0°, -15°, and -20°C levels were derived using the AMU RRA utility tool with the RAOB data set. All the raw temperature values were given in degrees Celsius, and heights were given in feet, therefore no further conversions were necessary.

4. Expert Meteorologist Input

We collected expert meteorologist information only on cloud top heights. Using their decades of experience, each expert provided their best approximation of the monthly average cloud top heights by layer (low, mid, and high). Once the experts submitted their inputs, we weighted each input equally and averaged them to determine an overall expert estimate of the cloud top heights. The formula for computing the expert meteorologist estimate is shown below. The results from applying this formula to the expert inputs are shown in Table 7.

$$\textbf{Monthly Average} = \frac{Expert\ 1 + Expert\ 2 + Expert\ 3 + Expert\ 4 + Expert\ 5}{5}$$

Monthly Average Cloud Top Heights Based on Expert Inputs			
Month	Mean Cloud Top Height (ft)		
	Low	Mid	High
Jan	5000	13000	27500
Feb	5000	13000	27500
Mar	7000	13500	28250
April	8500	16000	29250
May	11000	16500	31000
Jun	12750	18000	32000
Jul	13000	18000	32000
Aug	12750	18000	31500
Sep	10500	17500	29750
Oct	8500	16000	28500
Nov	7000	13000	28250
Dec	5250	13000	27500
Totals	8854	15458	29417

Table 7. Monthly average cloud top heights (in feet) for the three cloud layers, low, mid, and high. Values based on averaging the inputs from five expert meteorologists.

5. Data Quality Control

Since our process involves the application of multiple data sets, developing a quality control method was critically important. We divided our quality control efforts into four categories:

1. Cloud detection
2. Cloud bases
3. Cloud tops
4. Temperatures

For each of these categories and for each data set, we compared from one data to that from the others and to other meteorological information. Our objective was to identify the similarities and differences between each data set,

and to assess the accuracy of each data set. Ultimately, we wanted to determine the confidence to place in specific parts of each data set, and thereby determine if and how to apply those parts in the calculation of thick cloud LLCC climatologies. The following sections describe the processes and methods we developed and applied to the data sets in our quality control procedures. Unless otherwise noted, all data set comparisons were performed for 00Z and 12Z of January 1988 – Dec 2010. The specific results of these data set comparisons will be discussed in Chapter III.

a. Cloud Detection

We examined and compared the detection of clouds by the CFSR, METAR, and RAOB data sets. We defined cloud detection as the identification of any amount of cloud at any layer, time, or date. If no clouds were reported, then clear skies were identified. We calculated and compared the percentage of times that clouds and clear skies were detected by CFSR, METAR, and RAOB. We used percentages rather than total numbers because the number of times within the study period that data was available was different for each data set (see Table 2). For these comparisons, we assumed the METAR observations were a close representation of the real state of cloudy or clear sky conditions over the study region, and therefore used those observations as our ground truth. We compared both cloud and clear sky conditions. For each data set (CFSR, METAR, and RAOB), we applied the formula below (or a similar one for cloudy conditions. We applied this formula separately for 00Z data and 12Z data.

- $$\frac{\textit{Total number of times with clear skies reported}}{\textit{Total number of observations}} \cdot \mathbf{100}$$

In this formula, the number of number of times is the number of 00Z or 12Z occasions during the study period (Table 2).

b. Cloud Base Heights

Cloud base height comparisons were conducted using monthly averages for the entire data base. We compared CFSR, METAR, and RAOB

derived cloud base heights, separated by layer (low, mid, and high). For this study, we defined cloud layers using the information in Table 4. As with cloud detection, we assumed METAR observations to be a close representation of the actual cloud bases, and used them as our ground truth. Based on our procedures for identifying cloud bases in each data set (see prior sections), we calculated the cloud bases for each day in our data base, and then calculated the averages for each month. These monthly averages are what we used to make our final comparisons of the data sets.

c. Cloud Top Heights

Cloud top height comparisons were conducted using the same method as for the cloud bases, but with the one exception. METAR observations do not contain information on cloud top heights, so we used expert meteorologist Input as our ground truth for cloud top heights. The cloud top comparisons were conducted in the same way as for the cloud base comparisons.

d. Temperatures

Only two of our data sets included vertical profile temperature information, CFSR and RAOB. The only common variable between them was the height of the 0° Celsius isotherm. Similar to cloud detection, and cloud base comparisons, we wanted to identify a data set we could assume to be a close representation of the real state of the vertical temperature profile. For this, we assumed the data interpreted from the RAOBs would be an accurate measurement of the true heights of temperature levels over our study region. Thus, the RAOB data served as our ground truth for temperatures. Our objective in this comparison was to determine how much confidence to have in the CFSR and RAOB temperatures, so we could determine how to apply them in developing climatologies for the thick cloud LLCC.

6. Hybrid Process

Upon completion of the data set comparisons, we were able to compile a list of the strengths and weaknesses of each data set. Based on these results we produced a merged data set based on blending different parts of each of the four data sets. CFSR data composed the bulk of this merged data set, so we referred to the merged data set as the modified CFSR data set.

The CFSR was very complete spatially and temporally. But, as we discovered, CFSR values for some variables were not as accurate as the values from the other data sets (METAR, RAOB, expert meteorologist inputs). On the other hand, the METAR, RAOB, and expert meteorologist input information was spatially and/or temporally incomplete. Therefore, to create our merged data set, we used CFSR as the underlying foundation, and used data from the other data sets for the variables for which those other data sets appeared to provide more accurate information.

We began our development of the modified CFSR data set with the cloud base heights and cloud top heights. Due to the differences in the total observations contained in each data set, our comparisons of cloud base heights and cloud top heights were based on monthly average heights. We calculated the monthly averages of cloud base heights and cloud top heights for the entire study period. We separated the averages by time (00Z and 12Z), and by layer (low, mid, and high clouds). For this study, we assumed METAR cloud base heights to be the best representation of the real state of cloud base heights, and the expert meteorologist input to represent the real state of cloud top heights. Based on these assumptions, we applied the monthly average METAR cloud base heights to adjust the CFSR cloud bases, and the expert meteorologist input cloud top heights to adjust the CFSR cloud top heights.

These adjustments were made via corrections terms that we calculated by subtracting the monthly mean CFSR heights from the monthly mean heights from the alternative data set. Thus, for cloud base heights, we subtracted the monthly

mean CFSR cloud base height from the monthly mean METAR cloud base height; and for the cloud top heights, we subtracted the monthly mean CFSR cloud top height from the monthly mean expert meteorologist input cloud top heights. We derived these correction terms by layer, by time (00Z and 12Z), and by month for cloud bases and cloud tops. This gave us four correction term sets for each of the three layers and for each month. Examples of the 00Z sets of correction terms are given in Tables 8 and 9.

Cloud Base Height Correction Terms

Jan 1988 -Dec 2010		Correction Terms (ft)		
	Month	Low	Mid	High
00Z	*Jan*	-1933	-8226	-12851
	Feb	-2082	-7563	-12886
	Mar	-2248	-8280	-13493
	April	-2738	-8422	-14863
	May	-3663	-7591	-15888
	Jun	-4878	-6865	-19058
	Jul	-5177	-7432	-19540
	Aug	-4900	-7456	-20123
	Sep	-4467	-8376	-20273
	Oct	-3095	-8249	-18303
	Nov	-2243	-8618	-15708
	Dec	-1812	-8114	-14447
	Average	-3270	-7933	-16453

Table 8. Cloud base correction terms for 00Z calculated as monthly averages in feet for each cloud layer (low, mid, high). Terms calculated based on the difference: METAR cloud base height – CFSR Cloud base height.

Cloud Top Height Correction Terms				
Jan 1988 -Dec 2010		Correction Terms (ft)		
	Month	Low	Mid	High
00Z	*Jan*	-2656	-10619	-18927
	Feb	-2959	-9956	-18012
	Mar	-1368	-10404	-18534
	April	-356	-8179	-18918
	May	1086	-6803	-18194
	Jun	1619	-5649	-22191
	Jul	1930	-5851	-22034
	Aug	2021	-5926	-23402
	Sep	246	-7189	-26290
	Oct	-333	-8281	-24363
	Nov	-938	-10271	-21397
	Dec	-2288	-10149	-19928
	Average	-333	-8273	-21016

Table 9. Cloud top correction terms for 00Z calculated as monthly averages in feet for each cloud layer (low, mid, high). Terms calculated based on the difference: Expert meteorologist input cloud top height – CFSR Cloud top height.

This correction terms were then applied to the original CFSR data set according to the month being computed. For example, to calculate the low cloud base height for 00Z for an individual January day, we subtracted a value of 1,933 feet (see Table 8) from the original CFSR cloud base height. For February we did the same except that we subtracted a value of 2,082 feet. We continued this process for each day in the data base for 00Z and 12Z, as well as for each layer. Once these correction terms were applied, we were left with a modified set of CFSR cloud base heights and top heights that were adjusted toward the METAR cloud base heights, and the expert meteorologist input cloud top heights.

Our comparisons of the RAOB and CFSR temperature profiles for the study period and region showed that the two data sets provided very similar information. Thus, there was no need to correct the CFSR temperature height level data. However, since the CFSR data set only contained the heights of the

0° C level, we used the RAOB data to determine the heights of the -15° and -20° C level and to supplement the CFSR data.

Figure 16 outlines the methods we used to determine the cloud base height, cloud top height, and temperature height level data that we included in our modified CFSR data set.

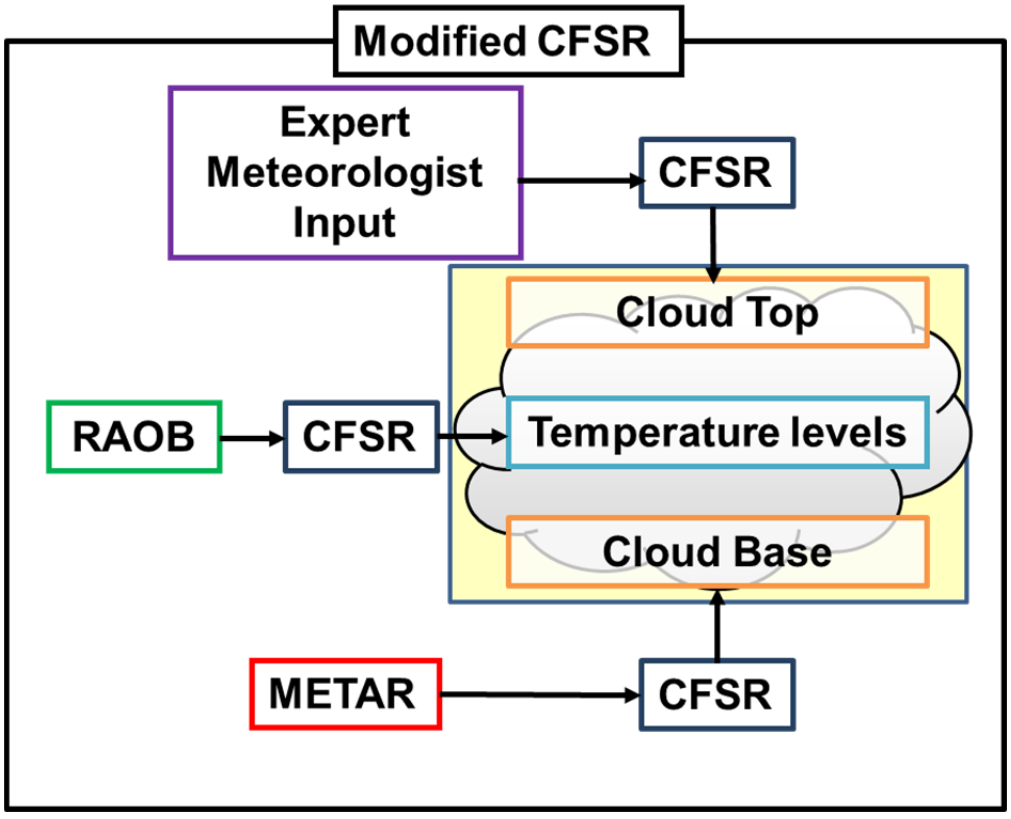

Figure 16. Schematic of the processes used to develop the cloud base height, cloud top height, and cloud temperature height level data included in the modified CFSR data set. Data flows into CFSR represent the use of non-CFSR data to evaluate CFSR and to adjust and/or supplement CFSR data. METAR data were used to modify CFSR cloud base heights. Expert meteorological input was used to modify CFSR cloud top heights. RAOB data were used to confirm and supplement CFSR temperature height levels.

7. Climatology and Probability

a. Initial Climatology and Probability

Once the correction terms were applied, and we constructed the modified CFSR data set. We then used that data set to calculate cloud base height, cloud top height, cloud thickness (using the hypsometric equation as described above), and the heights of the 0°, -15°, and -20°C levels for each cloud layer and for 00Z and 12Z of each date in the entire study period.

The thick cloud LLCC is complex due to the varying temperature constraints applied to the general violation of 4,500 ft thickness. In determining our final climatological probabilities, we used a series of logical tests for each time, date, and cloud layers. We determined a violation of the thick cloud LLCC had occurred if one of the conditions below was met.

1. Low cloud thickness was greater than or equal to 4,500 ft, and low cloud top height was higher than or at the height of the 0°C level

- Mid cloud thickness was greater than or equal to 4,500 ft, and the mid cloud top was located between or at the heights of the 0° and -20° levels

2. Mid cloud thickness was greater than or equal to 4,500 ft, and the mid cloud base height was higher than or at the height of the 0°C level, but lower than or at the height of the -20°C level

3. High cloud thickness was greater than or equal to 4,500 ft and the high cloud base height was located between or at the heights of the 0° and -20°C levels

If none of these conditions was met, then we determined that a violation of the thick cloud rule had not occurred for that time, date, and cloud layer. Additionally, once these logical tests were applied, we needed to account for the exceptions to the thick cloud LLCC. To accomplish this we applied

another series of logical tests to any indicated violation. We discounted a violation if any of the conditions below were satisfied.

1. Mid cloud thickness was greater than or equal to 4,500ft, and the cloud base height was higher than the height of the -20°C level
2. High cloud thickness was greater than or equal to 4,500ft, and the high cloud base height was higher than the height of the -15°C level
3. High cloud thickness was greater than or equal to 4,500ft, and the high cloud base height was higher than the height of the -20°C level

To calculate our final climatological probability of violation for each day at 00 and 12Z, we counted any violation at any layer as a violation for that date and time. We applied a final logical test to each observation time, and counted a violation for the date if any combination of the three layers indicated a violation. Once completed, our data set revealed a tally of violations by date and time for the entire study period. Our total data set accounted for twenty-three years of data, which implies twenty-three possibilities for each day of the year to violate the thick cloud LLCC for each time (00Z and 12Z). Our final calculation of the probability of violation (POV) of the thick cloud rule for any day of the year at either 00Z or 12Z is shown in the equation below. The process we used to generate the thick cloud LLCC climatologies and POVs is summarized in Figure 17.

$$\textbf{POV} = \frac{\boldsymbol{Total\ number\ of\ violations}}{\mathbf{23}} \cdot \mathbf{100}$$

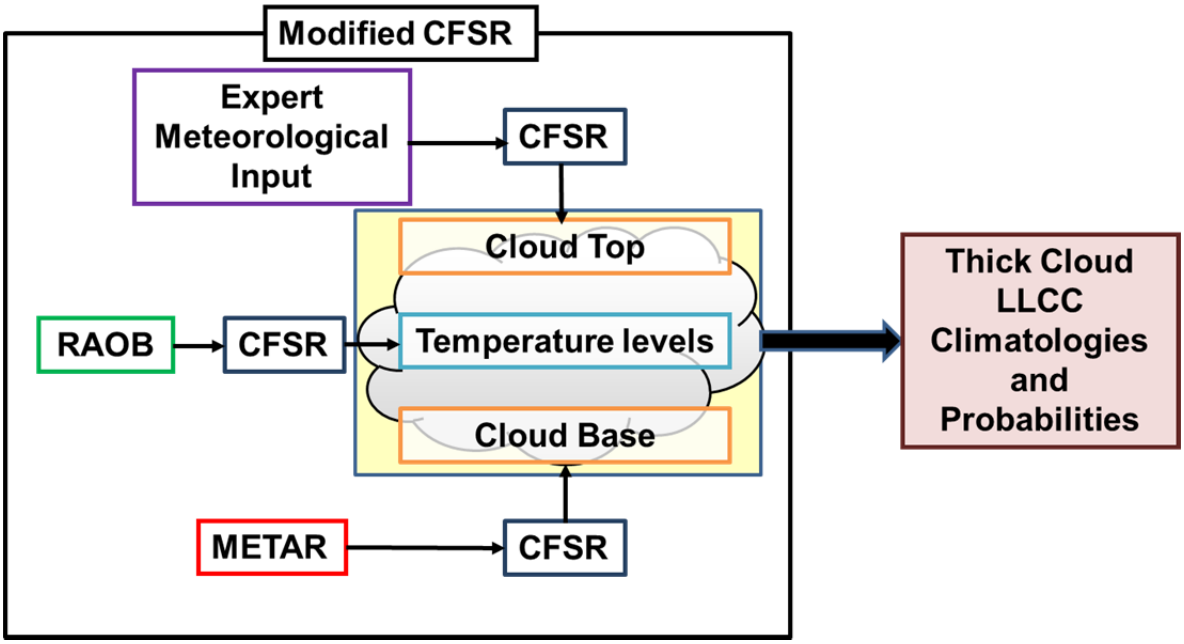

Figure 17. Schematic of the processes we used to: (1) develop the cloud base height, cloud top height, and cloud temperature height level data included in the modified CFSR data set; and (2) use that data set to calculate the thick cloud LLCC climatologies and probabilities of violations. See the Figure 16 caption for additional information.

b. Final POVs

We wanted to make the products from our research as operationally relevant and useful as possible, so we needed to fine-tune the final results. We determined that we could make our climatology products more useful by temporally smoothing them to reduce large day-to-day variations which appeared in our raw climatologies based on our 23 year long data set. This is the same approach Muller (2010) used in his work with natural lightning LLCC climatologies. Once the initial POVs were calculated, we applied a centered running mean smoother to them. We used five, seven, nine, eleven, thirteen, and fifteen day running means for each day of the year for both 00Z and 12Z. We then compared the smoothed results and settled on the fifteen day running mean results as the most operationally useful.

c. Sensitivity Analysis

We conducted a sensitivity analysis to assess the impacts of using different thickness thresholds, but with the same temperature constraints. To do so, we repeated the process for determining the POVs from the CFSR data set, but for a range of cloud thickness thresholds --- in particular, cloud thickness thresholds of 3,500, 4,000, 5,000, 5,500, 6,000, 6,500, 7,000, and 7,500 ft.

d. Case Studies

We conducted a small set of case studies of known thick cloud LLCC violations from 2005–2010. Our purpose was to do a sample validation of our POVs against known violations. As described in Chapter II, Section B.1, the LWOs identify thick cloud violations using several sources of meteorological input, including weather reconnaissance aircraft. Much of this information is contained only in written form in the LWOs mission folders, which are kept by each individual LWO for each launch mission. A known violation is defined as occurring if at any time during a launch countdown the launch weather team determined the thick cloud LLCC was violated.

Year	Month	Day
2002	May	30
2005	July	2
2006	January	18
2006	November	16
2007	June	8
2008	March	15
2009	December	4
2010	June	4

Table 10. Dates of known thick cloud LLCC violations. We used the dates of these violations to determine whether our calculated thick cloud LLC climatology data set also showed thick cloud violation on those dates.

We selected eight different missions during 2005–2010 for which LWO logs indicated the thick cloud rule had been violated (Table 10). For our study, we were only concerned with determining if the thick cloud LLCC was violated, and not with how long the violation lasted. We then determined whether our calculated thick cloud LLCC climatology data set showed violations at the same times and dates as the eight known violations. If our data set showed a violation at either 00Z or 12Z of a known violation date, then we determined our data set had correctly identified the known violation for that date.

III. RESULTS

A. DATA SET COMPARISONS

1. Overview

We evaluated the different data sets, and compared them to each other, to determine which components of each data set to include in our modified CFSR data set. As noted in Chapter II, we conducted our data set comparisons analyses, and our climatology data set development, for 00Z, and 12Z. The results from these two times were very similar to each other. The 00Z results are shown in Chapter III and the 12Z results are shown in Appendices A and C.

2. Cloud Detection

Using the methods described in Chapter II, Section E.5.a, we compared the cloud detections from CFSR, RAOB, and METAR. Figures 18-21 show the percentage of 00Z times during the study period when clouds and clear skies were detected by the CFSR, METAR, and RAOB data sets. The CFSR and METAR data sets both reported clouds 92% of the time, but the RAOB data set reported clouds only 28% of the time. As previously stated, since METAR surface weather data are based on a combination of instrument measurements and human observations, we determined that METAR observations were the most representative of the true state of cloudy and clear sky conditions over CCAFS and KSC. Thus, Figures 18-20 provide evidence that the CFSR data set did well at identifying cloudy conditions and clear skies, while the RAOB data set did not, with 64% fewer cloud detections than the other two data sets.

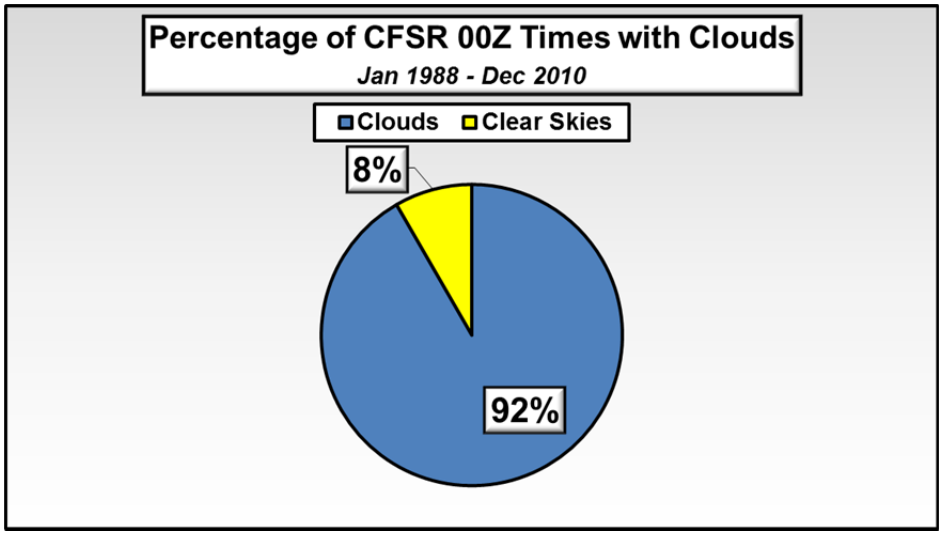

Figure 18. Percentage of all 00Z times in the study period for which CFSR indicated clouds (blue) and clear skies (yellow).

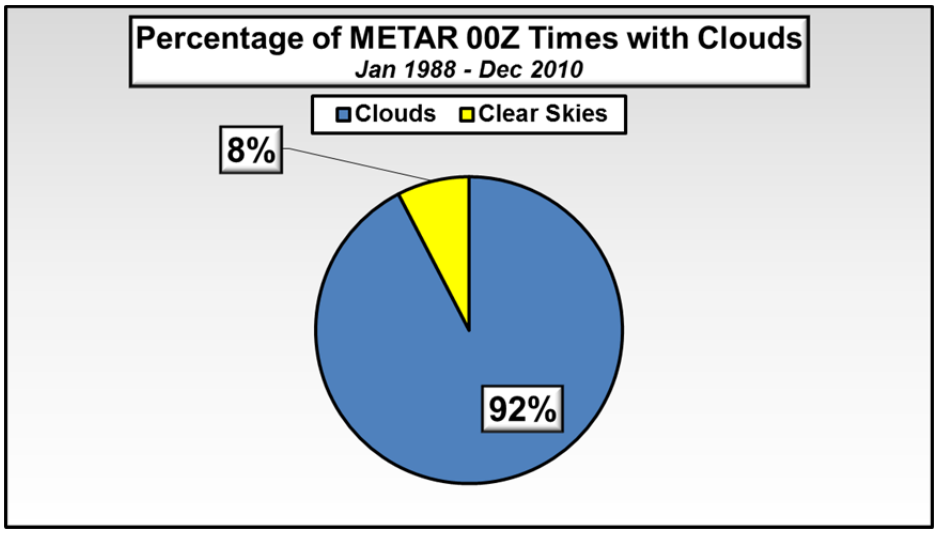

Figure 19. Percentage of all 00Z times in the study period for which METAR data indicated clouds (blue) and clear skies (yellow).

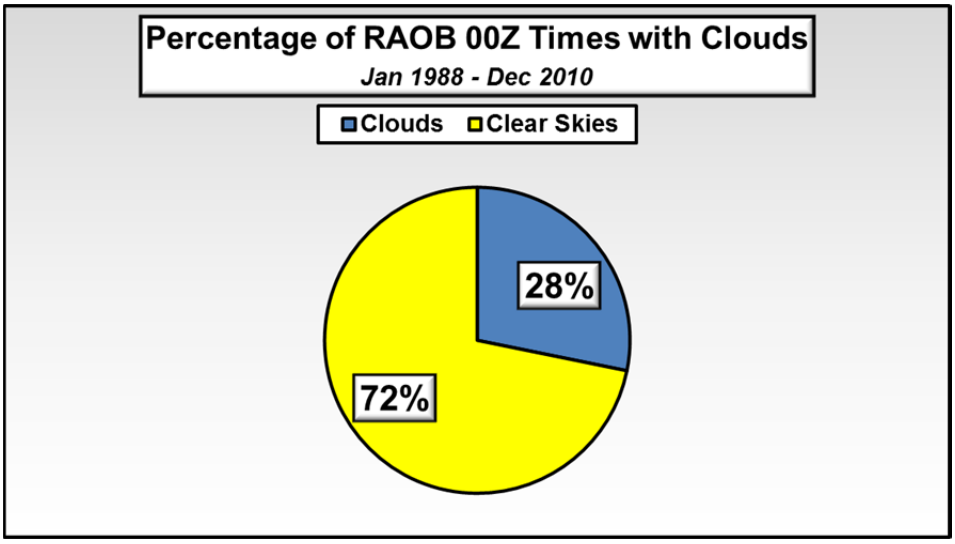

Figure 20. Percentage of all 00Z times in the study period for which RAOB data indicated clouds (blue) and clear skies (yellow).

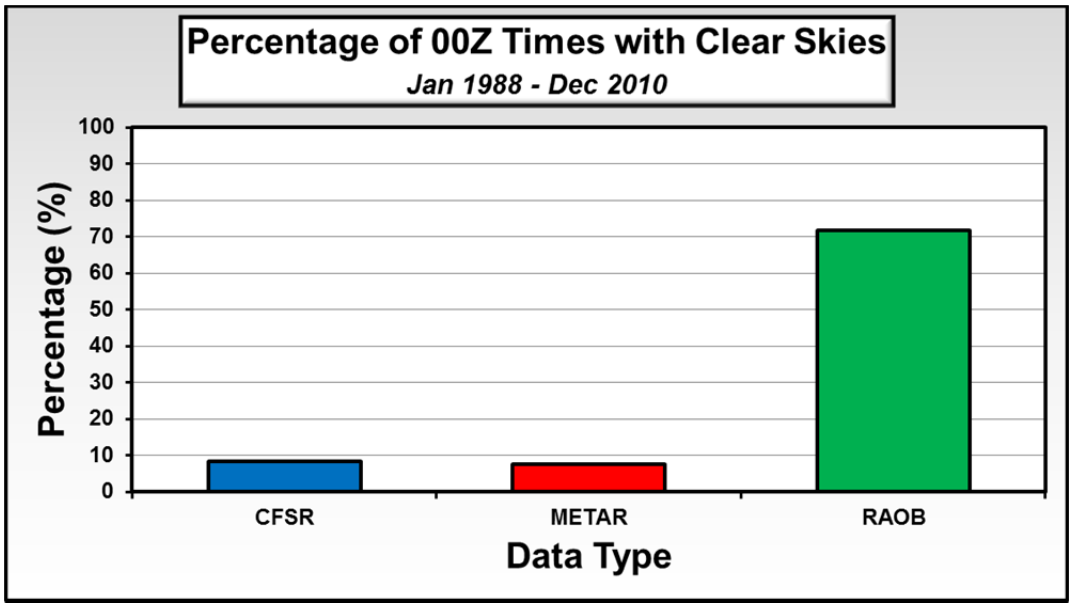

Figure 21. Percentage of all 00Z times in the study period for which the CFSR, METAR, and RAOB data sets indicated clear skies.

There are several possible reasons for the RAOB results. Recall from Chapter II, Section D.5, that the total number of times for which data was available were different for each data set, with the RAOB data set having a much lower number than the CFSR and METAR data sets. Additionally, we inferred

cloud occurrence from the RAOB data based on empirical rules using dew point depression and temperature relationships. This method could have led to missing days and times when clouds actually were present, but the RAOB data did not show those relationships. Additionally, days when the only clouds observed were in the mid and high cloud layers might have been missed by the RAOB due to wind drift of the RAOB away from the CCAFS and KSC location. This RAOB drift means the sensor could be tens of miles downstream of the study region by the time it reaches the heights of the mid and high cloud layers. This could lead to a RAOB sounding not detecting mid and high clouds over CCAFS or KSC, either missing them altogether, or observing clouds over an entirely different region.

Once the initial cloud detection comparisons were complete, we decided to look deeper into the relationship between CFSR and METAR to ensure they displayed similar characteristics. We conducted a comparison of cloud detection for all years in the study period for January and July only. We calculated the percentages of cloud detection for all January detections in the study period, and repeated the process for July. We selected January and July because are they are the climatological extreme months, with cloudy days being close to a minimum for the year in January and a maximum for the year in July, according to the 45 WS Forecast Reference Notebook (FRN). Both CFSR and METAR demonstrated what we expected in the January and July comparisons, with cloudy and clear sky percentages that were very similar to each other (Figure 22).

Overall, our cloud detection results provide evidence that CFSR data did well at distinguishing cloudy days from clear sky days, while the RAOB data did not perform as well, assuming that the METAR data is representative of the true cloud conditions over the study region.

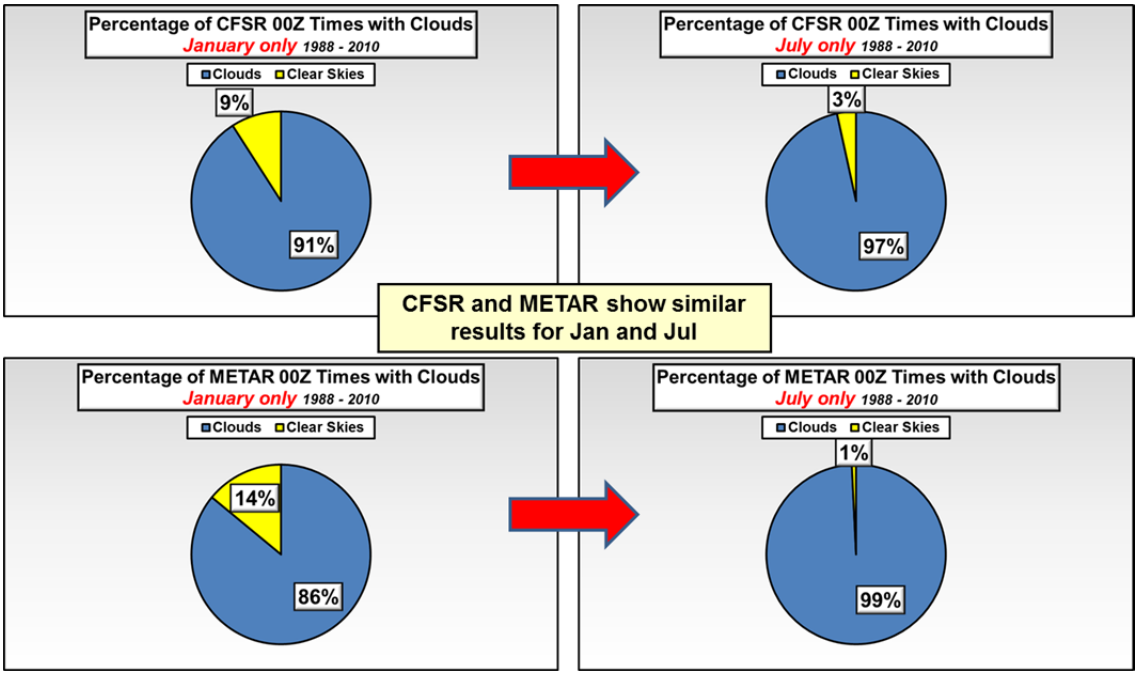

Figure 22. Percentage of all 00Z times in the study period for which the CFSR data set (top panels) and the METAR data set (bottom panels) indicated clouds (blue) and clear skies (yellow) for January (left panels) and July (right panels).

3. Cloud Base Heights

As with cloud detection, we treated the METAR data as our best indicator of the true cloud base heights over our study region. We used the processes outlined in Chapter II, Section 6.b, and the WMO cloud layer definitions (Table 4) to compare the cloud base heights from the three data sets (CFSR, METAR, and RAOB). Our objective was to determine which set to apply in developing our thick cloud climatology data set.

Figure 23 shows that the METAR and RAOB low cloud base heights were in generally good agreement, while the CFSR low cloud bases were significantly higher. The differences between CFSR and the other data sets ranged from approximately 2,000–3,000 feet in the winter, to 4,000–5,000 feet in the summer. Additionally, CFSR indicated a significant seasonal variation in cloud base heights, with an increase of nearly 3,000 feet in the low cloud base heights from

January to July. In contrast, the METAR data indicated a decrease of low cloud base heights of approximately 500 feet from winter to summer.

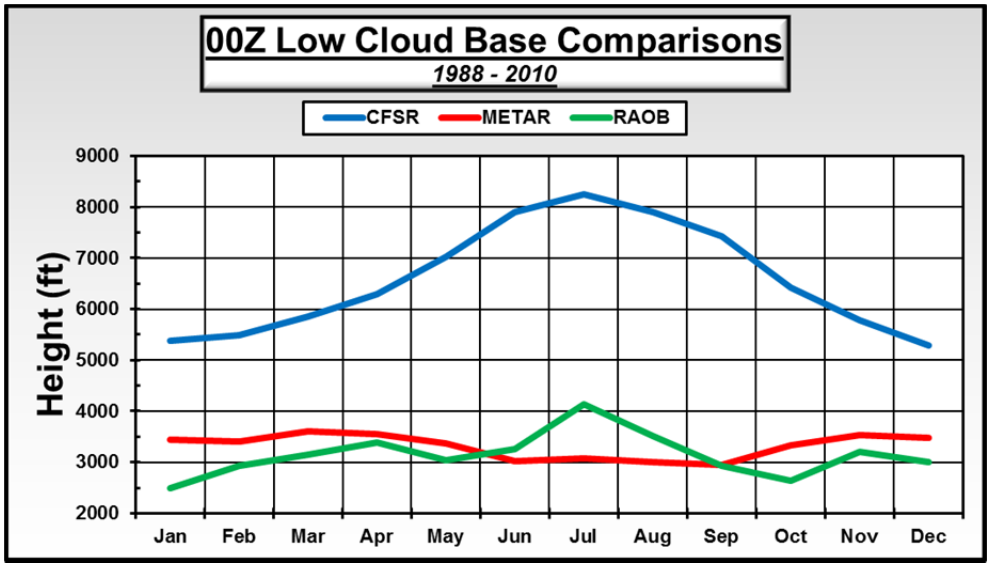

Figure 23. Monthly average low cloud base heights for each data set from 1988–2010.

The CFSR mid cloud base heights were between 7,000 and 9,000 feet higher than those from the METAR data (Figure 24). The RAOB mid cloud base heights were also higher than those from the METAR data by about 2,000 to 3,000 feet. For all three data sets, the seasonal variation in mid cloud base heights was small

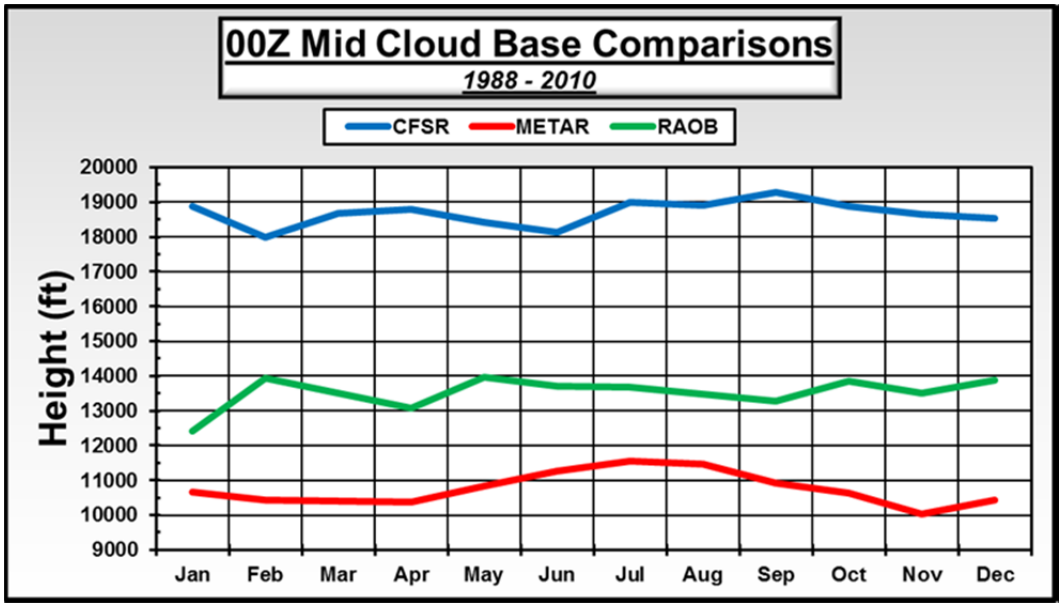

Figure 24. Monthly average mid cloud base heights for each data set from 1988–2010.

CFSR high cloud base heights were 13,000 to 20,000 feet higher than those from the METAR data, and those from the RAOB data were about 4,000 to 5,000 feet lower than those from the METAR data (Figure 25). Note in Figure 25 the lack of RAOB high cloud base heights for January through March. This is because our RAOB data set only contained information up to the height of the -20° C level. This limitation in our RAOB data set arose from our RAOB data request being based on the thick cloud LLCC -20° C temperature threshold. In January-March, the high cloud base heights tended to occur at temperatures colder than -20° C, so we did not capture these clouds in our RAOB data set. To correct for this limitation in our RAOB data, we used linear interpolation to estimate the January-March values. We selected this method was based in large part on the relatively constant RAOB high cloud base heights in April-December (Figure 25). The interpolation yielded an average value for January-March of 20,500 feet, very similar to the mean for the rest of the year of 21,000 feet.

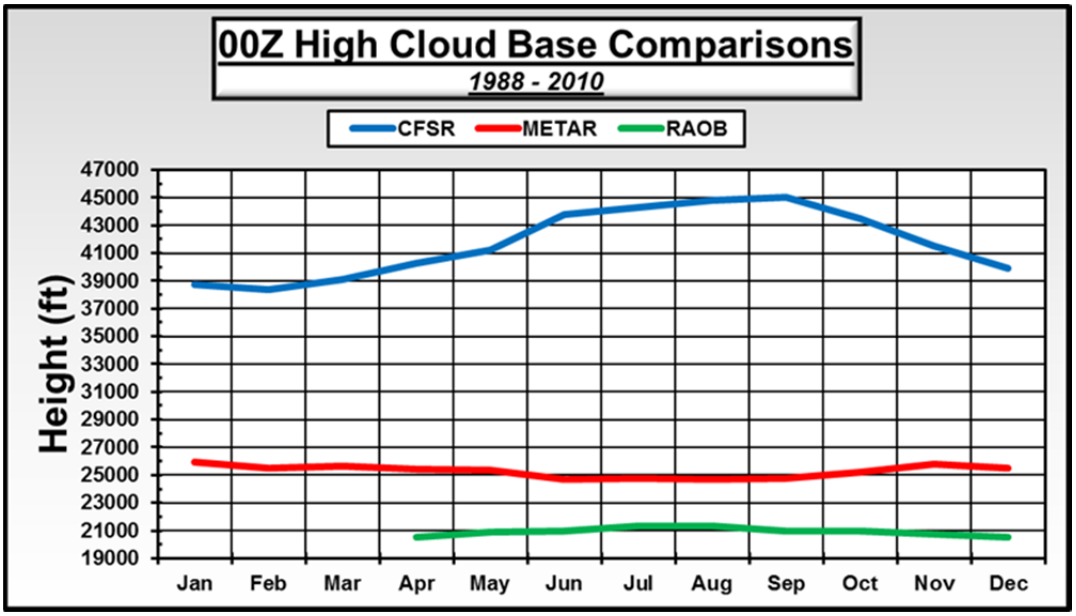

Figure 25. Monthly average high cloud base heights for each data set from 1988–2010.

To assess interannual variability in the cloud base heights, we conducted a comparison of the cloud base heights from each data set for January and July for all years in the study period. We did this in part to determine if the high CFSR cloud base heights were due to some extreme outlier years. None of the three data sets indicated any significant year-to-year variations in any layer for either January or July (results not shown).

We also analyzed variability in the METAR cloud base heights by calculating the upper and lower tercile limits of the monthly cloud base heights for based on data from all years. The results indicated very small magnitudes of difference between the upper and lower terciles for each layer (Table 11). Low cloud base heights only had a difference of 900–1700 ft between lower and upper terciles, mid clouds had a difference of 3,000–4000 ft, and high clouds had a difference of only 1,000 to 2,000 ft. This indicates relatively low variability in the METAR cloud base heights.

Jan 1988 -Dec 2010			Lower Tercile			Upper Tercile		
	Month	Total Obs	Low	Mid	High	Low	Mid	High
00 Z	*Jan*	29768	2100	9000	25000	3800	12000	27000
	Feb	27565	2200	9000	25000	3900	11000	26000
	Mar	28622	2500	9000	25000	4000	11000	26000
	April	27277	2600	9000	25000	4000	12000	26000
	May	28371	2500	9000	25000	3500	12000	26000
	Jun	28524	2200	10000	24000	3100	13000	25000
	Jul	29115	2300	10000	24000	3100	13000	25000
	Aug	28830	2200	10000	24000	3100	13000	25000
	Sep	27498	2200	10000	24000	3100	12000	25000
	Oct	28542	2500	9000	25000	3700	12000	26000
	Nov	27873	2500	8000	25000	4000	11000	27000
	Dec	29098	2300	8000	25000	4000	12000	26000
Totals & Averages		341083	2342	9167	24667	3608	12000	25833

Table 11. Monthly average lower and upper tercile values for METAR cloud base heights in feet for the three cloud layers (low, mid, high). We used these values to identify the typical range (middle third) of cloud base heights for each cloud layer.

Overall, the cloud base height comparisons revealed the CFSR cloud base heights were much higher than the METAR and RAOB cloud base heights. Additionally, applying experienced meteorological reasoning, much of the CFSR cloud bases appeared unrealistically high. For example, the average height of CFSR high cloud bases over our study region was 41,717 feet, corresponding to an average high cloud base height temperature of -57°C (using temperature climatology from RAOB data). The likelihood of cloud formation greatly diminishes at temperatures colder than –40°C (Rogers and Yau 1989). Also, the degree of separation between CFSR values and METAR values increased upward, from the smallest differences for the low cloud layer to the largest differences for the high cloud layer. Based on these results, we chose to use the METAR data to determine cloud base heights in the development of our thick cloud LLCC climatologies.

4. Cloud Top Heights

As defined in Chapter II, Section 6c, we conducted cloud top height comparisons using the same process as for cloud bases, except that we did not use METAR data and we did use expert meteorologist input. The expert meteorologist input is based on numerous years of monitoring varying weather conditions near CCAFS and KSC, using first-hand weather aircraft reports, radar, and satellite observations. So we regarded the expert cloud top heights for all three cloud layers as the most realistic.

We compared the cloud top height information from each data source (CFSR, Expert, RAOB) for each cloud layer. Figure 26 shows that the low cloud top heights were lower in winter and higher in summer for each data source. This is consistent with the expected thinning and thickening of the troposphere during winter and summer. This seasonal variation was largest (smallest) at about 8,000 (2,500) feet in the expert (RAOB) low cloud top heights.

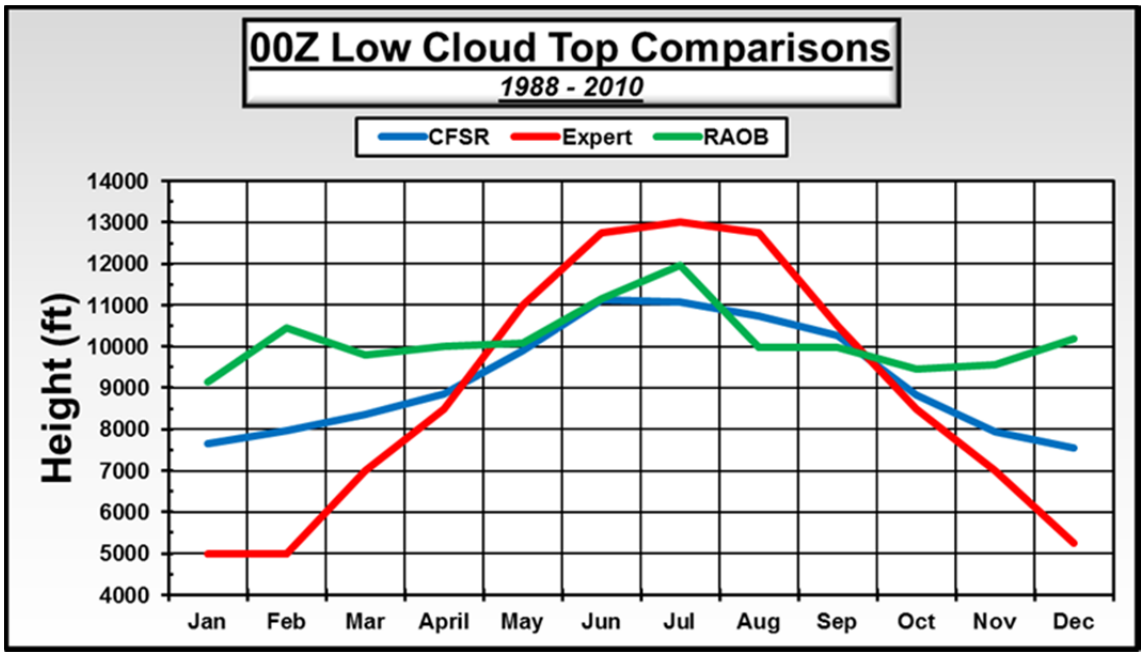

Figure 26. Monthly average low cloud top heights for each data set from 1988–2010.

The CFSR low cloud top heights showed a seasonal cycle that was in phase with the corresponding expert heights but with about half the amplitude of the expert seasonal cycle. One reason for this smaller seasonal variation may be that the CFSR low cloud base heights were too high (Figure 23). Recall that our cloud base height comparison showed that CFSR cloud bases for all cloud layers were significantly higher than those indicated by METAR data (Figures 23-25). Thus, CFSR would be expected to also give cloud top heights that are unrealistically high (cloud tops cannot be lower than cloud bases). Note that for January-March, the CFSR low cloud top heights were 1,000 – 3,000 feet higher than the corresponding expert values. For these months, the CFSR low cloud base heights were 2000 - 2500 feet too high (Figure 23). This suggests that this may be an example of the CFSR low cloud top heights being unrealistically high because the CFSR low cloud top heights were also too high.

Both the mid and high cloud top height comparisons yielded similar results (Figures 27-28). For both mid and high clouds, the expert meteorologist heights were significantly lower than the CFSR heights. This is most likely a result of the CFSR cloud bases also being too high, as previously discussed. The expert mid cloud top heights showed a pronounced seasonal cycle that was absent in the CFSR and RAOB heights. The expert high cloud top heights showed a pronounced seasonal cycle that was also present in the CFSR heights but with a lag of about two months. The RAOB mid (high) cloud top heights were much higher (moderately lower) than the expert. These differences may have been due to our method for identifying cloud layers based in RAOB data. As previously stated, we only calculated clouds form RAOB data up to a temperature of -20° C, therefore we may have effectively capped off high clouds at a lower level than what was actually observed. Additionally, as with cloud detection, the wind drift of a RAOB may result in the RAOB data describing mid and high clouds that are not over the CCAFS and KSC region.

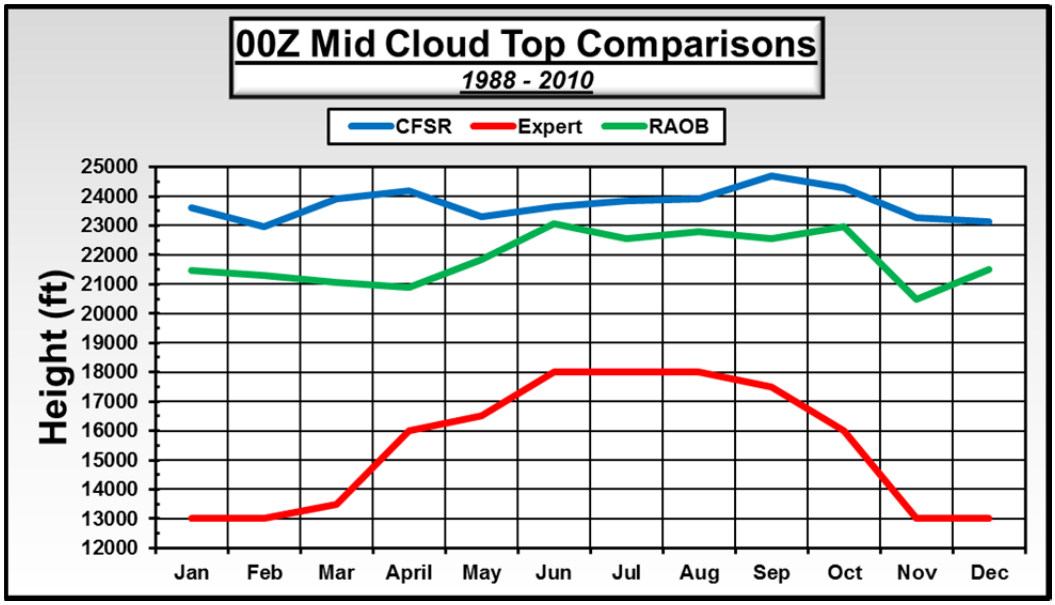

Figure 27. Monthly average mid cloud top heights for each data set from 1988–2010.

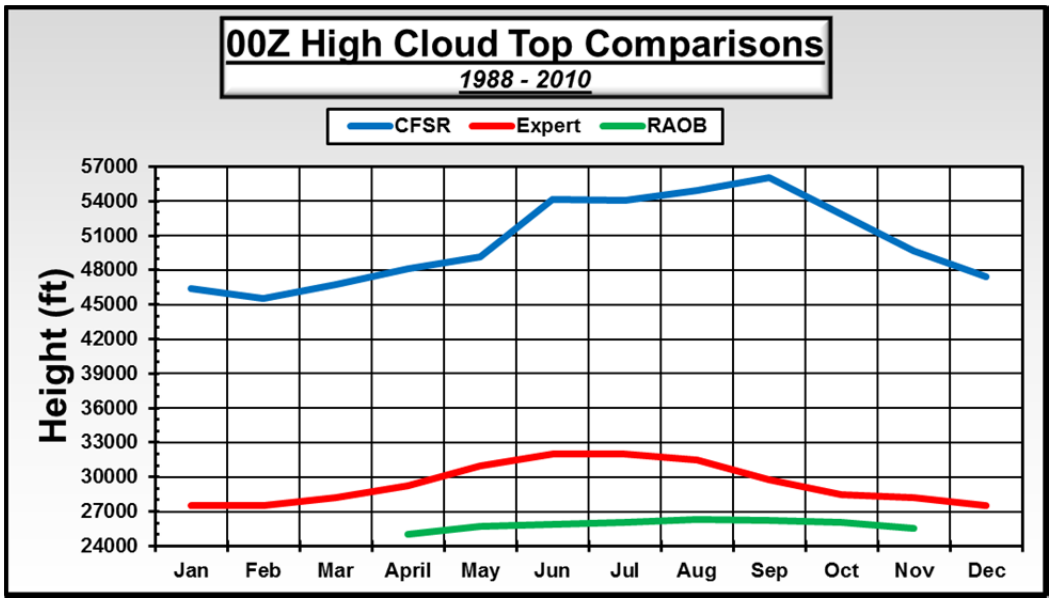

Figure 28. Monthly average high cloud top heights for each data set from 1988–2010.

The cloud top height comparisons led us to conclude that the CFSR cloud top heights were generally too high, with the exception of low cloud top heights during summer when they were too low. Additionally, we noted that the use in CFSR of fixed interface levels between low, mid, and high cloud layers may lead

to low and mid cloud top heights that are too low. We determined the RAOB cloud top height information was also problematic. We concluded that the expert meteorologist data on cloud top heights was the most realistic and the best choice for use in developing our thick cloud LLCC climatologies.

5. Temperatures

As previously stated, in our CFSR data set, the only direct information about temperature height level (i.e., the height of an isotherm) is for the 0° C level. To assess this CFSR information, we compared it to the corresponding RAOB data. Figure 29 shows the monthly average difference between the CFSR and RAOB values (CFSR minus RAOB). The average difference was 28 feet across all months in the study period. The main difference was in the late summer months when CFSR 0° C heights were 267 feet higher than the RAOB data, and in early winter, where the RAOB 0° C heights were 467 feet higher than the CFSR data. These small differences gave us confidence in using RAOB temperature height levels. Recall that our CFSR data set provided data for these heights only for the 0° C level, and not for the -15 and -20° C levels that we also needed. Thus, we decided to use RAOB temperature height level data in developing the thick cloud LLCC climatologies.

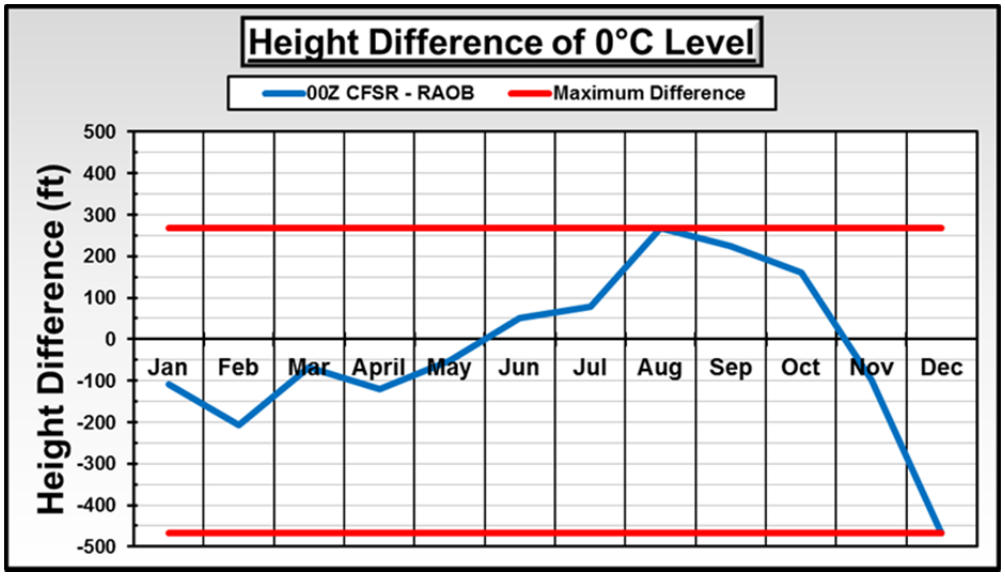

Figure 29. Monthly average difference between the CFSR 0° C height level and the RAOB 0° C height level (CFSR minus RAOB) in feet. Results based on 00Z values for all years in the study period. The red lines mark the largest differences. The average difference for all months was 28 feet.

6. Data Set Comparison Summary

We conducted extensive data set assessments and comparisons to: (a) determine the strengths and weaknesses of each of our four data sets; and (b) determine what information in each data set to use in developing our thick cloud LLCC climatologies. We found that both the METAR and CFSR data sets appeared to do well at the detection of cloud and clear sky conditions for our CCAFS and KSC study region, but the RAOB data set seemed not to perform as well. CFSR cloud base heights and top heights were too high, but METAR and expert meteorologist input, respectively, provided good alternative sources of information for these heights. RAOB temperature height level data matched well with CFSR temperature height level data, indicating we could comfortably use RAOB temperature height level data to supplement the CFSR data where needed. We concluded that no one data set by itself would be sufficient, but that a combination of information from the four data sets would provide the data we needed to develop thick cloud LLCC climatologies. We referred to this combined or merged data set as the modified CFSR data set, since most of the data in this

data set came from CFSR but with some important replacement and supplemental data from the METAR, RAOB, and expert meteorologist data sets (Figure 17). Our results from applying the modified CFSR data set are presented in the following sections.

B. CLOUD THICKNESSES

The results in this section are for calculations of cloud thickness only, and not for the full application of the thick cloud LLCC with temperature constraints applied. Our results for the full application are presented in a later section.

Figure 30 shows the monthly average cloud thicknesses for each of the three cloud layers, with the 4,500 ft thickness highlighted for comparison. The low cloud layer had the largest annual variation in average thicknesses, with a minimum of 1,586 ft in January and a maximum of 9,746 ft in July. This is consistent with the deeper convection and thicker atmosphere over the region in July. The mid and high cloud layers also had clear annual cycles that peaked in the summer months, but with a lower amplitude than for the low cloud layer.

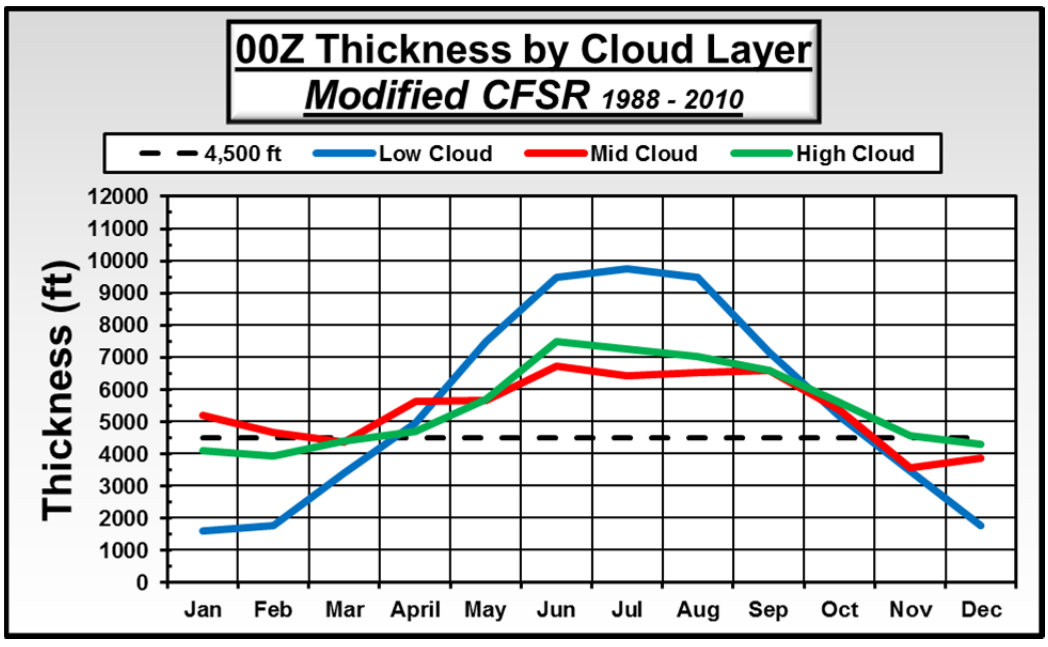

Figure 30. Monthly average cloud thicknesses by cloud layer based on the modified CFSR data set. The dashed black line represents the 4,500 ft thickness threshold in the thick cloud LLCC.

Our evaluations of the monthly averages shown in Figure 30 showed the low and high cloud thicknesses each exceeded the 4,500 ft threshold 58% of the time, while mid cloud thicknesses exceeded that threshold 83% of the time. Thus, when considering just cloud thickness, mid clouds provided the largest portion of the violations of the thick cloud LLCC.

We analyzed the interannual variations in cloud thickness for each cloud layer to identify: (a) differences in these variations by time of the year, especially for the transition seasons; and (b) extreme year variations that could skew our results. Figure 31 is a representative example of the results from our interannual analyses, in this case for low clouds. Note that there are no extreme years for any of months in any of the cloud layers. Note also that the thickest (thinnest) low clouds occurred in July (January), and that April and October were very similar to each other and close to the 4500 ft thickness threshold.

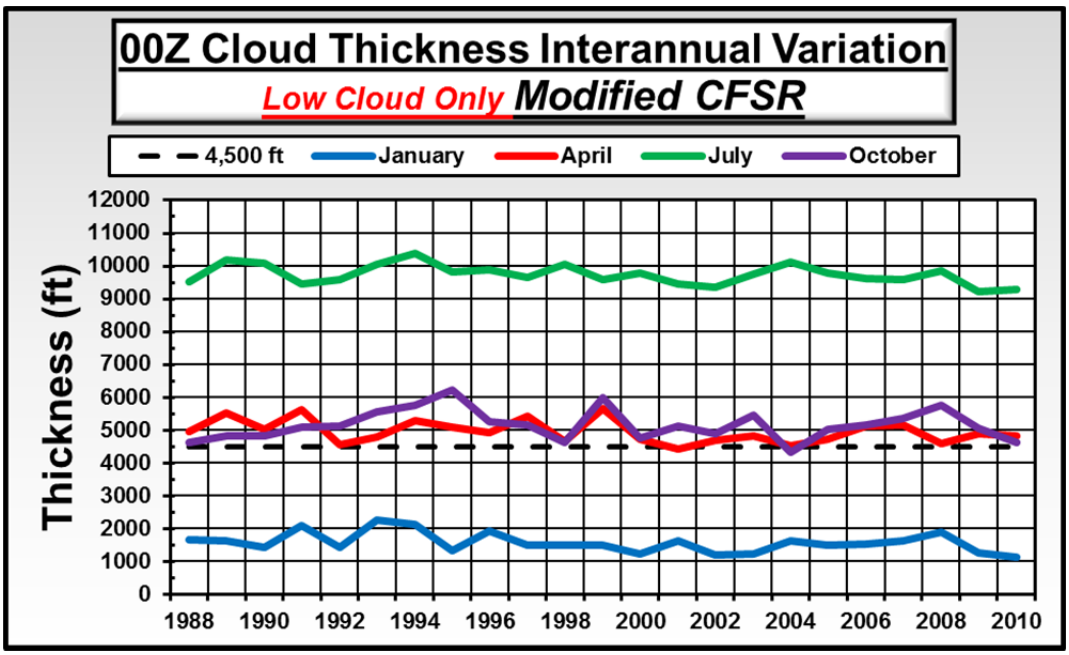

Figure 31. Interannual variation of low cloud thickness for January, April, July, and October for 1988–2010 based on the modified CFSR data set. The dashed black line represents the 4,500 ft thickness threshold in the thick cloud LLCC.

To further assess the modified CFSR cloud thickness values, we compared them to the un-modified CFSR thicknesses. The unmodified CFSR thicknesses are simply those from the original CFSR data, with no inputs or modifications based on METAR or expert meteorologist data. Figures 32-33 are representative examples of the comparison results, in these cases for low and high clouds. The low and high cloud thicknesses differed by an average of 2,849 ft, and 3,248 ft respectively. These differences indicate the extent to which the CFSR thicknesses were modified by the use of: (a) METAR data to adjust the CFSR cloud base heights; and (b) expert meteorologist data to adjust the cloud top heights. These results also show that had we not modified the CFSR data set, low cloud thicknesses would have never violated the 4,500 ft thickness threshold, and high cloud thicknesses would have always violated the 4,500 thickness threshold (Figures 32 and 33). The modified CFSR and unmodified CFSR cloud thicknesses matched very well, with an annual average difference in thicknesses of 334 ft (not shown).

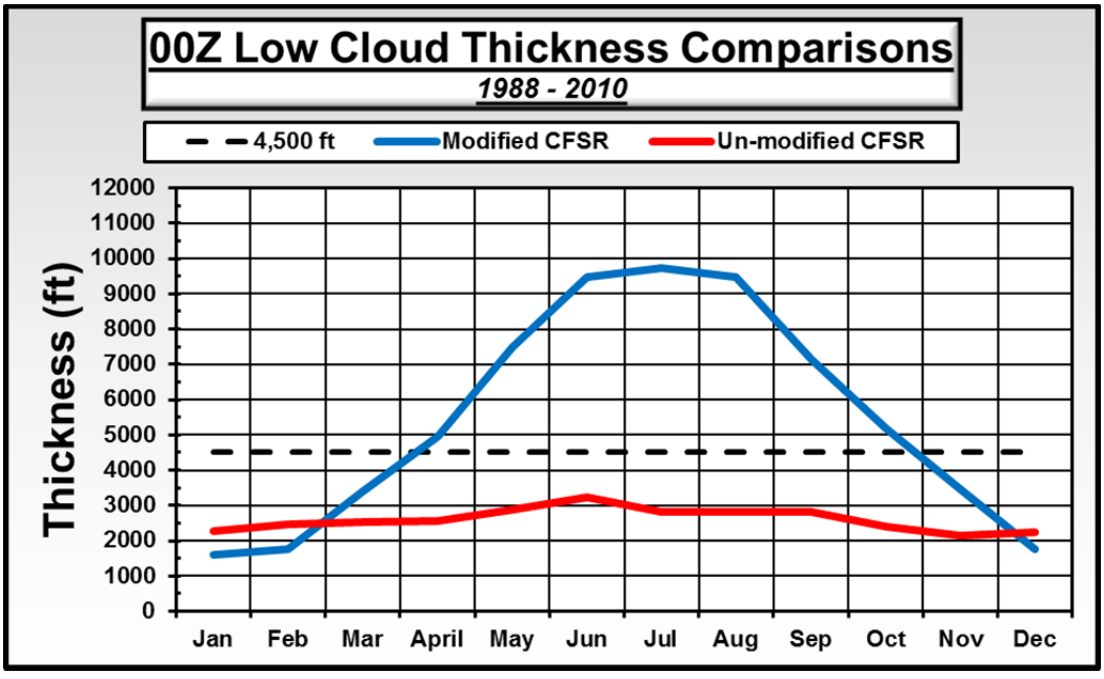

Figure 32. Monthly average low cloud thickness from the modified CFSR data set (blue) and un-modified CFSR data set (red).

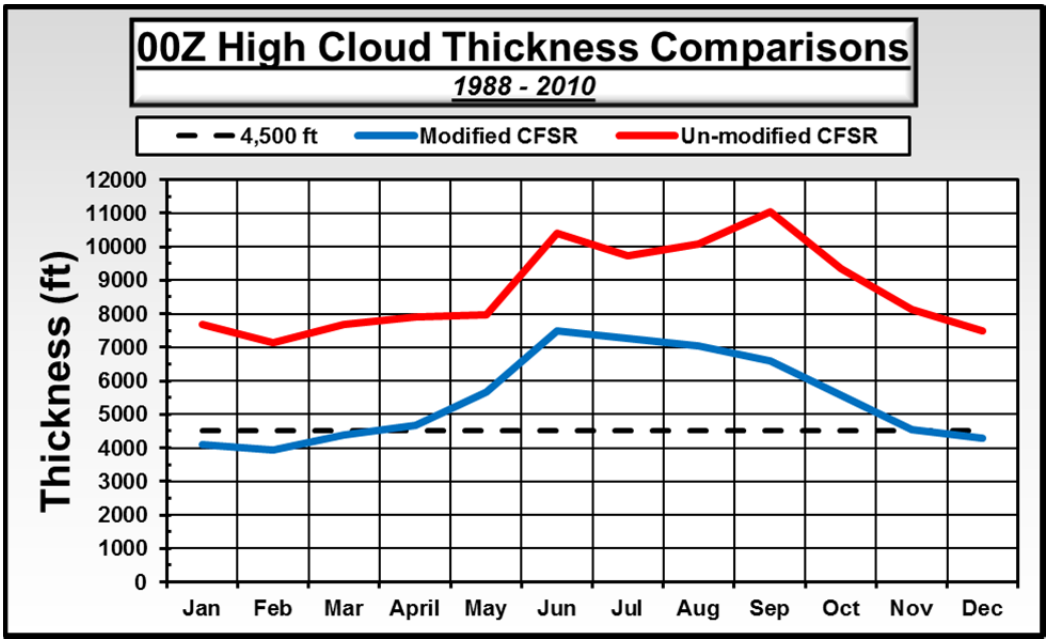

Figure 33. Monthly average low cloud thickness from the modified CFSR data set (blue) and the un-modified CFSR data set (red).

C. PROBABILITIES OF VIOLATION (POV)

1. Initial POVs

As described in Chapter II, Section E.8.a, we produced daily climatological POVs for 00 and 12Z for each day of the year based on the modified CFSR data for the 23 year study period, January 1988 – December 2010. Figure 34 shows the 00Z results. These POVs had the expected seasonal variations --- for example, the probabilities of violating the thick cloud LLCC were higher in the summer months, as expected given the thicker clouds during those months (Figure 30). For example, the average POV for November through January was 14.5%, while the average POV for June through August was 41.5%.

Note in Figure 34 that the POVs showed some large day-to-day variations. For example, the POV was 8.7% for January 8 but 39.1% for January 9, an increase of over 30% from one day to the next. Overall, the largest (smallest) differences from one day to the next occurred in the warmer (cooler) months.

For example, the maximum difference in August (November) was 30.4% (8.7%). In some periods, the day-to-day differences were very small or even non-existent.

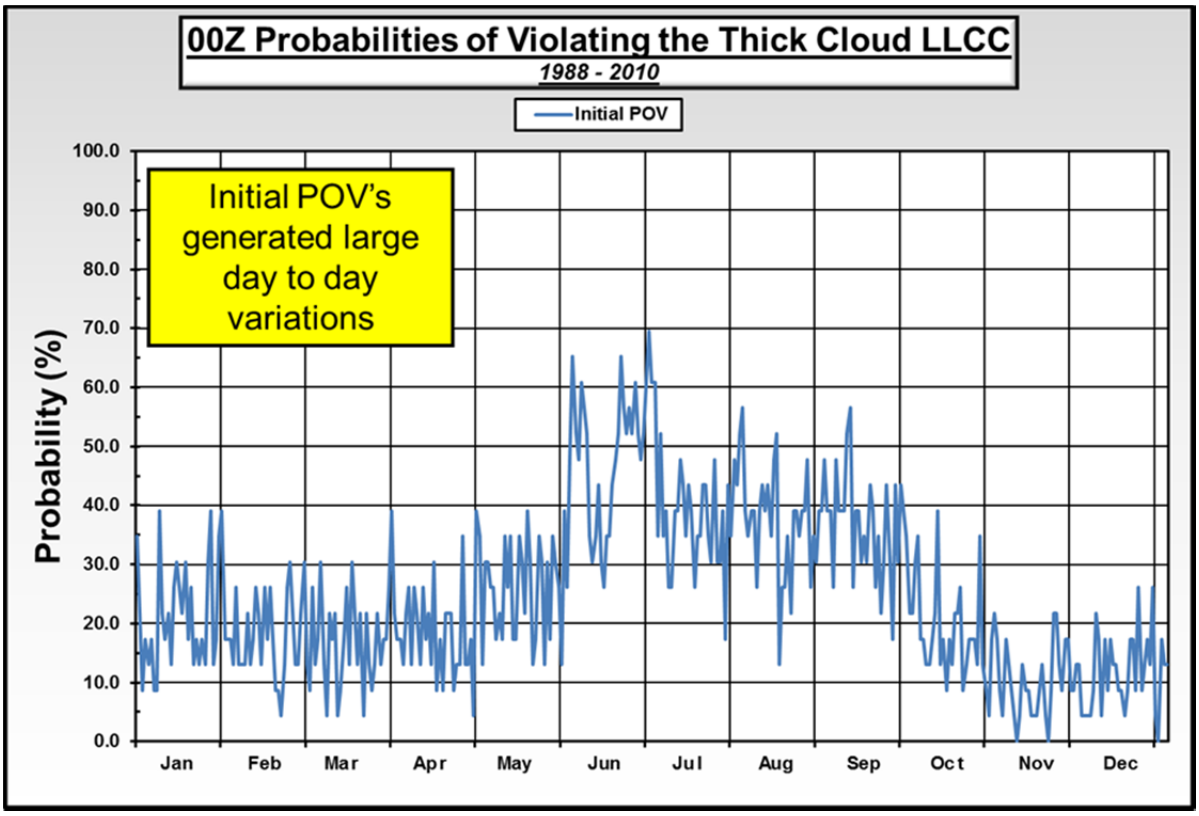

Figure 34. Daily probabilities of violating the thick cloud LLCC with no smoothing of the daily values. The probabilities are for each day of the year from 1 January through 31 December based on the modified CFSR data set for January 1988 – December 2010. Note the large day-to-day variations in the absence of any temporal smoothing.

These large temporal variations in the climatological POVs are probably not realistic and appear to be mainly a result of the limitations of our 23-year data set, for which only 23 values are available for each day of the year. The large day-to-day variations may also be linked to our use of four separate sources of data compute our results, which may have indirectly led to an increase in day-to-day variations. To address these problematic daily variations in the POVs, we applied temporal smoothing to the POVs, as discussed in the following section.

2. Final Probabilities

The large day-to-day variations in our initial thick cloud LLCC POVs make them difficult to apply as a useful operational tool for launch weather planning. For this reason, we chose to make use of several center weighted running averages in an attempt to produce a more smoothed daily climatological product. As stated in Chapter II, Section E.8.b, we computed the running average for five, seven, nine, eleven, thirteen, and fifteen day periods with the goal of minimizing the day to day variability. Additionally, we wanted to ensure we kept the final product as meaningful and operationally useful as possible. To do this, we first evaluated several of the running averages together to identify: (a) any significant differences between them; and (b) the temporal averaging period for which the overall POV variability appeared to be both realistic and small enough to allow the POVs to be operationally useful.

Figure 35 shows the results from smoothing the initial POVs (Figure 34) with running seven, eleven, and fifteen-day running averages. Note that the seven and eleven day running averages still showed some large day-to-day variations. The largest intra-month variations were also reduced (e.g., from about 35% in the unsmoothed POVs to about 15% in the 15-day smoothed POVs for June). As expected, using the 15-day running averages yielded the least amount of day-to-day variability.

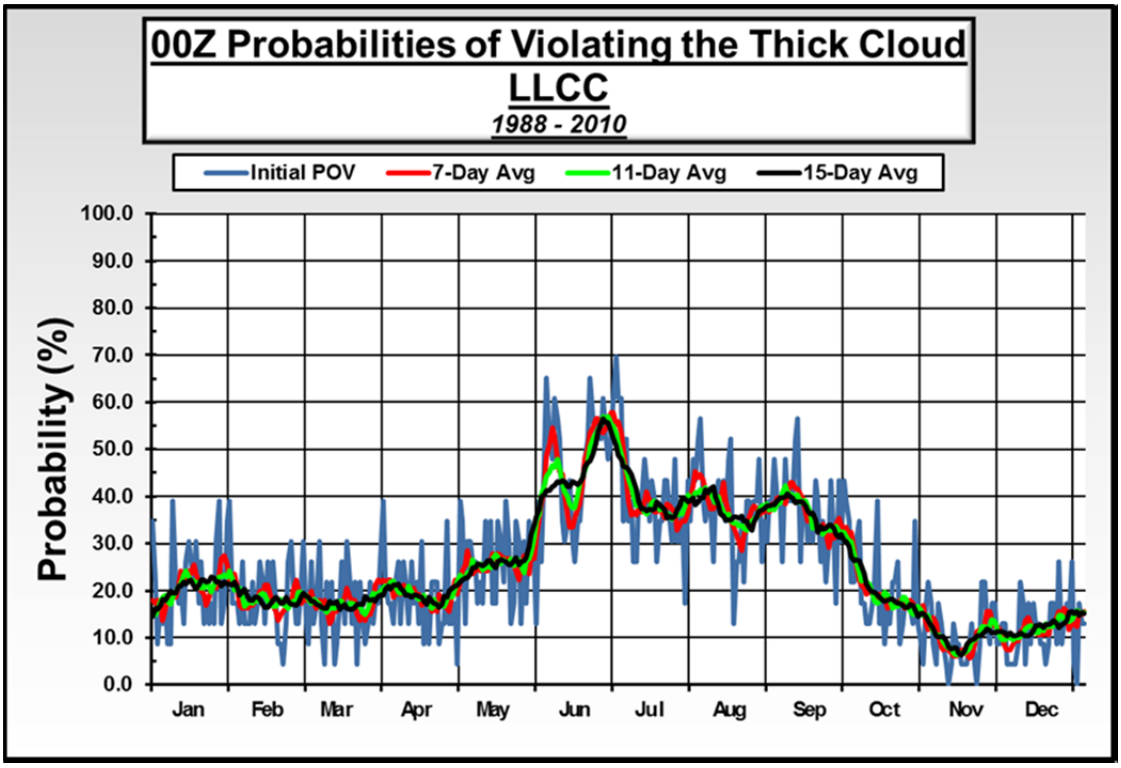

Figure 35. Daily probabilities of violating the thick cloud LLCC with no smoothing of the daily values (blue) with overlays of 7, 11, and 15-day center weighted running means of the probabilities. The probabilities are for each day of the year from 1 January through 31 December based on the modified CFSR data set for January 1988 – December 2010. Note the smaller day-to-day variations in the running mean probabilities.

To assess the full range of the smoothed POVs, we compared the initial unsmoothed POVs to the 5 and 15-day smoothed POVs (Figure 36). The maximum day-to-day variation was 39.1% for the unsmoothed POV,s 8.2% for the 5-day smoothed POVs, and 2.6% for the 15-day smoothed POVs.

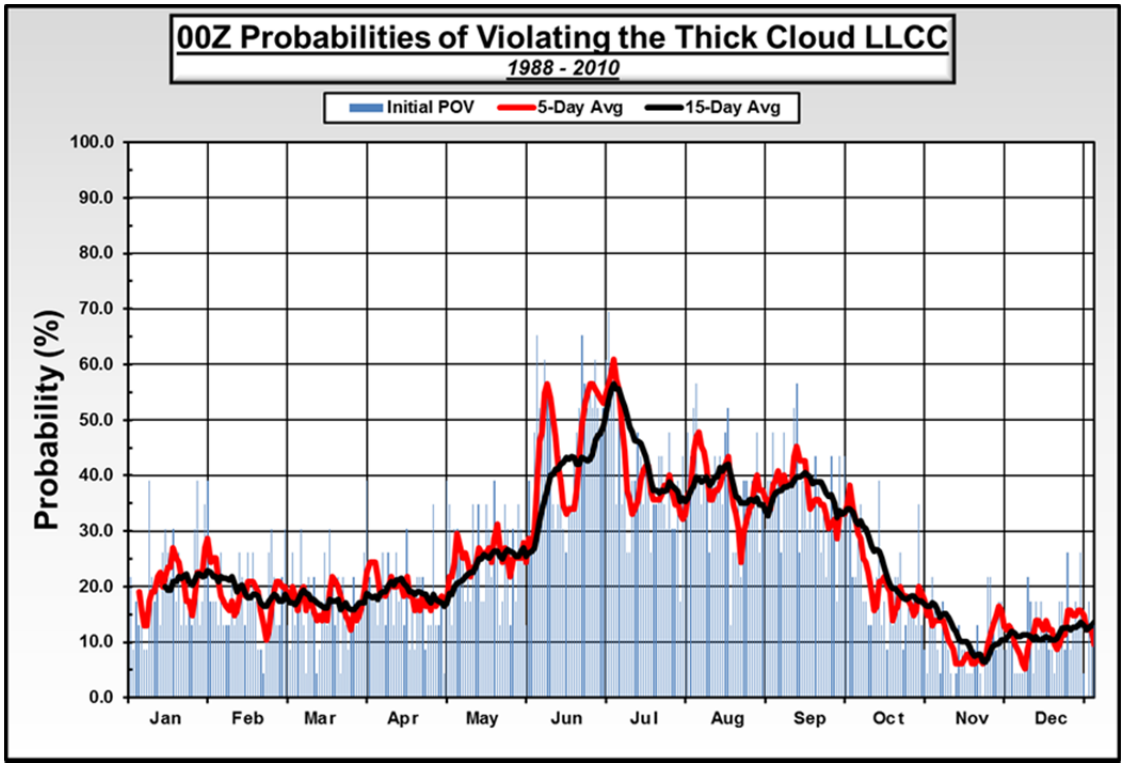

Figure 36. Daily probabilities of violating the thick cloud LLCC with no smoothing of the daily values (blue) with overlays of 5 and 15-day center weighted running means of the probabilities. The probabilities are for each day of the year from 1 January through 31 December based on the modified CFSR data set for January 1988 – December 2010. Note the smaller day-to-day variations in the running mean probabilities, especially the 15-day running mean probabilities.

Typically, the initial weather forecasts for a launch are issued at lead times of five to seven days. At these lead times, weekly mean POVs are especially relevant. Thus, we also analyzed the week-to-week variations in the smoothed POVs. The five, seven, and nine day running averages offered similar results, with maximum week-to-week variations of 30.2%, 27.3%, and 23.2% respectively.

After balancing all of the POV results with operational needs, we determined that the 15-day running average POVs provided the best balance of realism and operational utility.

Thus, our final POVs are based on 15-day running means of the initial POVs. Figure 37 and Table 12 present these smoothed POVs. Table 12 also shows the monthly average POVs (highlighted in yellow).

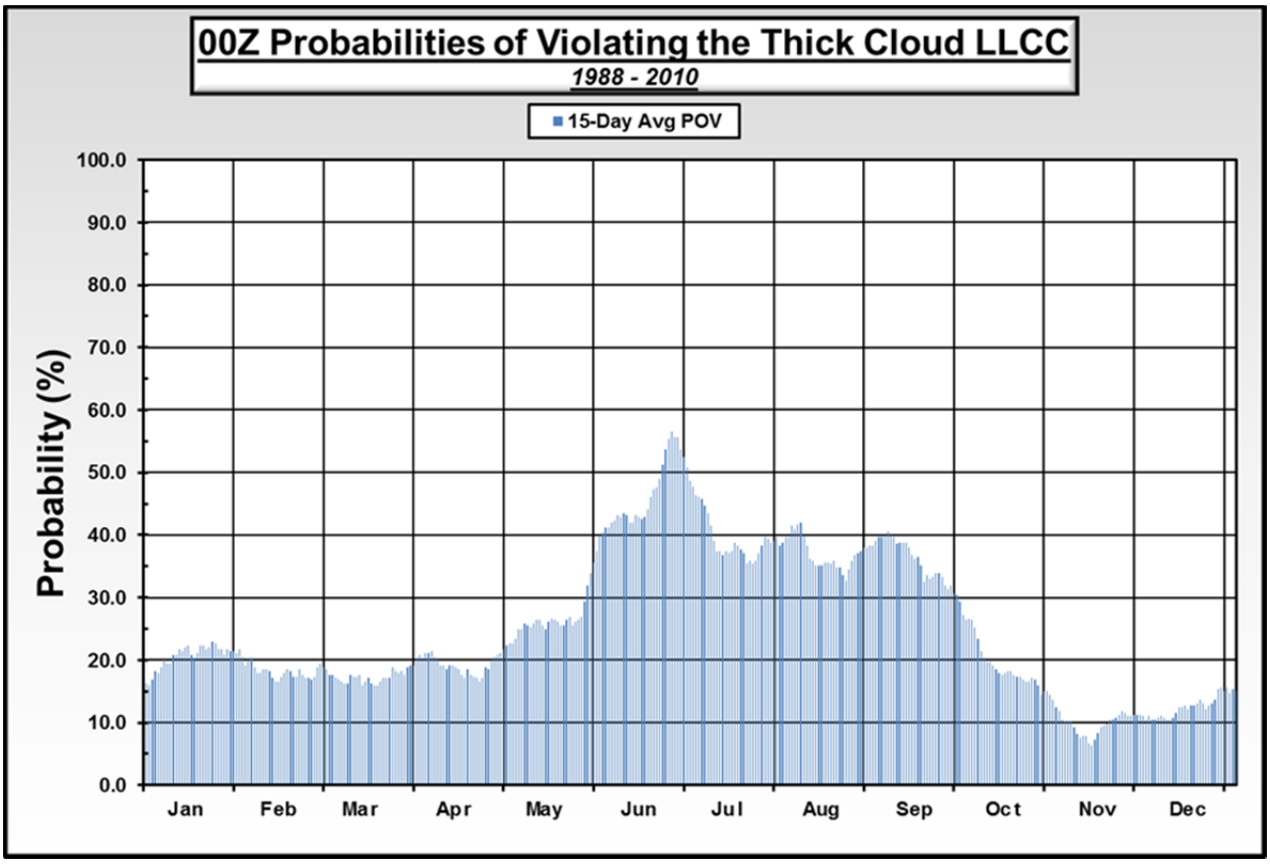

Figure 37. Daily probabilities of violating the thick cloud LLCC after applying a 15-day center weighted running mean smoothing of the initial probabilities (Figure 34). The probabilities are for each day of the year from 1 January through 31 December based on the modified CFSR data set for January 1988 – December 2010.

Probabilities of Thick Cloud Rule LLCC Violation												
	00Z											
	Jan	Feb	Mar	Apr	May	Jun	Jul	Aug	Sep	Oct	Nov	Dec
1	14.5	21.2	19.4	19.1	21.7	37.4	50.7	38.3	38.3	27.2	12.5	10.4
2	16.2	21.7	18.8	20.3	22.3	40.0	48.7	38.8	39.1	26.4	11.9	11.0
3	15.9	20.6	18.6	20.9	22.6	40.3	47.8	39.7	39.7	26.7	10.4	10.4
4	16.8	19.1	17.7	20.3	22.6	41.2	46.4	39.7	39.7	26.4	10.1	10.4
5	18.3	20.0	17.7	21.2	23.5	41.2	46.1	41.4	40.0	25.2	10.1	10.7
6	18.0	20.3	17.1	21.2	24.9	42.0	45.8	40.9	40.6	23.5	10.1	11.0
7	18.8	18.8	16.8	21.4	24.9	42.3	44.6	41.7	40.0	21.4	9.3	10.7
8	20.0	18.0	16.5	20.6	25.8	43.2	43.5	42.0	39.7	20.3	8.1	10.4
9	19.4	18.0	16.2	20.0	25.5	42.9	41.4	40.0	38.6	19.7	7.5	10.4
10	19.4	18.6	16.2	19.1	25.2	43.5	39.1	38.3	38.8	19.7	7.8	10.7
11	20.9	18.6	17.7	19.1	25.8	43.2	37.4	36.2	38.8	19.1	7.8	11.6
12	20.9	18.3	17.4	18.6	26.4	42.0	37.4	35.9	38.8	18.6	6.7	12.5
13	21.7	17.1	17.4	19.1	26.4	42.0	36.8	35.1	38.0	18.0	6.4	12.5
14	21.4	16.5	17.7	19.1	25.5	43.2	37.4	35.1	36.8	17.7	7.2	12.8
15	22.0	16.5	15.9	18.8	24.9	42.9	37.1	35.1	36.2	18.0	8.4	12.2
16	22.3	17.4	16.5	18.6	26.1	42.6	37.4	35.7	36.5	18.3	9.3	12.8
17	20.9	18.0	17.1	17.7	26.7	42.9	38.8	35.7	35.1	18.3	9.6	12.8
18	20.3	18.6	16.2	17.1	26.4	44.1	38.3	35.4	32.5	17.7	9.9	13.0
19	21.2	18.3	15.9	18.6	26.1	46.1	37.7	35.9	33.6	17.4	10.4	13.6
20	22.3	17.4	15.9	17.7	25.5	47.2	37.1	34.8	33.0	17.4	10.4	13.0
21	22.3	17.4	16.5	17.4	25.5	47.5	35.4	34.8	33.3	16.8	10.7	12.2
22	21.7	18.6	17.1	17.1	26.4	49.0	35.9	33.6	33.9	16.5	11.3	12.8
23	22.0	17.7	17.1	16.5	27.0	51.3	35.4	32.8	33.9	16.5	11.9	13.0
24	22.9	17.1	17.1	17.1	25.5	53.6	35.9	34.5	33.3	17.1	11.6	13.6
25	22.6	17.1	18.8	18.8	26.1	55.4	37.1	35.9	31.9	16.8	11.0	15.4
26	21.7	16.8	18.3	18.6	26.4	56.5	38.3	36.8	31.3	15.9	11.0	15.7
27	21.7	17.4	18.0	20.0	27.0	55.7	39.7	37.1	31.9	14.5	11.3	15.1
28	20.9	18.8	18.3	20.6	29.3	55.7	39.4	37.4	30.7	15.1	11.3	15.7
29	21.7		17.7	20.9	31.9	53.6	38.8	38.0	30.4	15.1	11.3	14.8
30	21.4		18.8	21.2	33.9	52.5	39.1	38.0	29.3	14.5	11.0	15.4
31	21.4		19.1		35.7		39.7	38.3		13.6		15.1
Avg	20.4	18.3	17.4	19.2	26.2	46.0	40.1	37.2	35.8	19.0	9.9	12.6
Results based on thesis research by Capt. Greg Strong, USAF, Naval Postgraduate School, March 2012												

Table 12. Daily probabilities of violating the thick cloud LLCC after smoothing the initial probabilities (Figure 34) with a 15-day center weighted running mean smoother. The probabilities are for each day of the year from 1 January through 31 December based on the modified CFSR data set for January 1988–December 2010. Monthly average POVs are shown in yellow highlighted row at the bottom of each monthly column.

3. POVs by Cloud Layer

We also separately calculated the climatological probabilities of violating the thick cloud LLCC for each of the three cloud layers. Our objectives were to: (a) isolate the layer that made largest contribution to the violations; and (b) provide decision makers with information to use when considering potential modifications of the thick cloud LLCC. Figure 38 shows the results for the 00Z probabilities. Mid cloud violations dominated the violations of the thick cloud LLCC with 76% of the total violations.

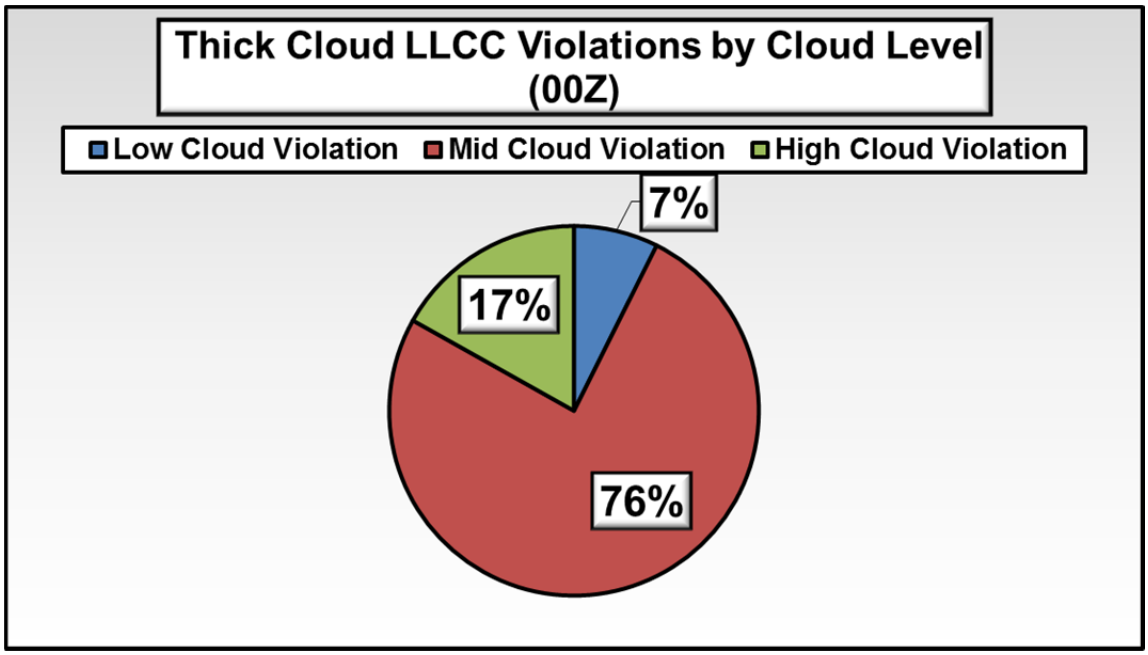

Figure 38. Percentage of 00Z thick cloud LLCC violations by cloud layer.

Recall that the thick cloud LLCC says that any part of a cloud greater than or equal to 4,500 ft thick must also be located between the 0° and -20° C levels to be considered a violation. Figure 30 shows that, on a monthly average basis, mid cloud thicknesses were greater than or equal to 4,500 ft in all months except November and December (i.e., 83% of the time). Additionally, Figure 39 shows that, on a monthly average basis, the 0°C level was located within the mid cloud layer (somewhere between the cloud base and cloud top) in all months except November and December (i.e., 83% of the time). These results indicate why mid

cloud lead to a high probability of violating the thick cloud LLCC, because 83% of the time mid clouds meet both the thickness and temperature threshold requirements.

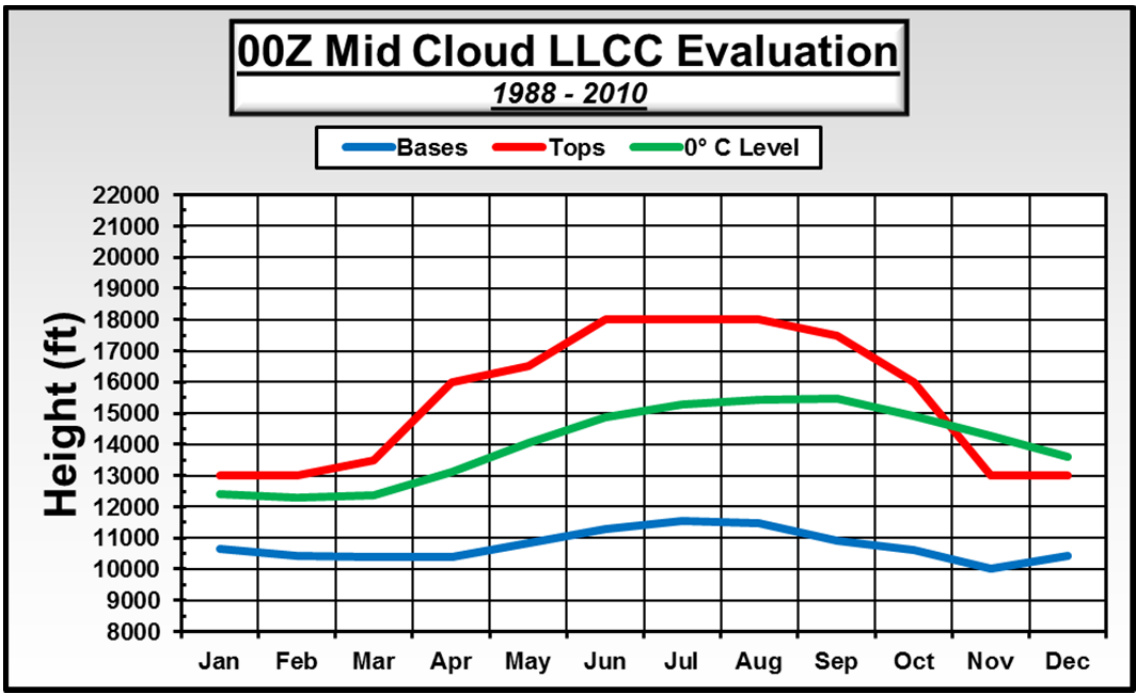

Figure 39. Monthly average mid cloud base heights and top heights, and the height of the 0° C level. Note that monthly average height of the 0° C level was located between the monthly average mid cloud base height and top height in all months except November and December. These results indicate that mid clouds tend to produce many of the violations of the thick cloud LLCC.

Low and high cloud layers contribute relatively few violations (Figure 38) because these layers do not typically meet one of the prescribed temperature thresholds. Figure 40 shows that, on a monthly average basis, the low cloud tops are always below the height of the 0° C level. This means that low clouds: (a) tend not to have top heights that exceed the 0° C height; and (b) produce relatively few violations of the thick cloud LLCC. Similarly, Figure 41 shows that, on a monthly average basis, the high cloud bases are located above the -20° C level 67% of the time, and above the -15° C level 100% of the time. Assuming high clouds meet the requirements defined in Chapter II, Section E.8.a, these

monthly averages imply high clouds tend to produce few violations of the thick cloud LLCC, due to their base heights being higher than the height of the -15° C level.

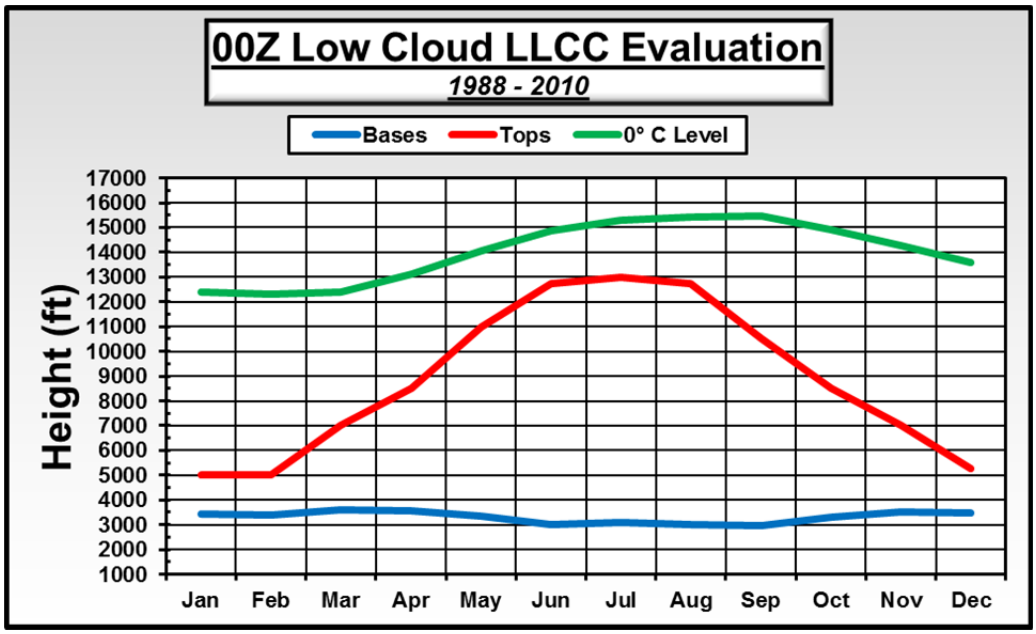

Figure 40. Monthly average low cloud base heights and top heights, and the height of the 0° C level. Note that monthly average height of the 0° C level was located above the monthly average mid cloud base height and top height in all months.

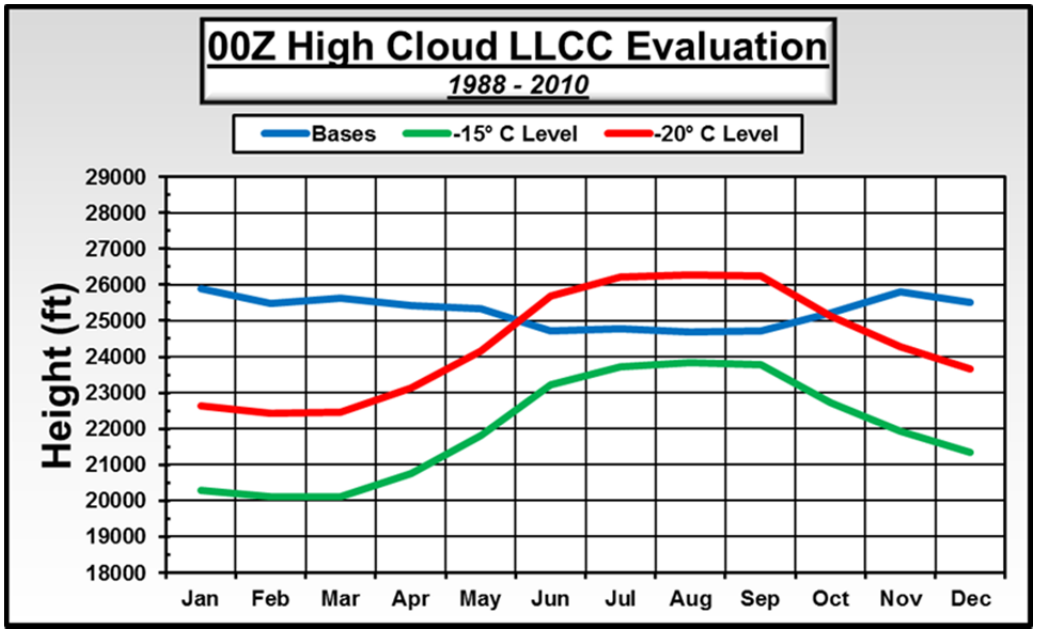

Figure 41. Monthly average high cloud base heights, and the heights of the -15° C and -20° C levels. High cloud top heights not shown because the high cloud base heights were the interacting cloud feature for determining thick cloud LLCC violations in this layer. Note that monthly average height of the -15° C level was located below the monthly average high cloud base height in all months.

To further understand the implications of thick cloud LLCC probabilities of violation by layer (Figure 38), we isolated these probabilities by month. Figures 42-43 show the results for January and July --- examples of months with relatively low and high probabilities, respectively (Figure 37). The mid cloud violations decreased by from 95% in January to 68% in July, while the low and high cloud violations both increased (Figures 42 and 43). This was an expected result, considering the information in Figures 39–41. While the monthly averaged low cloud tops never exceeded the height of the 0° C level, they were the closest to doing so in the warmer summer months (Figure 40). Therefore, we would expect, using daily computations, to find a higher chance in the summer months of low clouds violating the thick cloud rule.

The large percentage increase in high cloud violations from January to July (from 4% to 25% of the total violations) is consistent with the corresponding January to July decrease in the high cloud base heights and increase in the heights of the -15° and -20° C levels shown in Figure 41.

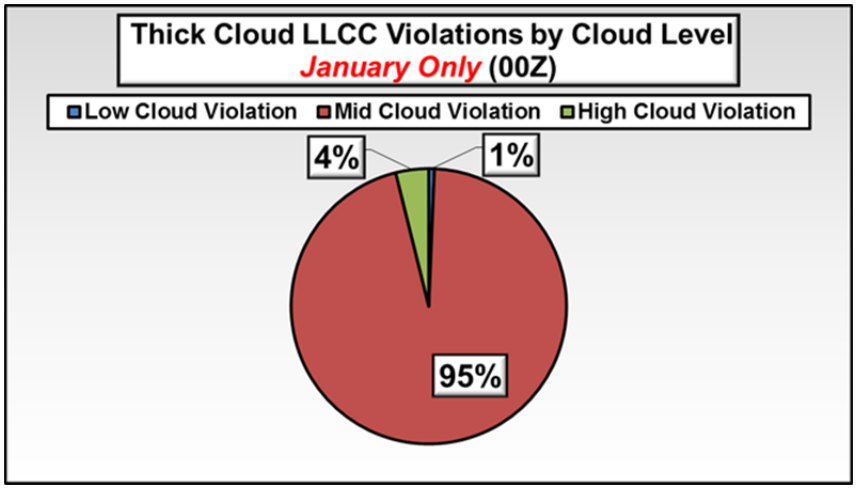

Figure 42. Percentages of 00Z thick cloud LLCC violations by cloud layer for January.

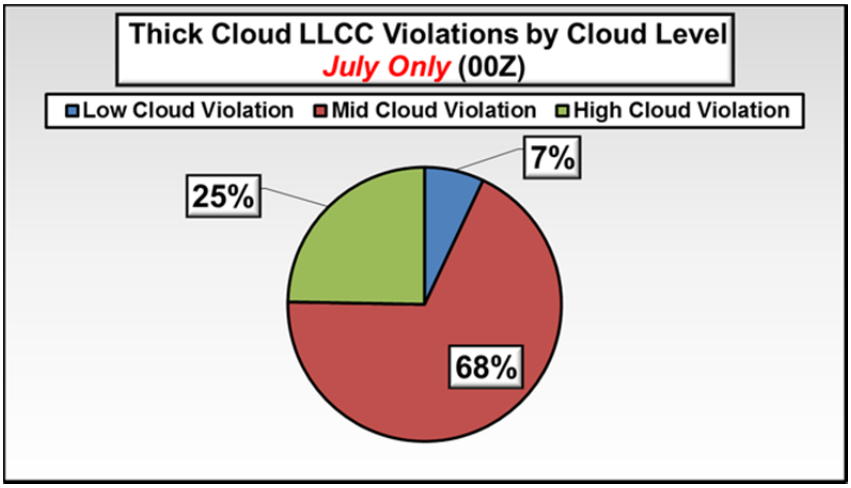

Figure 43. Percentages of 00Z thick cloud LLCC violations by cloud layer for July.

D. SENSITIVITY ANALYSIS

We conducted a sensitivity analysis of the thick cloud LLCC climatologies to determine if relatively small increases in the cloud thickness threshold might

lead to large decreases in the climatological probabilities of violations. Decrease in these probabilities could be operationally important because they could increase launch opportunities for the launch customers. We compared the POVs for the thickness thresholds listed in Chapter II, Section E.8.c, from 3,500 ft to 7,500 ft. The monthly mean results are shown in Figure 44. The probabilities of violating the thick cloud LLCC decreased as the thickness threshold increased (as expected) and also vary by month. As an example, the difference between the probabilities for the 3,500 and 7,500 ft thresholds were relatively small for November-February, with an average decline of about 10%, and large for June-September, with an average decline of about 30%. The larger differences in June-September are consistent with the relatively large number of thicker clouds and POVs during those months (e.g., Figures 30, 37).

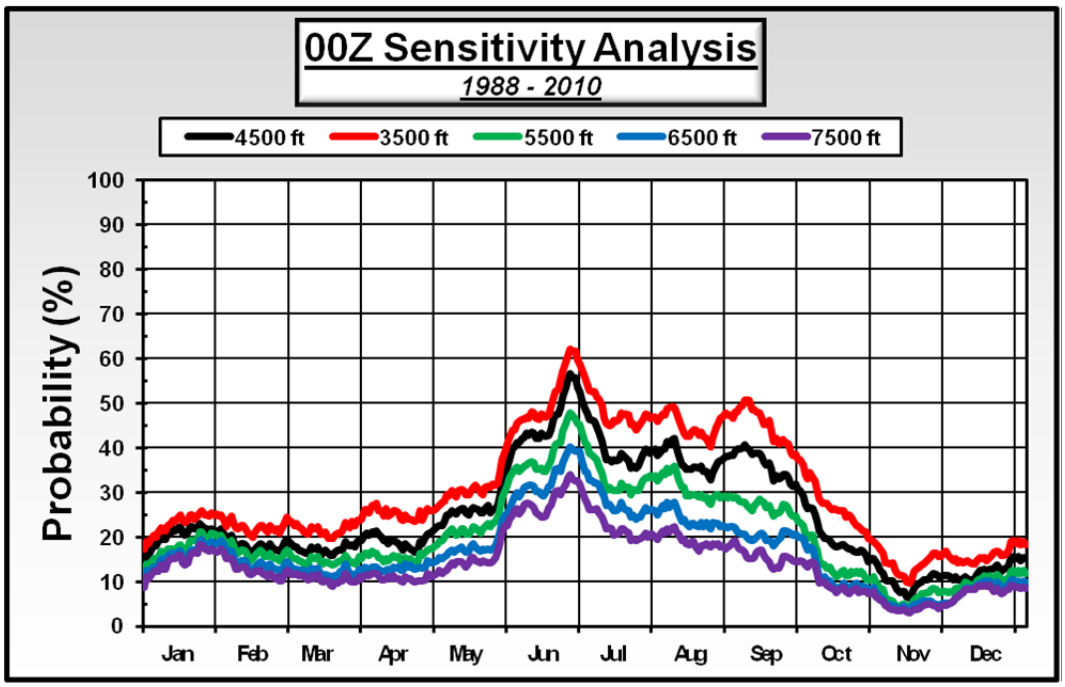

Figure 44. Daily probabilities of violating the thick cloud LLCC when using a thickness threshold of 3,500 ft (red), 4,500 ft (black), 5,500 ft (green), 6,500 ft (blue) and 7,500 ft (purple). The probabilities have been smoothed using a 15-day center weighted running mean smoother. The probabilities are for each day of the year from 1 January through 31 December based on the modified CFSR data set for January 1988 – December 2010.

The Figure 44 results showed that the POV reduction from a potential reduction in the thickness threshold varied by month. To assess the impacts on an annual basis, we computed the corresponding annual mean POV reductions. Figure 45 shows the changes in the annual mean probability of violation of the thick cloud rule for each of the thickness thresholds (bottom axis). For example, if the thick cloud LLCC thickness threshold was changed to 3,500 ft, the average POV would be 5.44% higher than the current 4,500 ft thickness threshold. However, if the thick cloud LLCC thickness threshold was 7,500 ft, the average POV would be 10.98% lower than for the current 4,500 ft threshold. This shows that even if we were to add 3,000 ft to the current rule (change from 4,500 ft to 7,500 ft), we would only expect only about an 11% decrease in the 00Z POVs for the year as whole. The annual average POV was 25.22%, when using the 4,500 ft thickness threshold but 14.24% when using the 7,500 ft thickness threshold. To put this into perspective, the annual average POV for the present thickness threshold of 4,500 ft is 25.22%. But if scientific evidence indicated the thickness threshold could be increased to 7,500 ft, then the POV would be 14.24%. Figure 45 suggests a linear relationship between variations in thickness threshold and POV. We found in a separate analysis that: (a) every 1,000 ft increase in the thickness threshold led to a reduction in the POV of about 2.05%; and (b) there is a strong linear relationship between threshold changes and POV changes (R^2 value of 0.984).

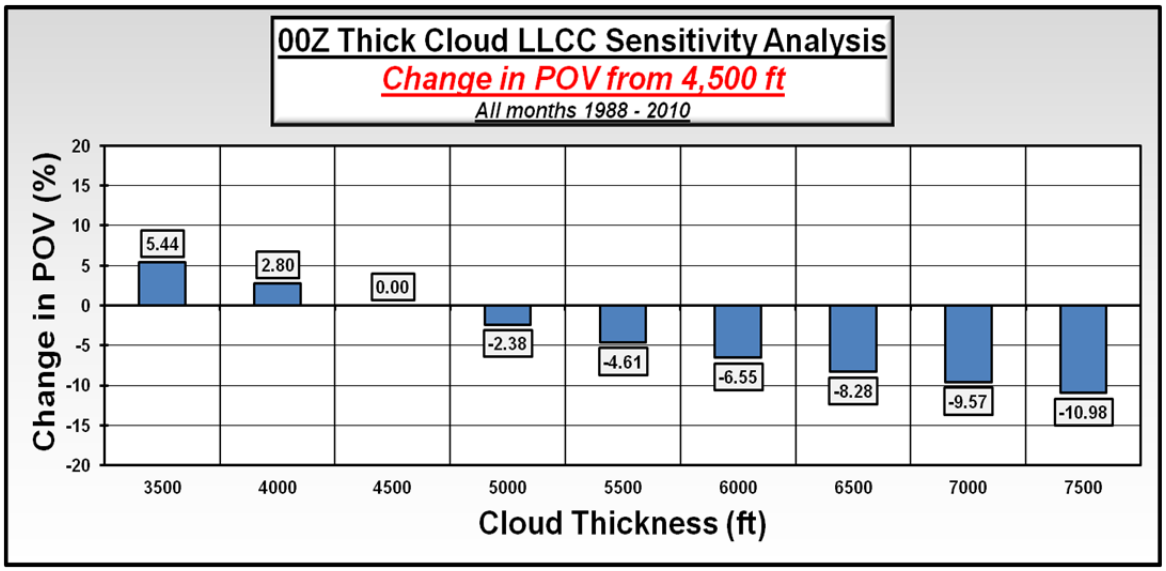

Figure 45. Daily mean change in the climatological probabilities of violating the thick cloud LLCC based on using alternative thickness thresholds rather than the present threshold of 4,500 ft. The alternative thresholds are shown on the horizontal axis.

E. CASE STUDIES

We conducted eight case studies to gain insight into the validity of our calculated POVs. The cases were for the eight recorded, or known, violations of the thick cloud LLCC from August 2005 through August 2010. For the eight days on which these cases occurred, our average calculated POV was a relatively high 32% (recall from the prior section that the annual average POV was 25%). Of the eight cases, five were correctly identified in our modified CFSR data set --- that is, in our daily calculated violations from which we calculated our POVs. This means that our modified CFSR data set correctly identified, on a daily basis, violations of all components of the thick cloud LLCC at the times and dates of 62% of the known violations (Figure 46).

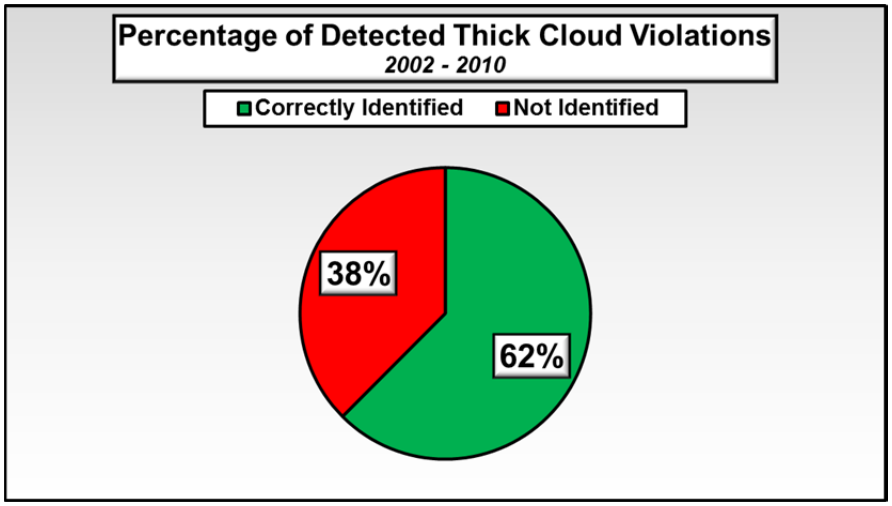

Figure 46. Percentage of known thick cloud LLCC violations during 2005–2010 that were identified correctly (green) and incorrectly (red) in the modified CFSR data set.

We then attempted to determine why our modified CFSR data set did not properly identify the remaining 38% of the known violations. To do so, we applied the thick cloud LLCC as if cloud thickness was the only factor, and neglected the temperature factors. We wanted to see if our data set correctly identified at least the 4,500 ft thickness factor properly. The result was that 87% of the known violations (seven of the eight cases) were properly identified in our data set when accounting for only the thickness factor (Figure 47). For the one case that was not correctly identified, our data set had a computed cloud thickness of 4,493 ft, only 7 ft below the thickness threshold of 4,500 ft.

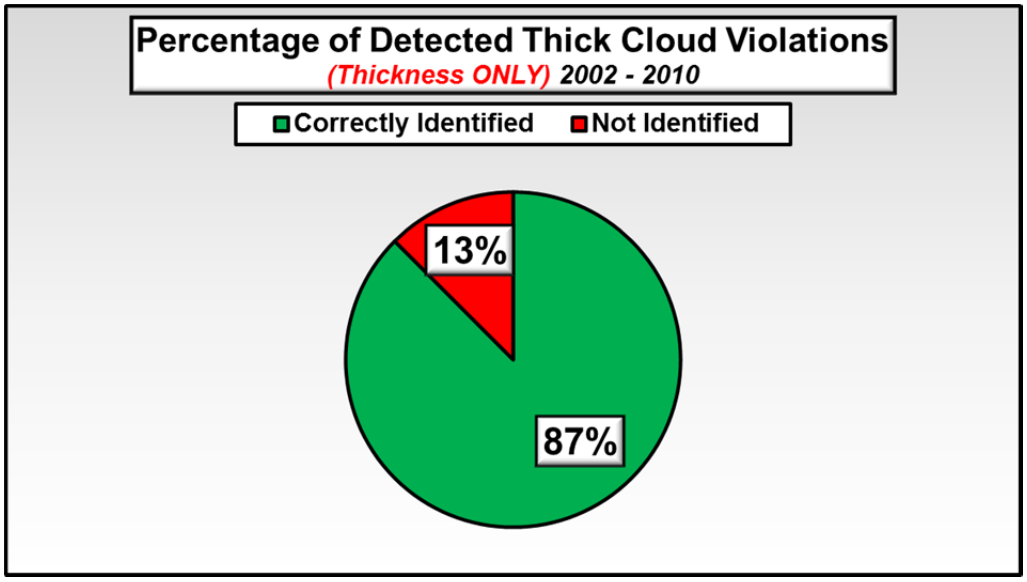

Figure 47. Percentage of known thick cloud LLCC violations during 2005–2010 that were identified correctly (green) and incorrectly (red) in the modified CFSR data set when calculating violations using only the 4,500 ft cloud thickness threshold and neglecting the temperature thresholds.

These case study results suggest that the data sets and processes we used to develop our modified CFSR data set, and to calculate the probabilities of violations, are valid. They also indicate that the relationships between the cloud base heights, cloud top heights, and temperature height levels in the data set could be improved. This led us to conclude that there is a need for a more in depth study of the relationship of these variables, as well as expanded validation studies.

IV. SUMMARY, CONCLUSIONS, AND RECOMMENDATIONS

A. KEY RESULTS AND CONCLUSIONS

This thesis explored the potential for merging multiple data sets together to create valid climatological probabilities of violating the thick cloud layer LLCC. Our primary focus was on: (1) assessing the needed data sets; (2) developing and testing the merger process; (3) calculating the probabilities; (4) validating the merged data set and the resulting probabilities; and (5) generating operationally useful products for use by the 45 WS. In this process, we also demonstrated that no individual data set is adequate for constructing the climatological probabilities of violations, but that comparative analyses of individual data sets could help identify the strengths and weaknesses of individual data sets, and which components of those data sets to use in constructing the merged data set. To do these comparative analyses, we developed detailed control methods to help ensure that the strongest components of each data set were identified and matched with those from the other data sets. The net result of our data set merger process was our modified CFSR data set, spanning January 1988 – December 2010, a 23-year period. We constructed the modified CFSR data set by merging together information from four individual data sets: CFSR, METAR, RAOB, and expert meteorologists.

We used this data set to calculate the climatological probabilities of violations (POVs) of the thick cloud LLCC. To adjust for the relatively short period of record for our modified CFSR data set (23 years), we smoothed our POVs using a center weighted 15-day running average smoother. We also separately computed the POVs for low, mid, and high cloud layers, to ensure that we captured enough detail for validation testing, operational applications, and determining potential focus areas for future work. Our results indicated mid clouds accounted for the majority of thick cloud LLCC violations, with the highest probabilities occurring in the warmer summer weather regime (June through September).

We then conducted a sensitivity analysis of the thick cloud LLCC POVs to the determine the extent to which increases in the thickness threshold lead to reductions in the POVs. Our objective was to uncover relatively small threshold increases that could potentially lead to large decreases in the POVs. We found for every 1,000 ft increase in the cloud thickness threshold, there was a corresponding POV decrease of 2.05%.

We conducted eight case studies to validate our methods, our modified CFSR data set, and our climatological POVs. Our cases were ones in which launch mission information indicated that the thick cloud LLCC had been violated (i.e., the thick cloud LLCC requirements had been met or exceeded). Our modified CFSR data set correctly identified: (1) violations of the 4,500 ft thickness threshold in seven out of the eight cases; and (2) violations of both the thickness and temperature height level thresholds in five out of the eight cases.

B. DELIVERABLES TO 45 WS

The main goal of this study was to develop operationally relevant, meaningful, and useful tools for delivery to the 45 WS. The purposes of the tools range from aiding in the production of a launch forecast at one to seven day lead times to planning for future modifications of the thick cloud LLCC. Launch operations are extremely weather sensitive, and many critical decisions are made based on weather forecasts. Our study produced not only climatological probabilities of violating the thick cloud LLCC, but several other deliverable products as well. These products for delivery to the 45 WS are summarized below.

1. Climatological probabilities of violating the thick cloud LLCC for 00Z and 12Z for each day of the year
2. Monthly averages of climatological probabilities of violating the thick cloud LLCC for 00Z and 12Z

3. Climatological probabilities of violating the thick cloud LLCC for 00Z and 12Z by cloud layer (low, mid, and high layers)
4. Climatological probabilities of violating the thick cloud LLCC for 00Z and 12Z by cloud thickness threshold (3500 ft to 7500 ft, in 550 ft increments)
5. Climatologies of the variables used to compute thick cloud LLCC probabilities, including monthly averages of the variables listed below at 00Z and 12Z.
    a. Cloud bases by layer
    b. Cloud tops by layer
    c. Cloud thickness by layer
    d. Heights of temperature levels

C. AREAS FOR FURTHER RESEARCH

The results from this research highlighted the complex nature of computing cloud related LLCC climatologies. Due to this complexity, there are other areas that need to be researched to improve the development of these climatologies, and especially the climatological probabilities of violations for the LLCC. Our recommendations for future research are listed below.

1. Our study used the CFSR data at a single grid point (28.5° N; 80.5°W; Figure 10). Reanalyzing the thick cloud LLCC climatologies using data from several grid points surrounding the average launch point may offer additional information.

2. Due to time constraints with our research, we only computed climatological probabilities over the twenty-three year study period for 00Z and 12Z. To better identify possible diurnal variations of the thick cloud LLCC variables and POVs, and to develop an improved operational tool, we recommend computing climatologies and probabilities at 06Z and 18Z as well.

3. We used CFSR data from a 0.5 degree horizontal resolution gird, but data is also available on a Gaussian grid at a 0.3 degree horizontal resolution and should be considered in planning future research projects. In addition, the North American Regional Reanalysis (NARR) data set should also be considered.

4. The thick cloud LLCC is only one of eleven total LLCC, but it is one of six dealing specifically with clouds. Additionally, one of the factors in the full thick cloud LLCC is the association of a thick cloud layer with specific cloud types, in particular, anvil cloud and convective clouds. We investigated the potential for including cloud type information in the development of our modified CFSR data set. But we set this topic aside, due to the limitations of the cloud type data sets, and our time and scope. Our plan was to collect and/or generate climatological cloud type probabilities and apply them as weighting terms to our climatological probabilities of violating the thick cloud LLCC. The CFSR data set provides information on the occurrence of convective and non-convective clouds, which could be useful. While we are confident in our results, the inclusion of cloud type information would certainly help to improve our results. Developing a method to incorporate cloud type information into our process may also help with computing climatological probabilities of violating other cloud related LLCC, such as anvil clouds, debris, and cumulus clouds.

5. Our case studies investigated known thick cloud LLCC violations during the years of 2005–2010, the only years of LLCC violations for which data is kept in electronic format. However, the LWOs maintain hard copy copies of violation information for each launch mission. Compiling this hardcopy information into an electronic data base for each LLCC violation may prove useful for further research and development on LLCC climatologies. Additionally, we recommend evaluating all known thick cloud LLCC violations from 1 Jan 1988–31 Dec 2010 against our existing thick cloud LLCC climatological probabilities of violation.

THIS PAGE INTENTIONALLY LEFT BLANK

APPENDIX A. CLIMATOLOGICAL TABLES

Probabilities of Thick Cloud Rule LLCC Violation												
	00Z											
	Jan	Feb	Mar	Apr	May	Jun	Jul	Aug	Sep	Oct	Nov	Dec
1	14.5	21.2	19.4	19.1	21.7	37.4	50.7	38.3	38.3	27.2	12.5	10.4
2	16.2	21.7	18.8	20.3	22.3	40.0	48.7	38.8	39.1	26.4	11.9	11.0
3	15.9	20.6	18.6	20.9	22.6	40.3	47.8	39.7	39.7	26.7	10.4	10.4
4	16.8	19.1	17.7	20.3	22.6	41.2	46.4	39.7	39.7	26.4	10.1	10.4
5	18.3	20.0	17.7	21.2	23.5	41.2	46.1	41.4	40.0	25.2	10.1	10.7
6	18.0	20.3	17.1	21.2	24.9	42.0	45.8	40.9	40.6	23.5	10.1	11.0
7	18.8	18.8	16.8	21.4	24.9	42.3	44.6	41.7	40.0	21.4	9.3	10.7
8	20.0	18.0	16.5	20.6	25.8	43.2	43.5	42.0	39.7	20.3	8.1	10.4
9	19.4	18.0	16.2	20.0	25.5	42.9	41.4	40.0	38.6	19.7	7.5	10.4
10	19.4	18.6	16.2	19.1	25.2	43.5	39.1	38.3	38.8	19.7	7.8	10.7
11	20.9	18.6	17.7	19.1	25.8	43.2	37.4	36.2	38.8	19.1	7.8	11.6
12	20.9	18.3	17.4	18.6	26.4	42.0	37.4	35.9	38.8	18.6	6.7	12.5
13	21.7	17.1	17.4	19.1	26.4	42.0	36.8	35.1	38.0	18.0	6.4	12.5
14	21.4	16.5	17.7	19.1	25.5	43.2	37.4	35.1	36.8	17.7	7.2	12.8
15	22.0	16.5	15.9	18.8	24.9	42.9	37.1	35.1	36.2	18.0	8.4	12.2
16	22.3	17.4	16.5	18.6	26.1	42.6	37.4	35.7	36.5	18.3	9.3	12.8
17	20.9	18.0	17.1	17.7	26.7	42.9	38.8	35.7	35.1	18.3	9.6	12.8
18	20.3	18.6	16.2	17.1	26.4	44.1	38.3	35.4	32.5	17.7	9.9	13.0
19	21.2	18.3	15.9	18.6	26.1	46.1	37.7	35.9	33.6	17.4	10.4	13.6
20	22.3	17.4	15.9	17.7	25.5	47.2	37.1	34.8	33.0	17.4	10.4	13.0
21	22.3	17.4	16.5	17.4	25.5	47.5	35.4	34.8	33.3	16.8	10.7	12.2
22	21.7	18.6	17.1	17.1	26.4	49.0	35.9	33.6	33.9	16.5	11.3	12.8
23	22.0	17.7	17.1	16.5	27.0	51.3	35.4	32.8	33.9	16.5	11.9	13.0
24	22.9	17.1	17.1	17.1	25.5	53.6	35.9	34.5	33.3	17.1	11.6	13.6
25	22.6	17.1	18.8	18.8	26.1	55.4	37.1	35.9	31.9	16.8	11.0	15.4
26	21.7	16.8	18.3	18.6	26.4	56.5	38.3	36.8	31.3	15.9	11.0	15.7
27	21.7	17.4	18.0	20.0	27.0	55.7	39.7	37.1	31.9	14.5	11.3	15.1
28	20.9	18.8	18.3	20.6	29.3	55.7	39.4	37.4	30.7	15.1	11.3	15.7
29	21.7		17.7	20.9	31.9	53.6	38.8	38.0	30.4	15.1	11.3	14.8
30	21.4		18.8	21.2	33.9	52.5	39.1	38.0	29.3	14.5	11.0	15.4
31	21.4		19.1		35.7		39.7	38.3		13.6		15.1
Avg	20.4	18.3	17.4	19.2	26.2	46.0	40.1	37.2	35.8	19.0	9.9	12.6
Results based on thesis research by Capt. Greg Strong, USAF, Naval Postgraduate School, March 2012												

Table 13. Daily probabilities of violating the thick cloud LLCC after smoothing the initial probabilities with a 15-day center weighted running mean smoother.

Probabilities of Thick Cloud Rule LLCC Violation												
	12Z											
	Jan	Feb	Mar	Apr	May	Jun	Jul	Aug	Sep	Oct	Nov	Dec
1	16.8	16.8	15.4	18.3	20.6	31.9	44.6	28.7	30.4	25.2	10.4	13.9
2	16.5	16.8	16.8	18.3	20.6	31.9	43.5	29.3	30.4	25.2	9.9	16.2
3	16.5	17.7	16.5	18.0	20.6	32.5	41.2	29.9	30.7	26.4	9.3	15.9
4	16.8	17.1	16.2	18.8	20.9	32.8	40.0	29.0	30.1	25.8	8.7	16.5
5	16.5	16.8	16.8	20.3	20.6	31.9	38.8	29.0	29.9	24.1	7.5	17.4
6	15.9	17.1	16.8	20.3	21.7	33.3	38.3	30.4	30.4	22.0	7.8	18.3
7	15.9	16.8	17.1	19.7	22.9	31.9	36.8	30.7	32.2	20.3	7.0	18.3
8	15.9	17.4	16.2	20.9	21.4	31.0	36.8	30.4	31.3	19.7	7.0	17.7
9	15.7	17.7	16.2	20.9	20.9	30.7	35.9	29.3	31.0	20.0	7.0	18.3
10	14.5	17.4	16.8	20.9	21.4	30.1	34.5	29.0	29.9	18.8	7.2	18.6
11	13.9	16.8	16.5	21.7	21.7	31.3	33.0	27.2	29.6	17.1	7.0	18.8
12	13.0	17.4	17.1	22.3	22.6	31.0	33.6	27.2	28.1	16.8	6.4	19.1
13	13.3	17.4	16.8	22.3	22.3	31.3	32.8	27.5	27.5	15.9	7.0	19.7
14	13.3	17.1	16.8	21.4	22.6	31.3	31.3	27.2	26.1	15.9	7.0	18.6
15	14.2	17.1	17.1	20.0	23.2	31.3	31.6	26.7	25.8	15.4	7.5	18.6
16	13.9	17.4	16.8	19.7	23.8	31.3	31.9	27.0	25.5	15.4	7.5	18.6
17	14.5	18.0	15.4	19.7	24.3	33.0	31.3	27.5	25.5	14.5	7.2	17.4
18	14.5	17.1	15.4	20.3	24.3	35.4	30.7	27.5	24.9	13.0	8.1	18.0
19	13.6	17.1	15.4	19.1	24.1	37.1	29.6	27.2	25.8	12.2	8.4	17.7
20	13.9	16.2	15.7	18.6	24.3	38.3	30.1	27.8	26.7	11.9	8.7	17.4
21	15.1	16.5	15.1	18.6	24.9	39.7	28.4	27.0	27.2	12.8	8.4	17.4
22	14.5	16.5	15.7	18.3	23.2	41.7	29.0	25.8	27.0	12.5	9.3	17.1
23	14.8	16.5	17.4	19.1	24.1	43.5	28.4	24.9	26.7	12.2	9.6	18.0
24	14.2	16.2	16.5	20.0	24.9	44.3	28.4	27.0	26.7	11.3	10.1	18.0
25	15.4	15.7	15.7	20.0	25.8	46.4	27.8	27.2	27.0	11.3	10.7	18.0
26	16.2	15.7	15.7	19.7	27.2	47.0	27.2	29.0	27.0	11.3	11.9	17.7
27	16.8	15.4	15.1	19.7	26.4	46.1	27.2	29.3	27.2	11.0	12.8	17.1
28	16.5	15.4	15.7	20.3	27.8	46.1	27.5	29.9	27.2	11.6	11.6	18.0
29	16.8		15.9	20.3	28.7	46.4	27.5	30.1	27.0	11.0	13.0	17.7
30	16.2		16.8	20.9	29.9	44.9	27.5	30.7	26.1	11.3	13.3	17.1
31	16.8		17.7		31.6		28.4	30.7		10.7		17.4
Avg	15.3	16.8	16.3	19.9	23.9	36.5	32.7	28.4	28.0	16.2	8.9	17.7
Results based on thesis research by Capt. Greg Strong, USAF, Naval Postgraduate School, March 2012												

Table 14. Daily probabilities of violating the thick cloud LLCC after smoothing the initial probabilities with a 15-day center weighted running mean smoother.

Jan 1988 -Dec 2010			Mean Cloud Thickness (ft)		
	Month	Total Obs	Low	Mid	High
00Z	Jan	713	1586	5206	4109
	Feb	644	1757	4648	3927
	Mar	713	3399	4369	4391
	April	690	4948	5618	4688
	May	713	7481	5662	5677
	Jun	690	9473	6730	7502
	Jul	713	9746	6437	7251
	Aug	713	9487	6533	7030
	Sep	690	7141	6584	6581
	Oct	713	5174	5370	5585
	Nov	690	3464	3574	4561
	Dec	713	1772	3873	4300
	Totals	8395	5452	5384	5467

Table 15. Table of values for 00Z monthly mean cloud thicknesses as calculated by modified CFSR process.

Jan 1988 -Dec 2010			Mean Cloud Thickness (ft)		
	Month	Total Obs	Low	Mid	High
12Z	Jan	713	2034	4253	3873
	Feb	644	2133	4491	3681
	Mar	713	4011	4041	3813
	April	690	5437	5120	4301
	May	713	7528	5455	4925
	Jun	690	9716	5945	6503
	Jul	713	10115	5596	6571
	Aug	713	9726	5763	5958
	Sep	690	7100	5910	5575
	Oct	713	5445	5059	5033
	Nov	690	3780	3470	4359
	Dec	713	2123	5400	4147
	Totals	8395	5762	5042	4895

Table 16. Table of values for 12Z monthly mean cloud thicknesses as calculated by modified CFSR process.

THIS PAGE INTENTIONALLY LEFT BLANK

APPENDIX B. FIGURES VALID FOR 00Z

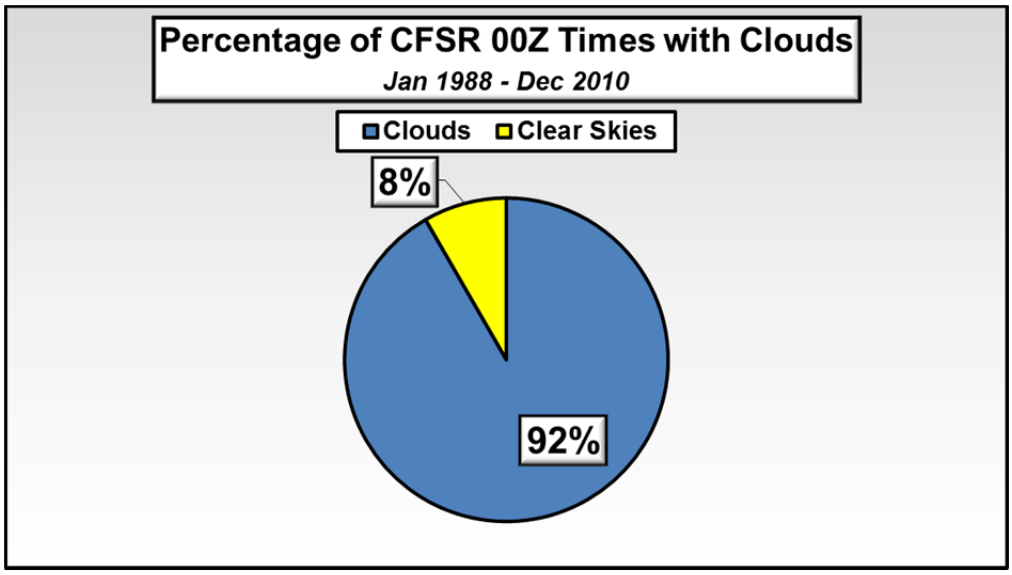

Figure 48. Percentage of all 00Z times in the study period for which CFSR indicated clouds (blue) and clear skies (yellow).

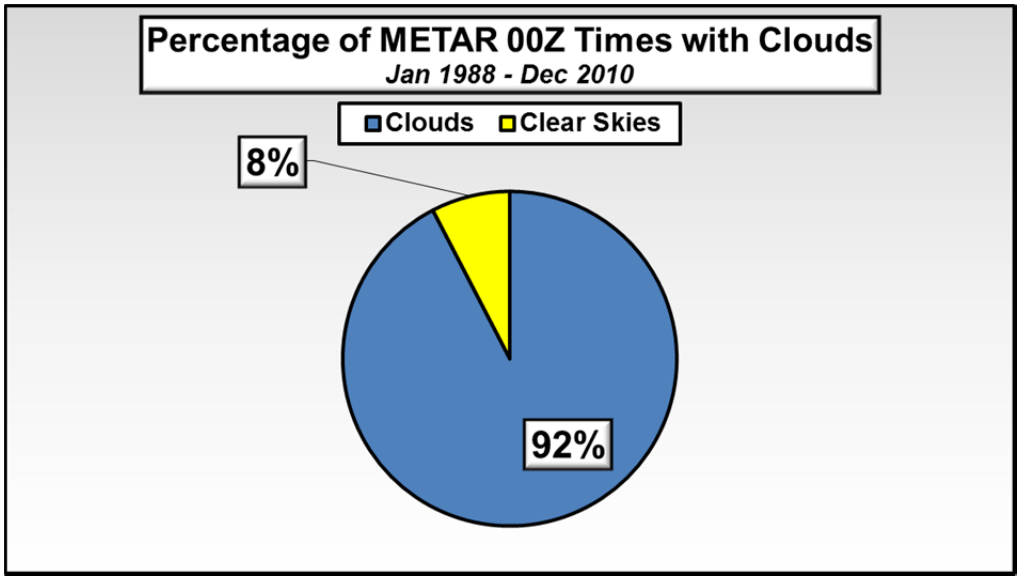

Figure 49. Percentage of all 00Z times in the study period for which METAR indicated clouds (blue) and clear skies (yellow).

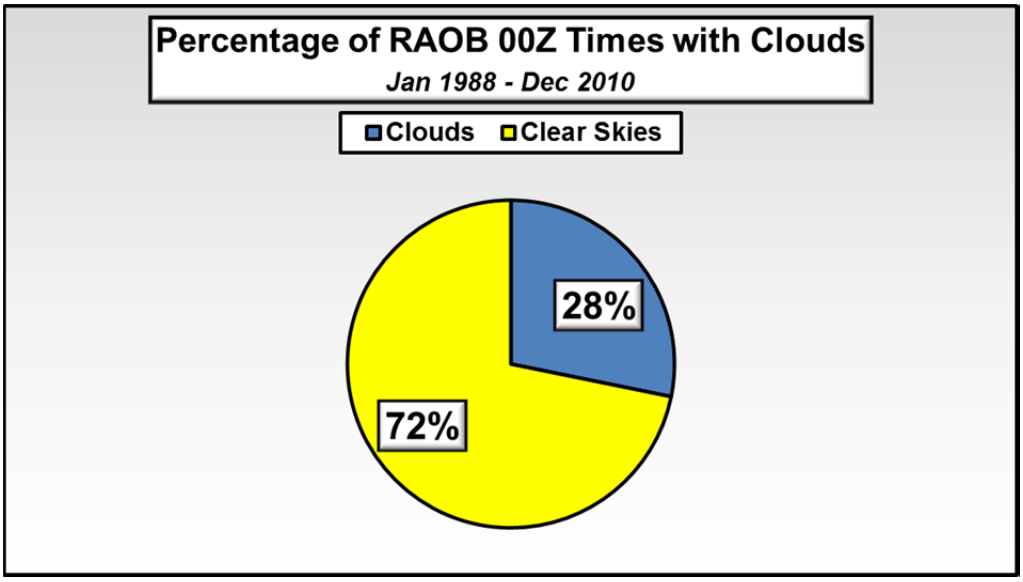

Figure 50. Percentage of all 00Z times in the study period for which RAOB indicated clouds (blue) and clear skies (yellow).

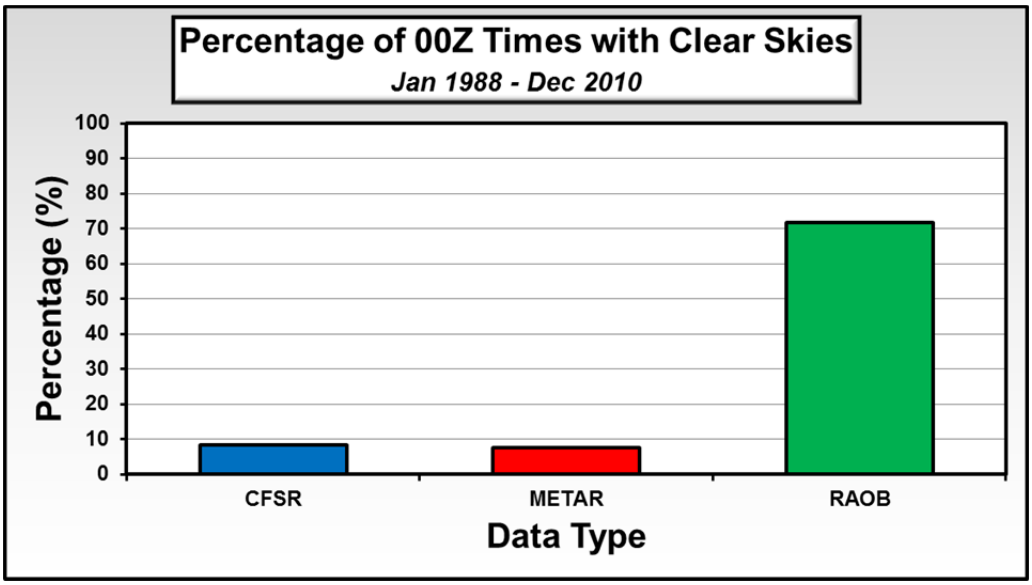

Figure 51. Percentage of all 00Z times in the study period for which the CFSR, METAR, and RAOB data sets indicated clear skies.

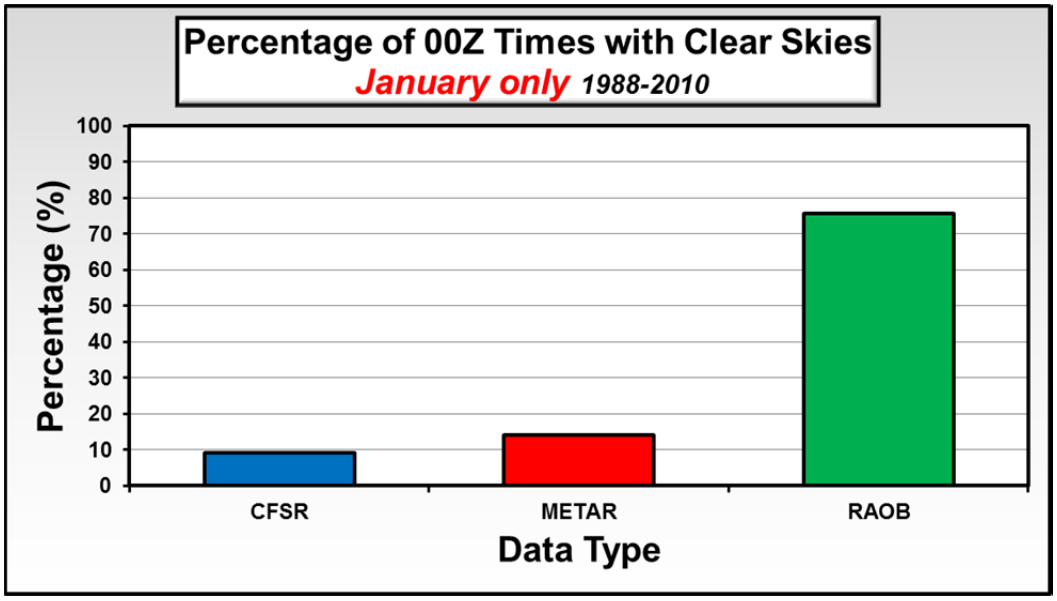

Figure 52. Percentage of all January 00Z times in the study period for which the CFSR, METAR, and RAOB data sets indicated clear skies.

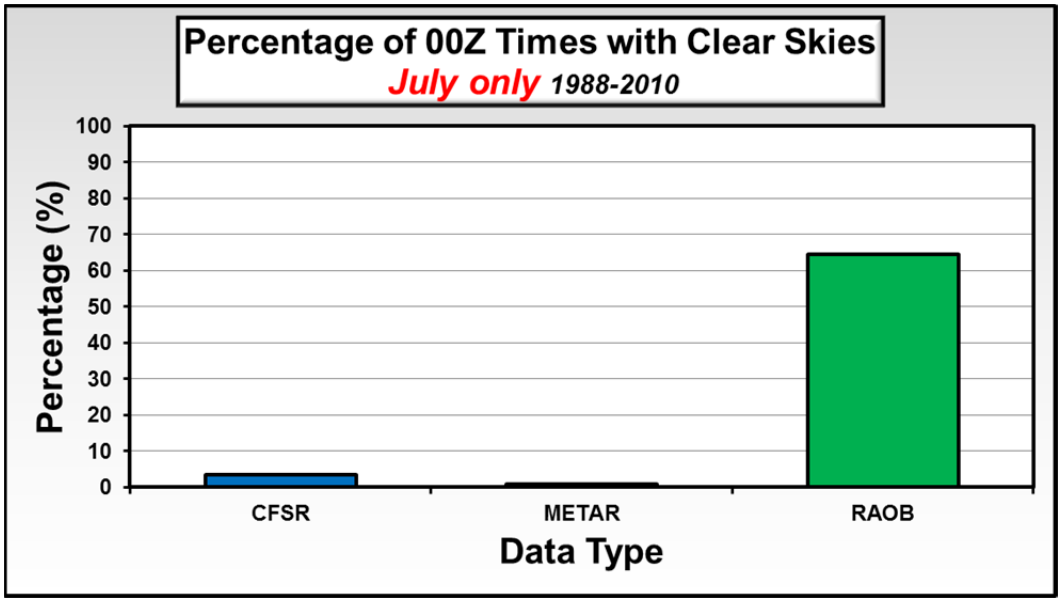

Figure 53. Percentage of all July 00Z times in the study period for which the CFSR, METAR, and RAOB data sets indicated clear skies.

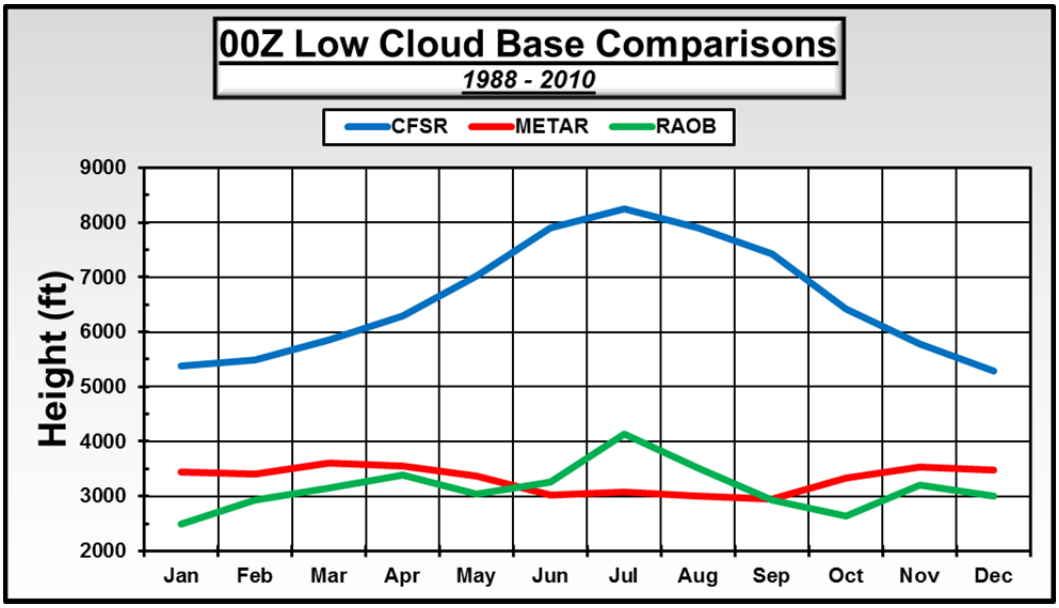

Figure 54. Monthly average low cloud base heights for each data set from 1988–2010.

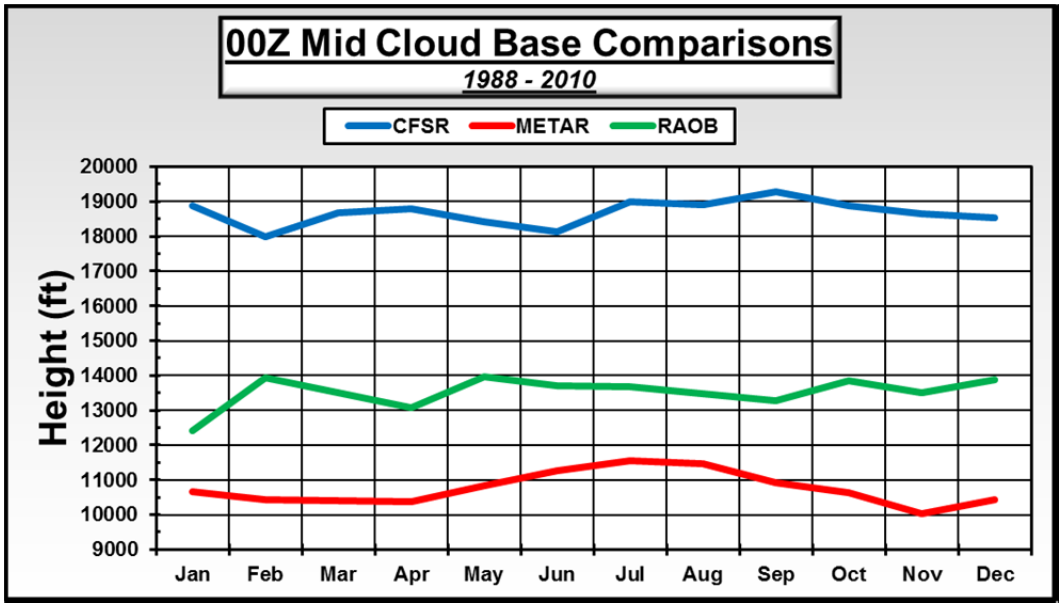

Figure 55. Monthly average mid cloud base heights for each data set from 1988–2010.

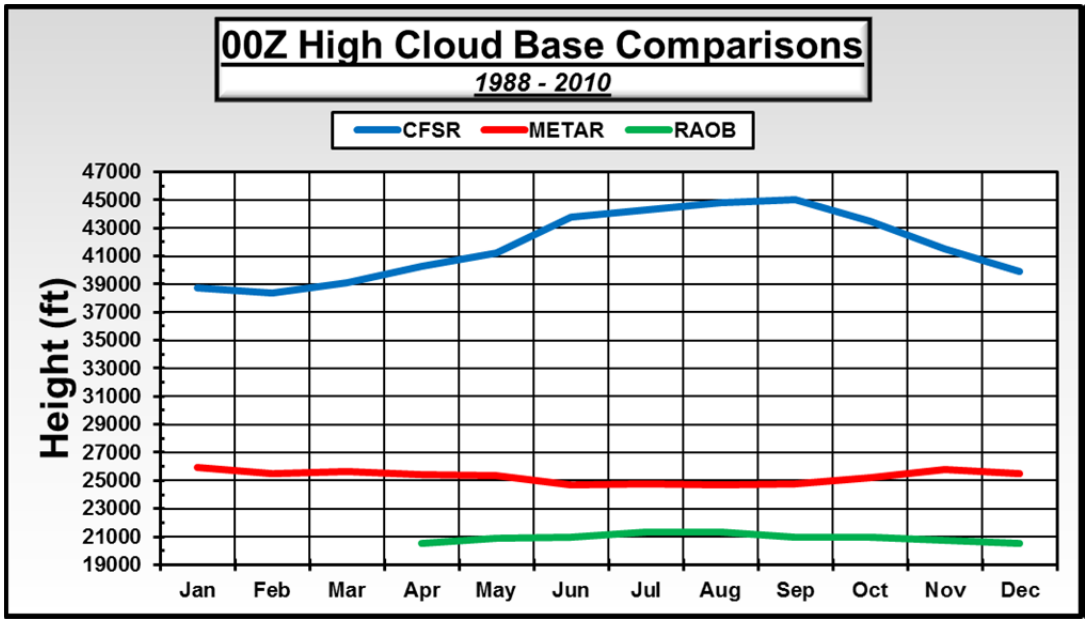

Figure 56. Monthly average high cloud base heights for each data set from 1988–2010.

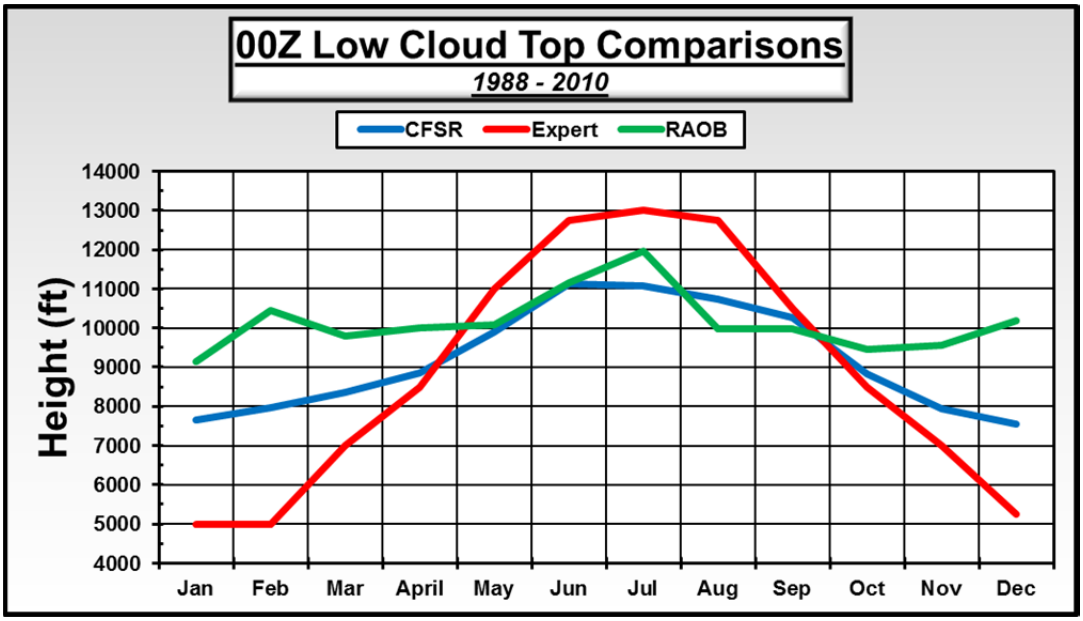

Figure 57. Monthly average low cloud top heights for each data set from 1988–2010.

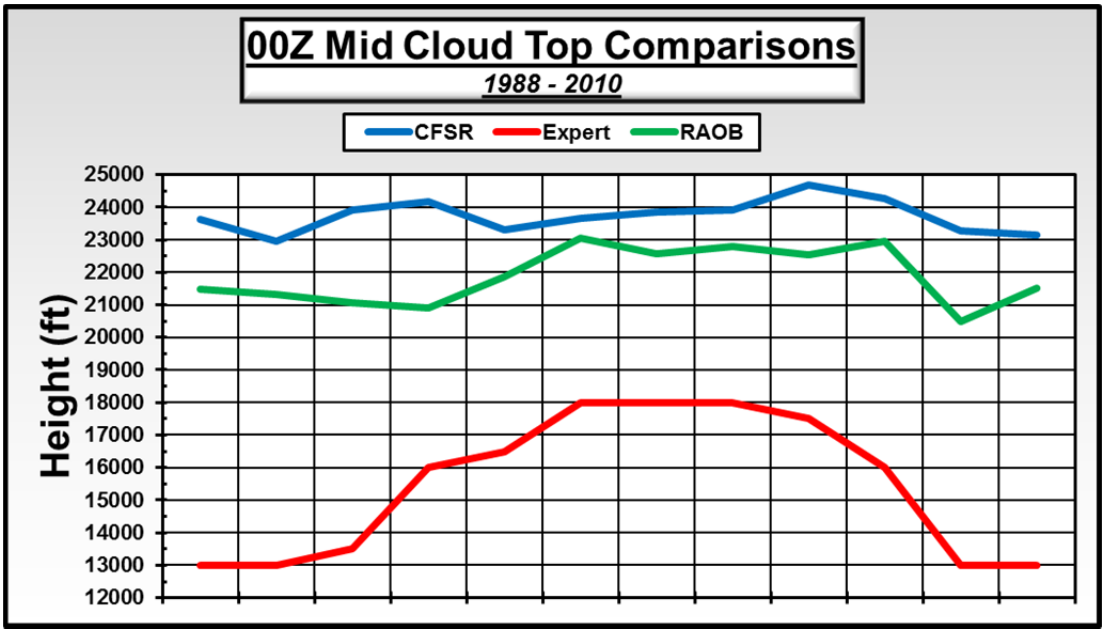

Figure 58. Monthly average mid cloud top heights for each data set from 1988–2010.

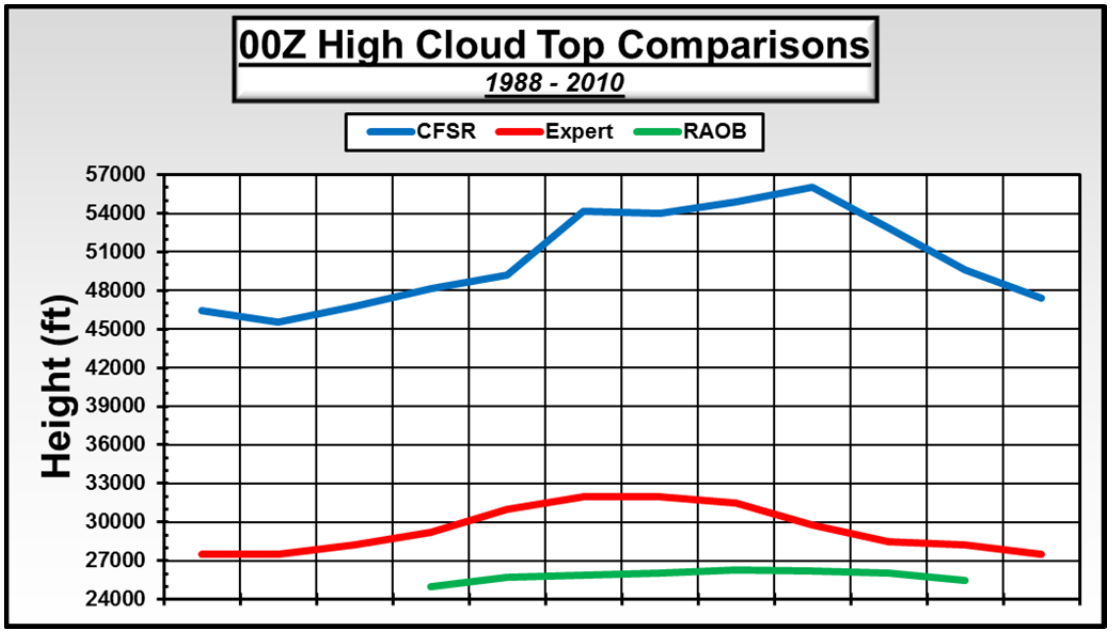

Figure 59. Monthly average high cloud top heights for each data set from 1988–2010.

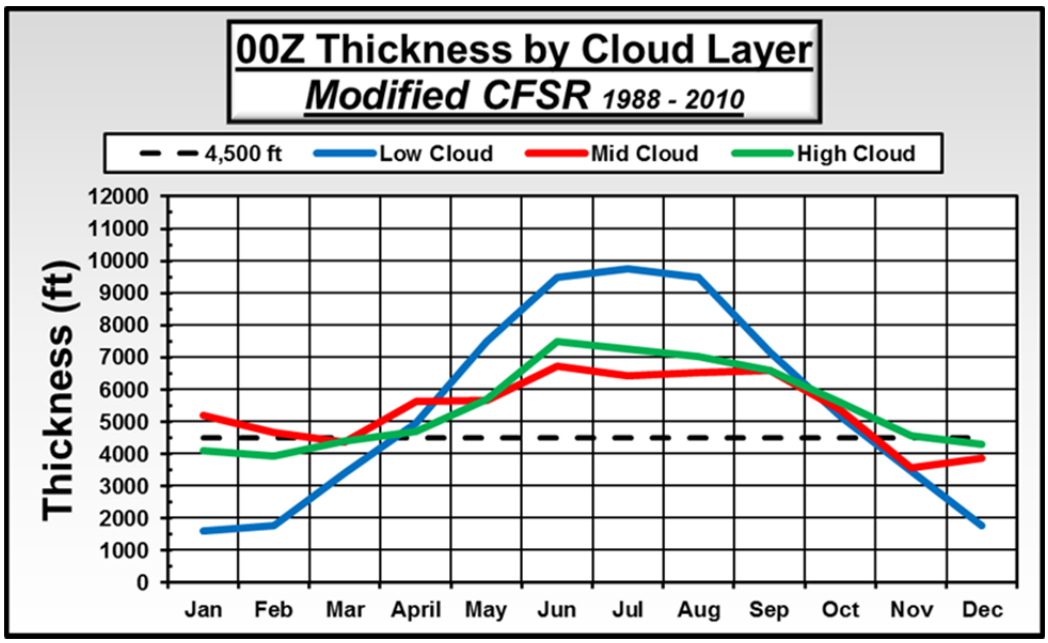

Figure 60. Monthly average cloud thicknesses by cloud layer based on the modified CFSR data set. The dashed black line represents the 4,500 ft thickness threshold in the thick cloud LLCC.

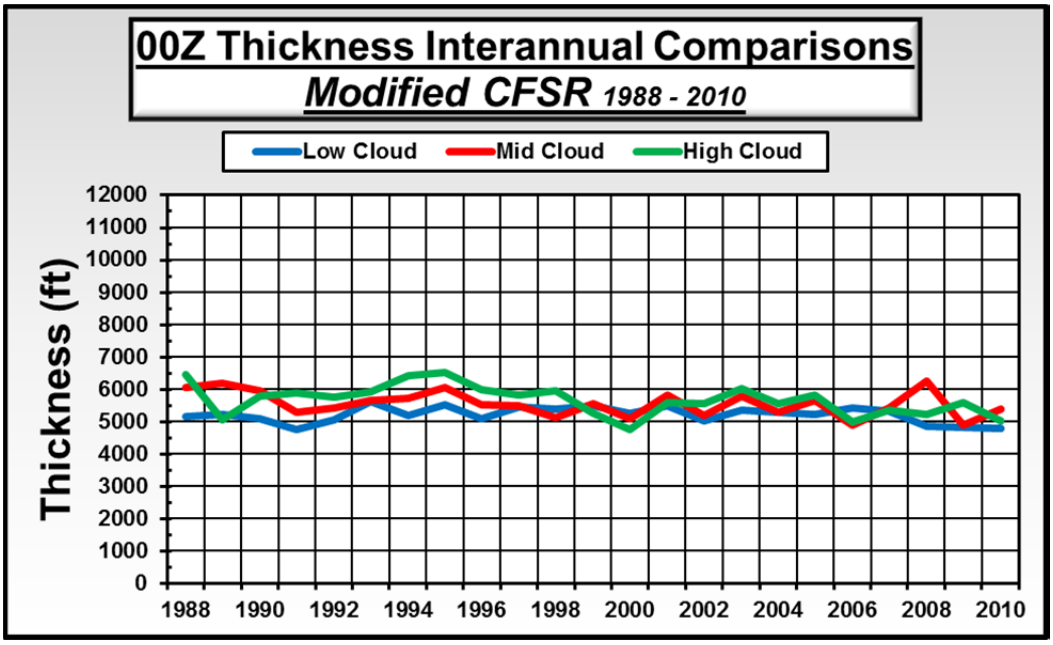

Figure 61. Interannual variation of cloud thickness separated by layer for 1988–2010 based on the modified CFSR data set.

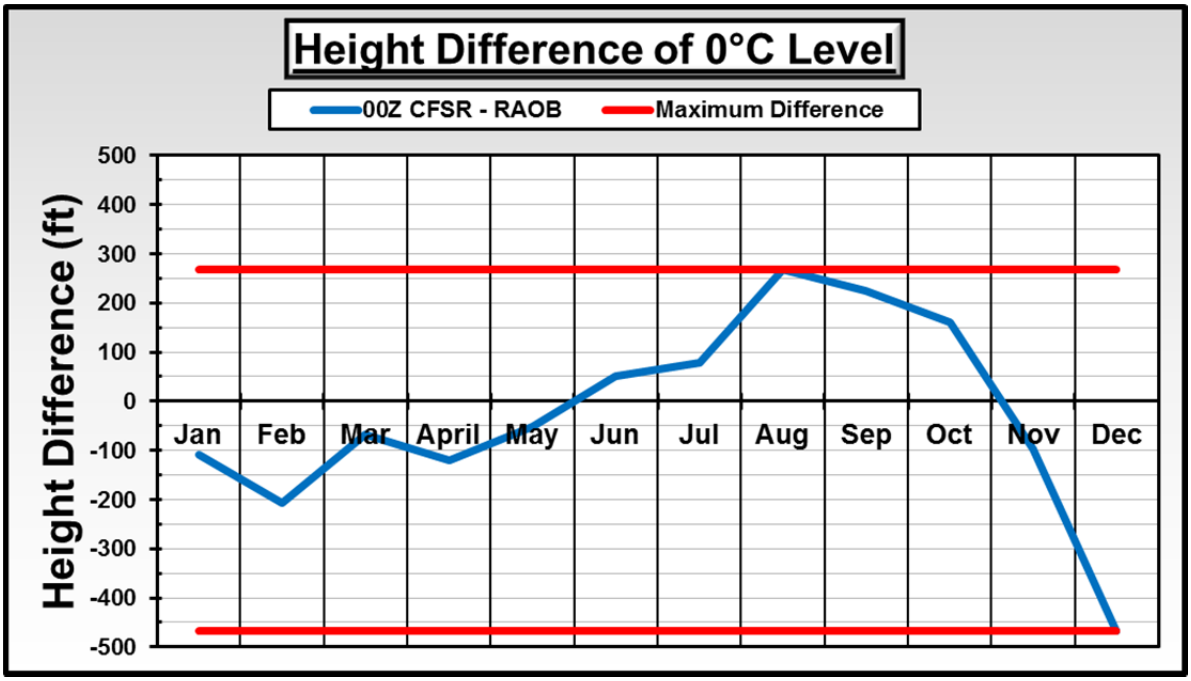

Figure 62. Monthly average difference between the CFSR 0° C height level and the RAOB 0° C height level (CFSR minus RAOB) in feet. Results based on 00Z values for all years in the study period. The red lines mark the largest differences. The average difference for all months was 28 feet.

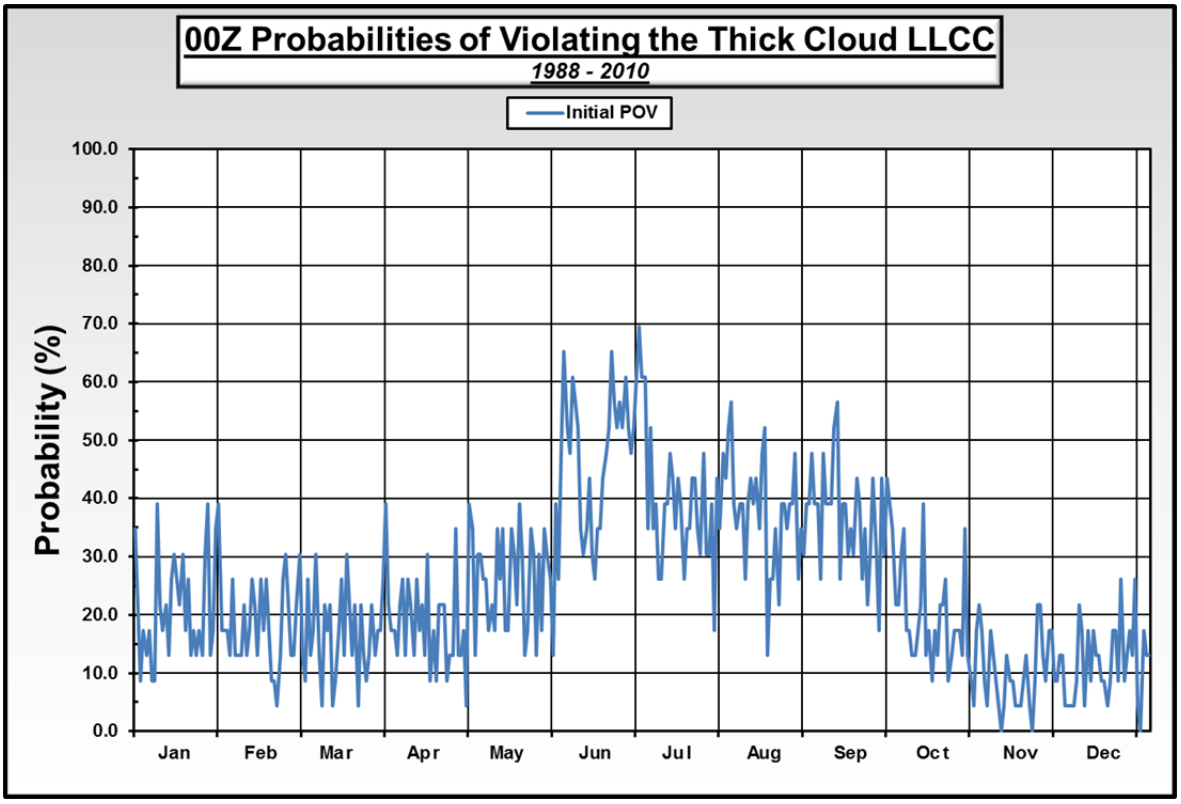

Figure 63. Daily probabilities of violating the thick cloud LLCC with no smoothing of the daily values. The probabilities are for each day of the year from 1 January through 31 December based on the modified CFSR data set for January 1988–December 2010. Note the large day-to-day variations in the absence of any temporal smoothing.

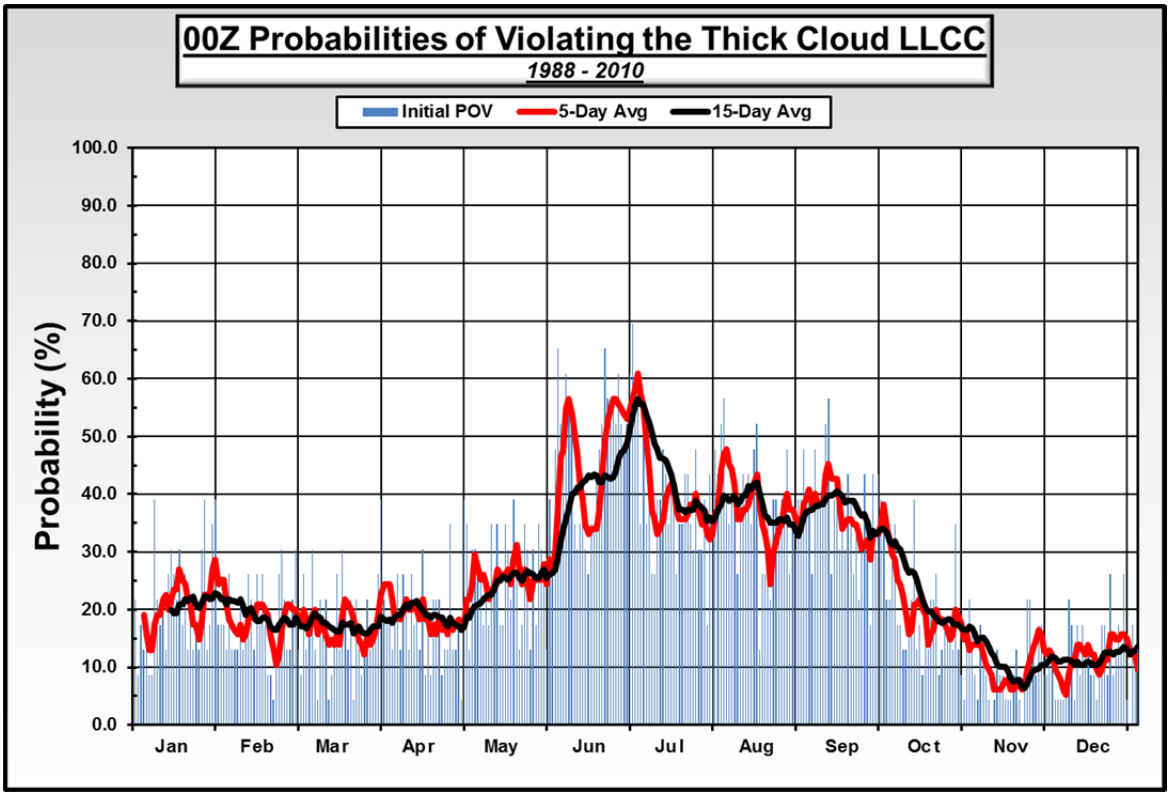

Figure 64. Daily probabilities of violating the thick cloud LLCC with no smoothing of the daily values (blue) with overlays of 5 and 15-day center weighted running means of the probabilities. The probabilities are for each day of the year from 1 January through 31 December based on the modified CFSR data set for January 1988–December 2010. Note the smaller day-to-day variations in the running mean probabilities, especially the 15-day running mean probabilities.

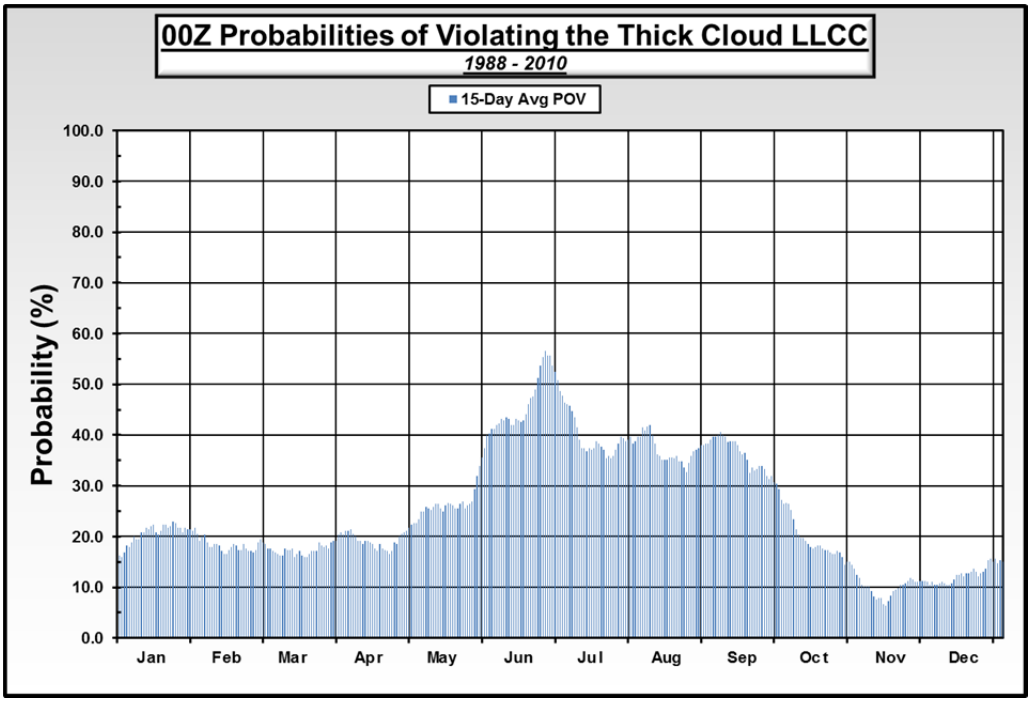

Figure 65. Daily probabilities of violating the thick cloud LLCC after applying a 15-day center weighted running mean smoothing of the initial probabilities (Figure 34). The probabilities are for each day of the year from 1 January through 31 December based on the modified CFSR data set for January 1988–December.

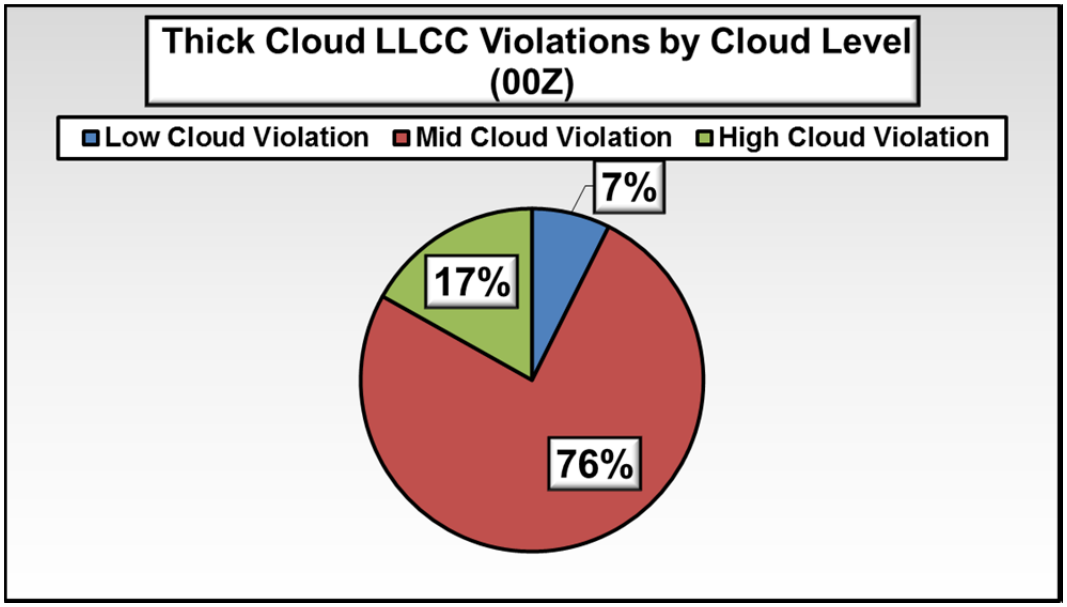

Figure 66. Percentage of 00Z thick cloud LLCC violations by cloud layer.

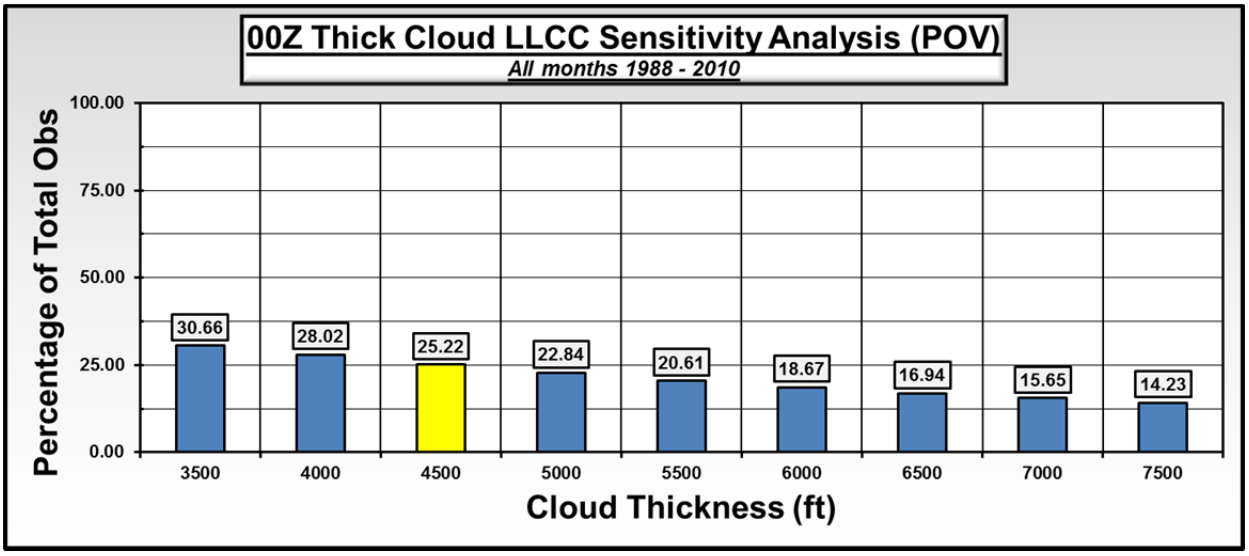

Figure 67. Daily mean climatological probabilities of violating the thick cloud LLCC based on using alternative thickness thresholds rather than the present threshold of 4,500 ft. The alternative thresholds are shown on the horizontal axis.

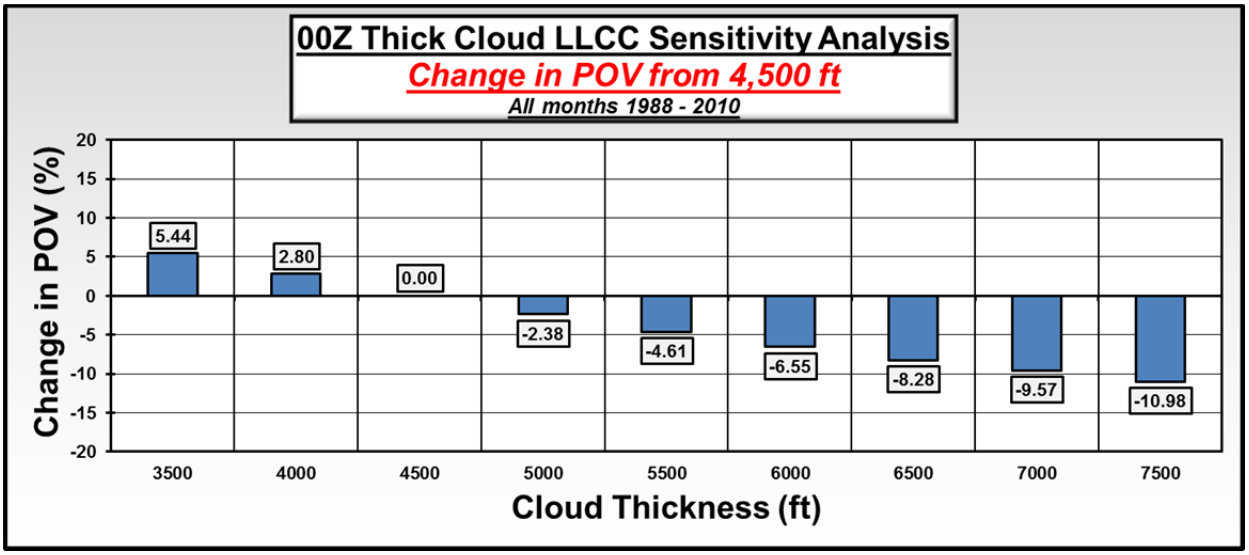

Figure 68. Daily mean change in the climatological probabilities of violating the thick cloud LLCC based on using alternative thickness thresholds rather than the present threshold of 4,500 ft. The alternative thresholds are shown on the horizontal axis.

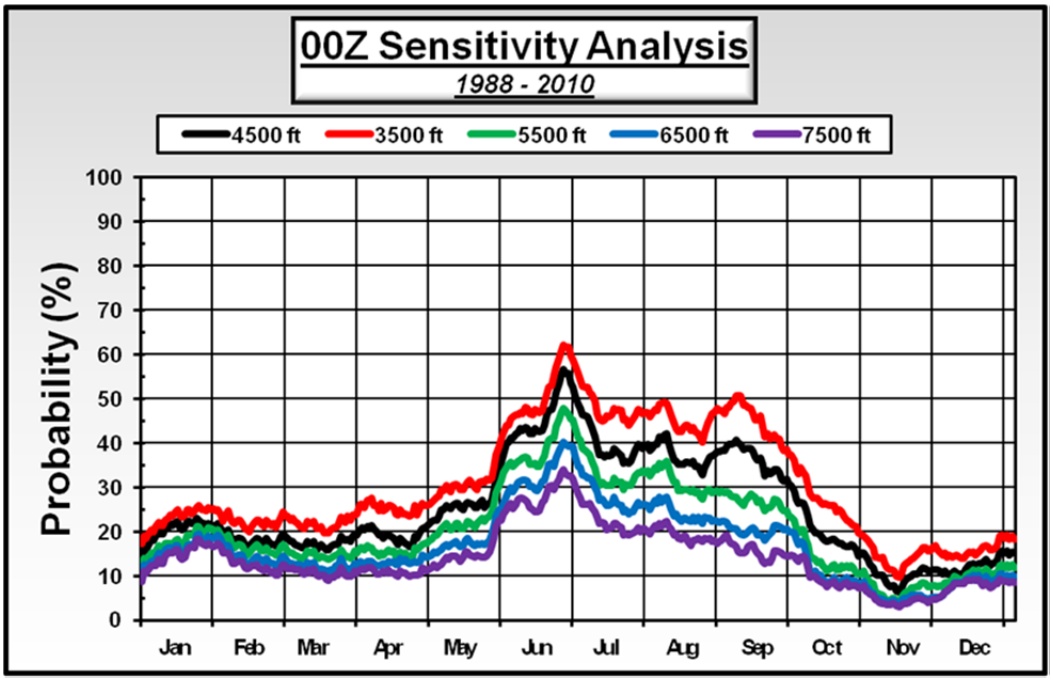

Figure 69. Daily probabilities of violating the thick cloud LLCC when using a thickness threshold of 3,500 ft (red), 4,500 ft (black), 5,500 ft (green), 6,500 ft (blue) and 7,500 ft (purple). The probabilities have been smoothed using a 15-day center weighted running mean smoother. The probabilities are for each day of the year from 1 January through 31 December based on the modified CFSR data set for January 1988–December 2010.

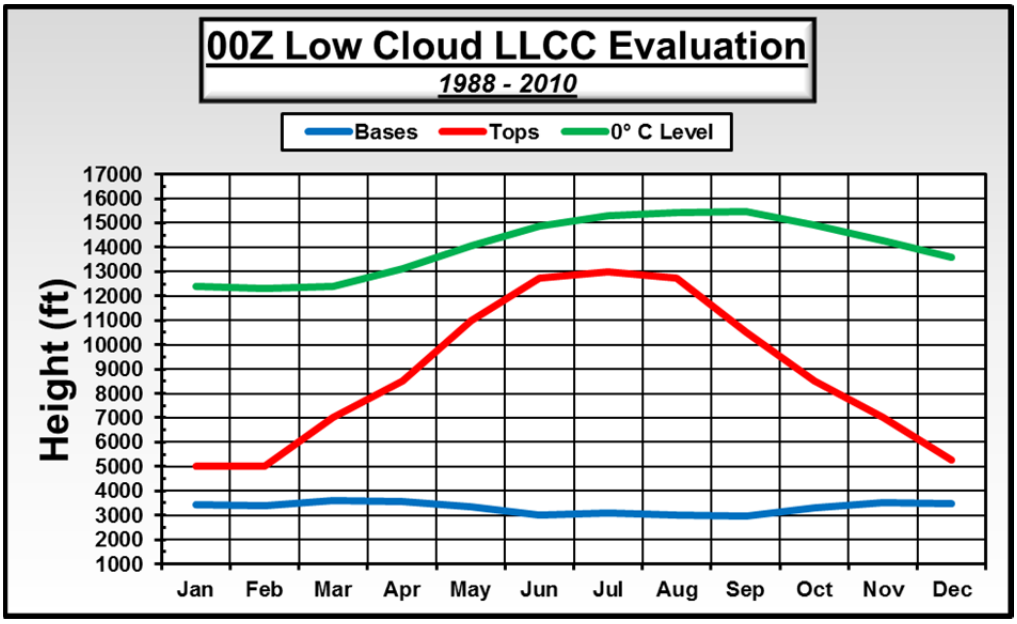

Figure 70. Monthly average low cloud base heights and top heights, and the height of the 0° C level. Note that monthly average height of the 0° C level was located above the monthly average mid cloud base height and top height in all months.

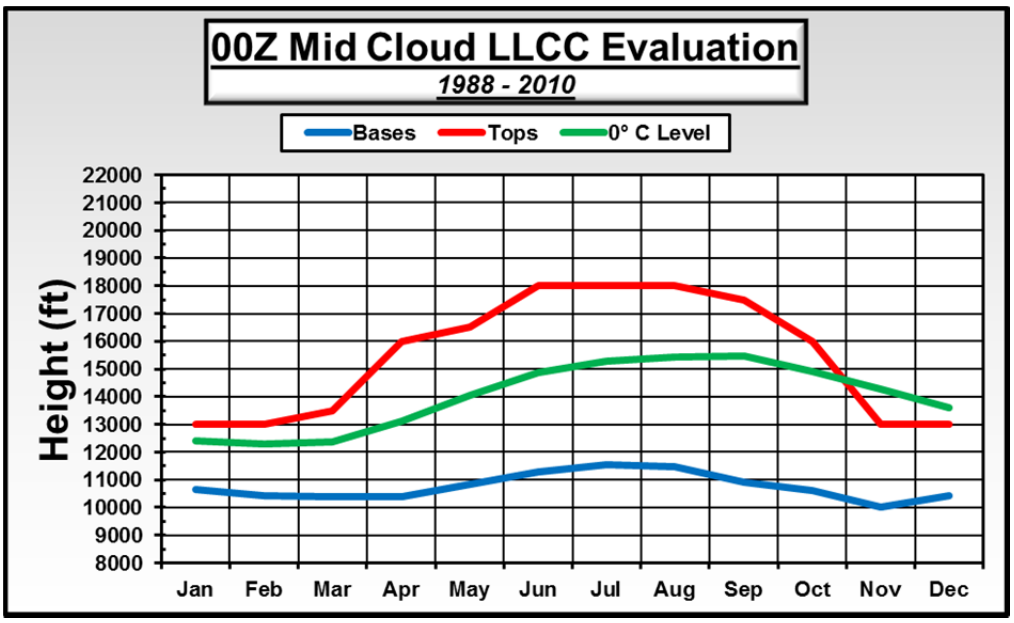

Figure 71. Monthly average mid cloud base heights and top heights, and the height of the 0° C level. Note that monthly average height of the 0° C level was located between the monthly average mid cloud base height and top height in all months except November and December. These results indicate that mid clouds tend to produce many of the violations of the thick cloud LLCC.

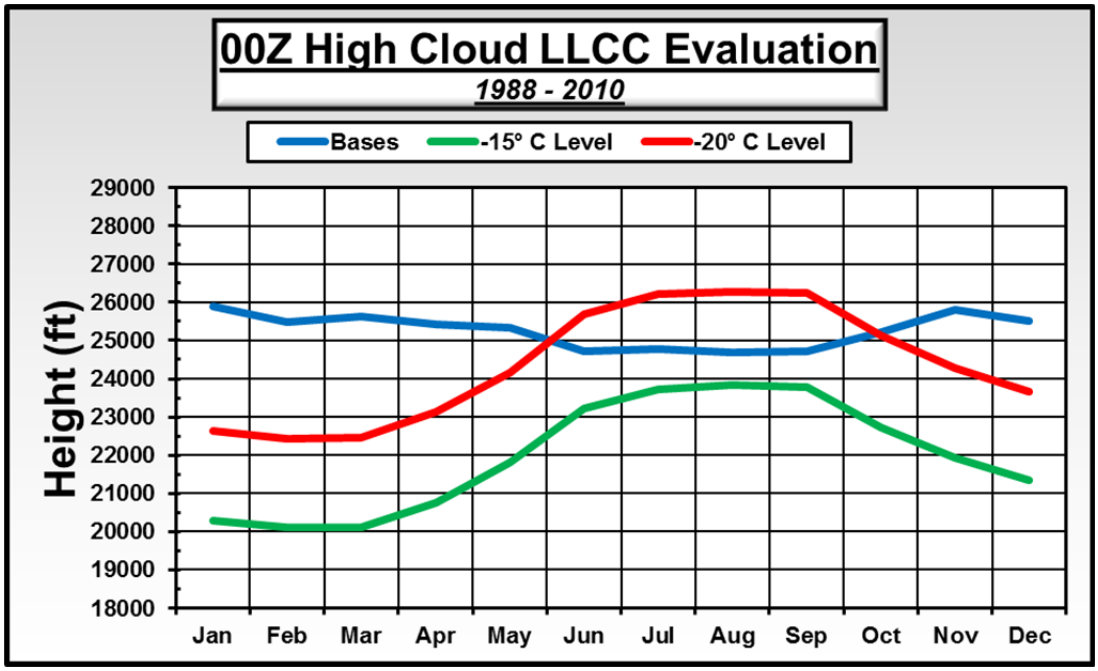

Figure 72. Monthly average high cloud base heights, and the heights of the -15° C and -20° C levels. High cloud top heights not shown because the high cloud base heights were the interacting cloud feature for determining thick cloud LLCC violations in this layer. Note that monthly average height of the -15° C level was located below the monthly average high cloud base height in all months.

THIS PAGE INTENTIONALLY LEFT BLANK

APPENDIX C. FIGURES VALID FOR 12Z

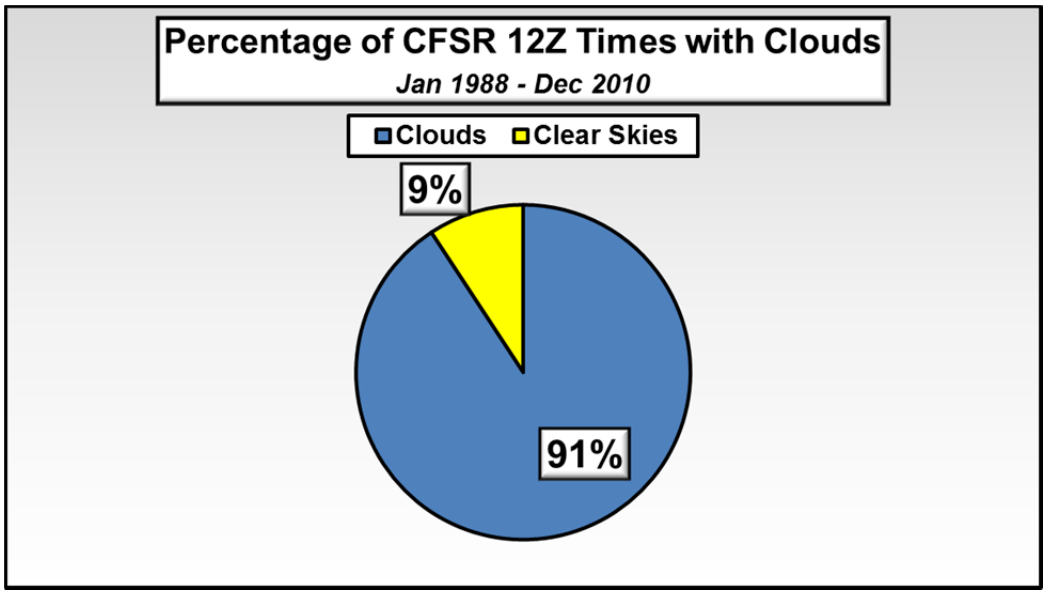

Figure 73. Percentage of all 12Z times in the study period for which CFSR indicated clouds (blue) and clear skies (yellow).

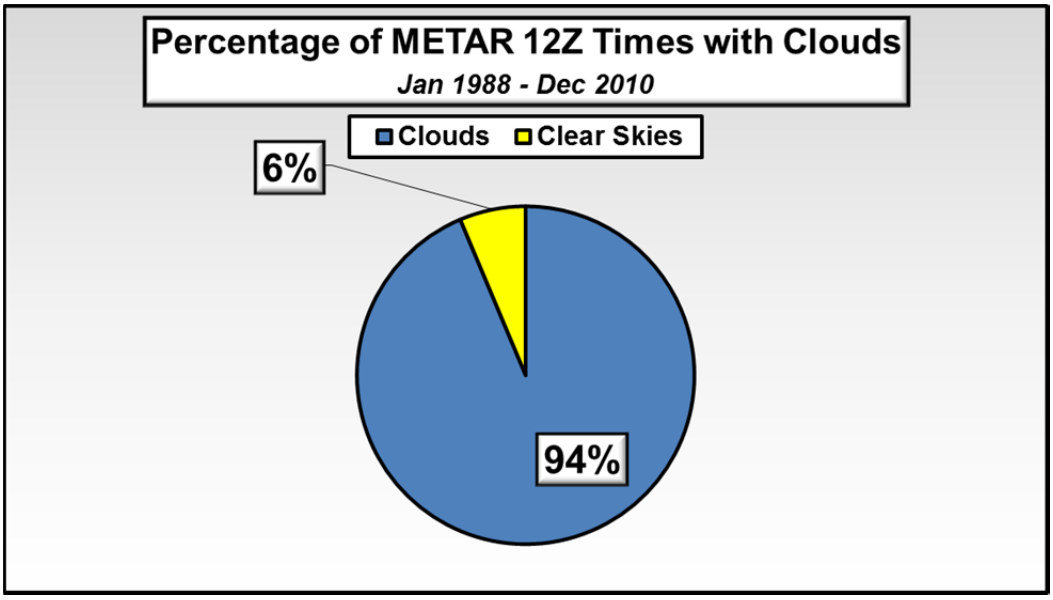

Figure 74. Percentage of all 12Z times in the study period for which METAR indicated clouds (blue) and clear skies (yellow).

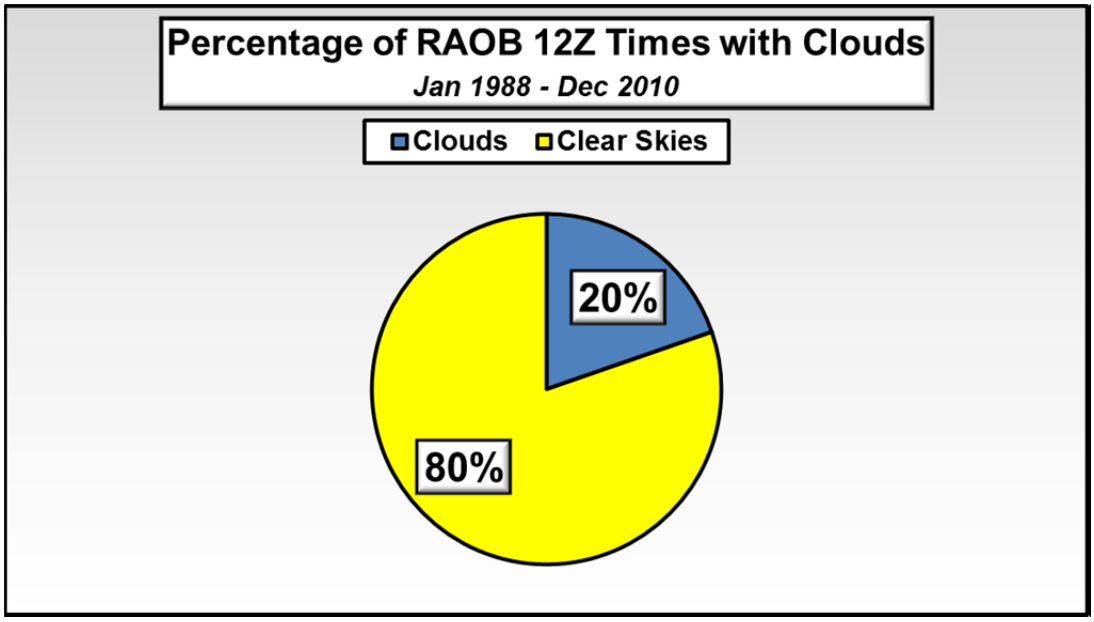

Figure 75. Percentage of all 12Z times in the study period for which RAOB indicated clouds (blue) and clear skies (yellow).

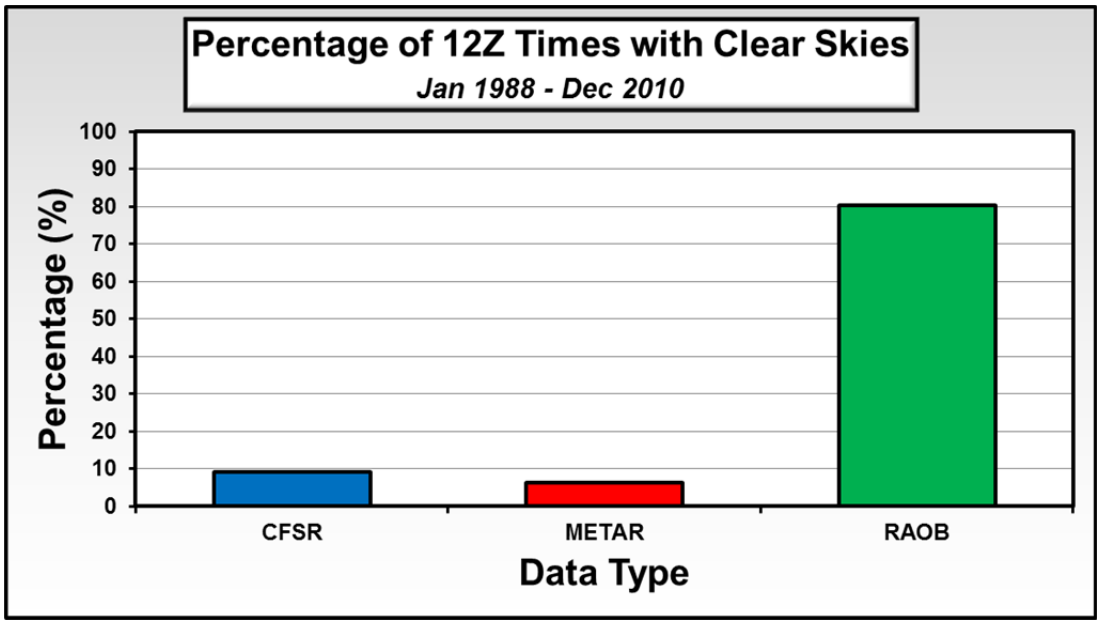

Figure 76. Percentage of all 12Z times in the study period for which the CFSR, METAR, and RAOB data sets indicated clear skies.

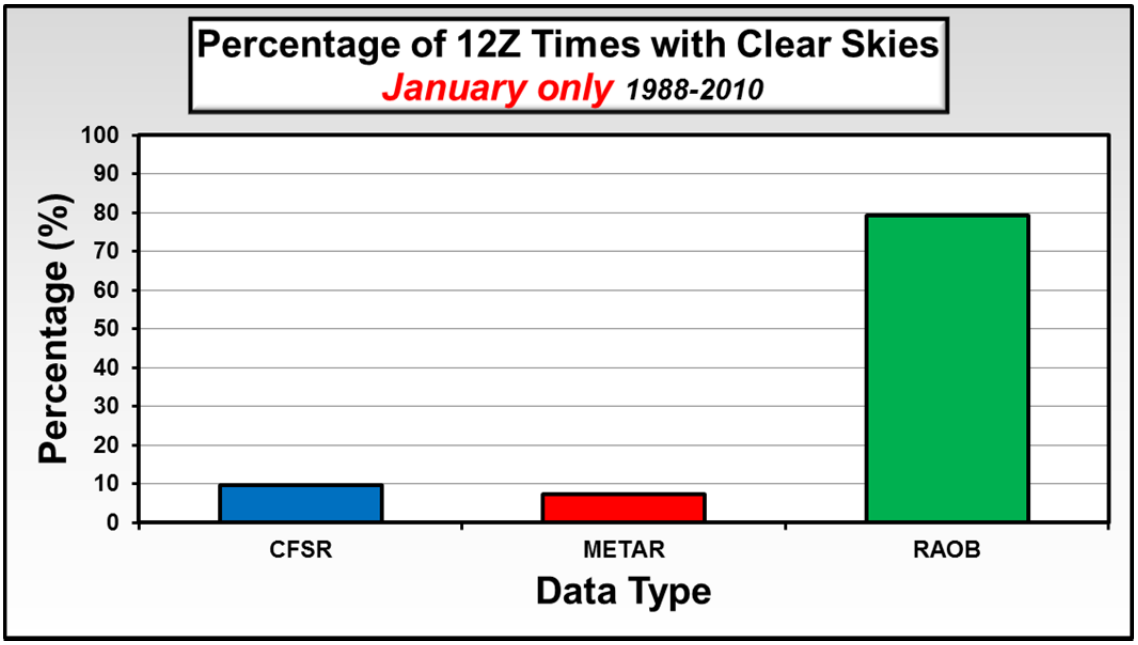

Figure 77. Percentage of all January 12Z times in the study period for which the CFSR, METAR, and RAOB data sets indicated clear skies.

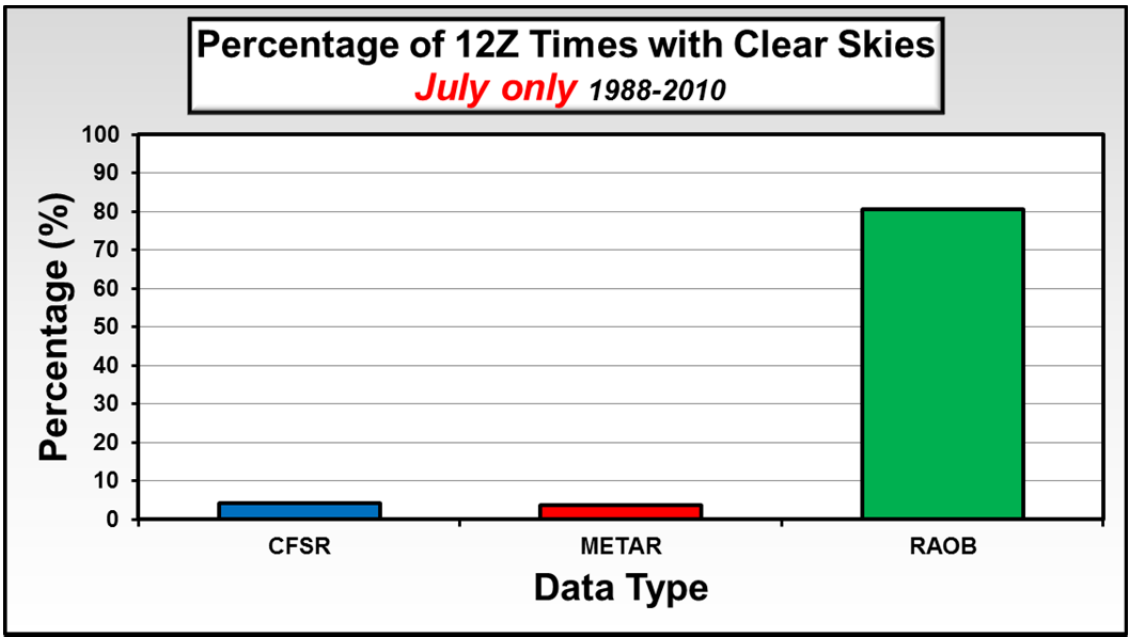

Figure 78. Percentage of all July 12Z times in the study period for which the CFSR, METAR, and RAOB data sets indicated clear skies.

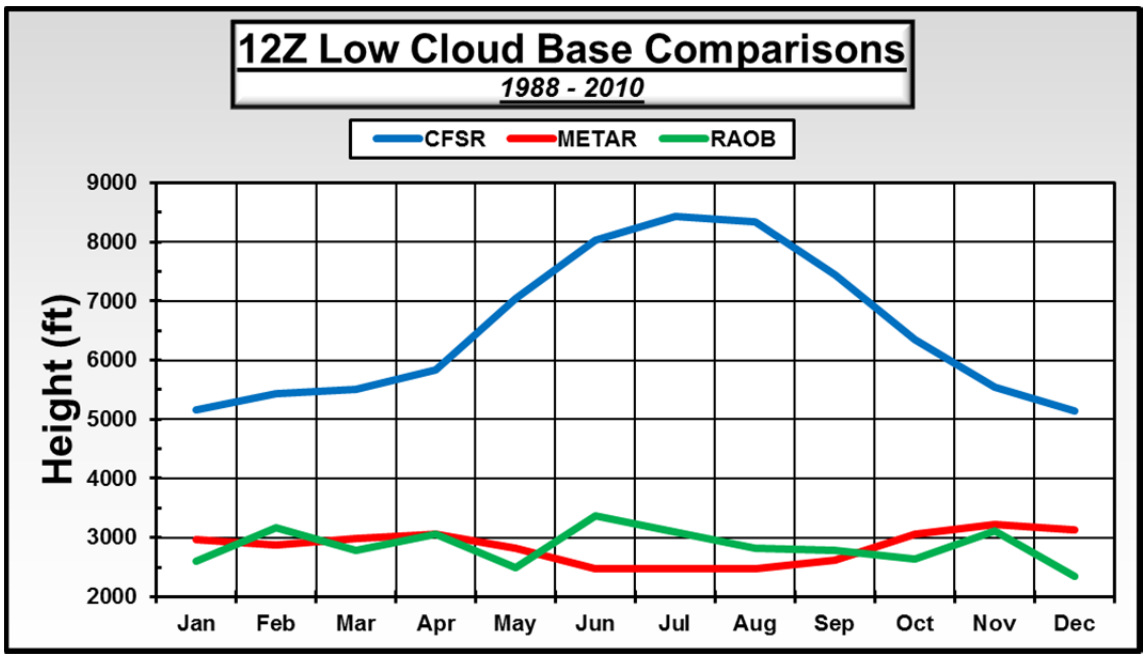

Figure 79. Monthly average low cloud base heights for each data set from 1988–2010.

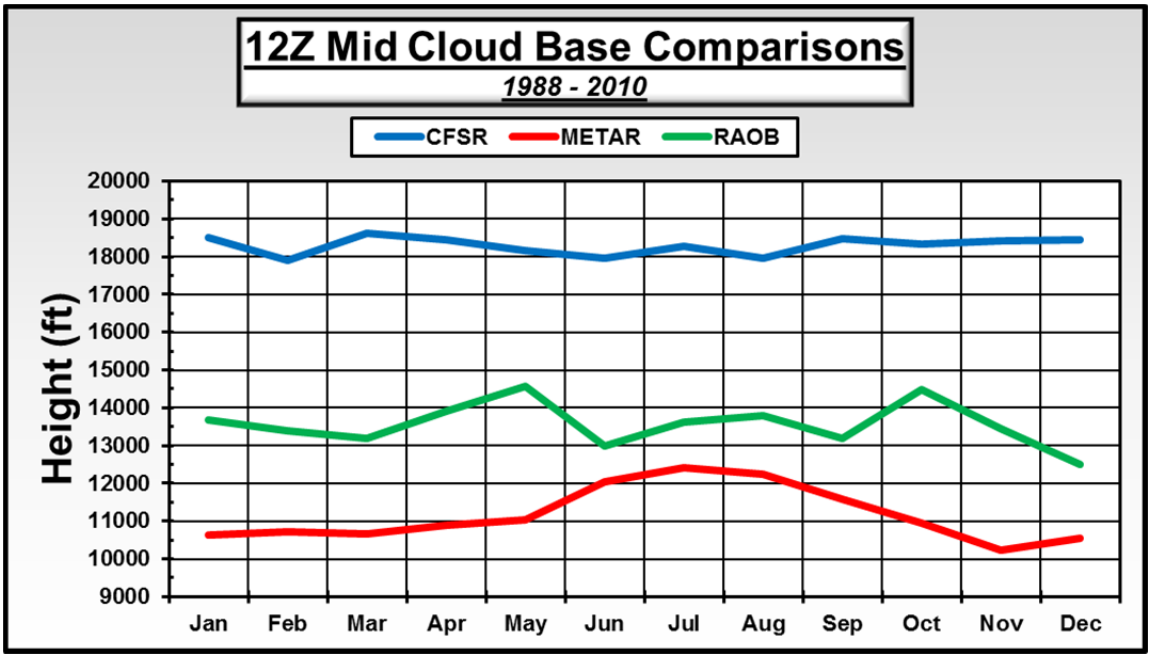

Figure 80. Monthly average mid cloud base heights for each data set from 1988–2010.

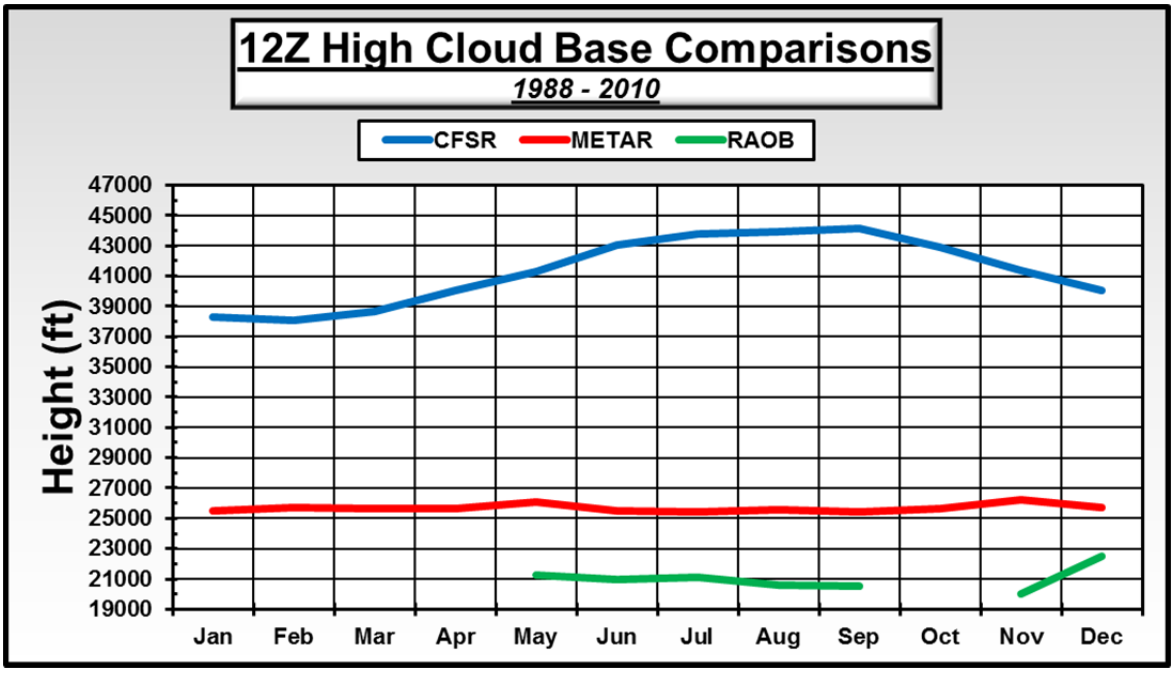

Figure 81. Monthly average low cloud base heights for each data set from 1988–2010.

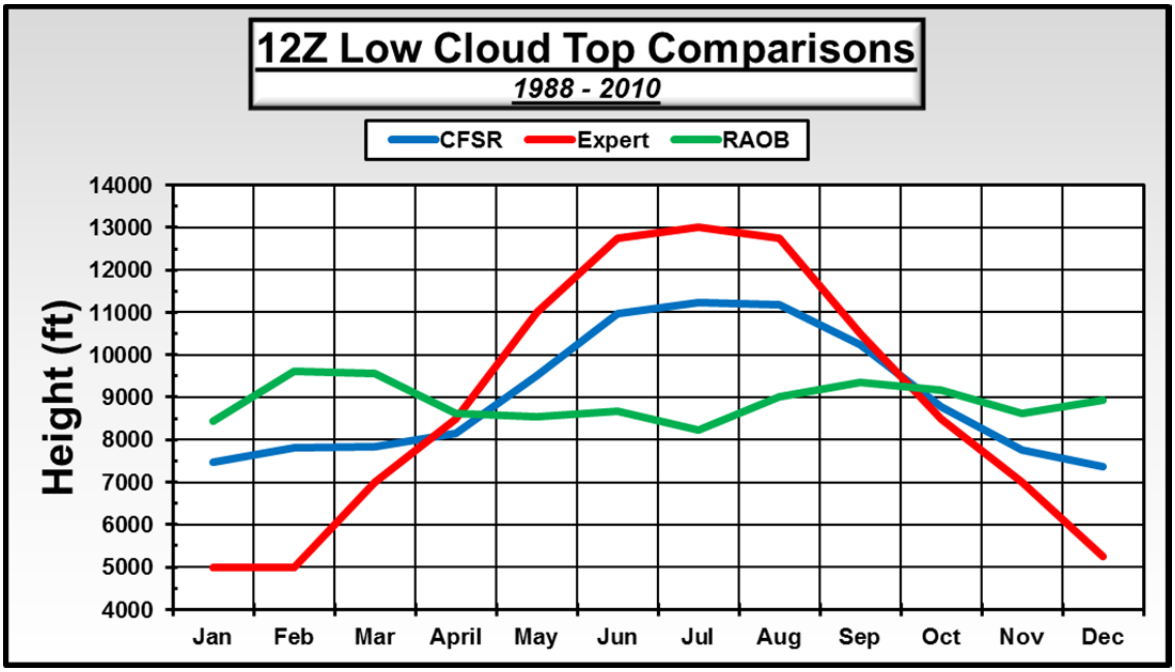

Figure 82. Monthly average low cloud top heights for each data set from 1988–2010.

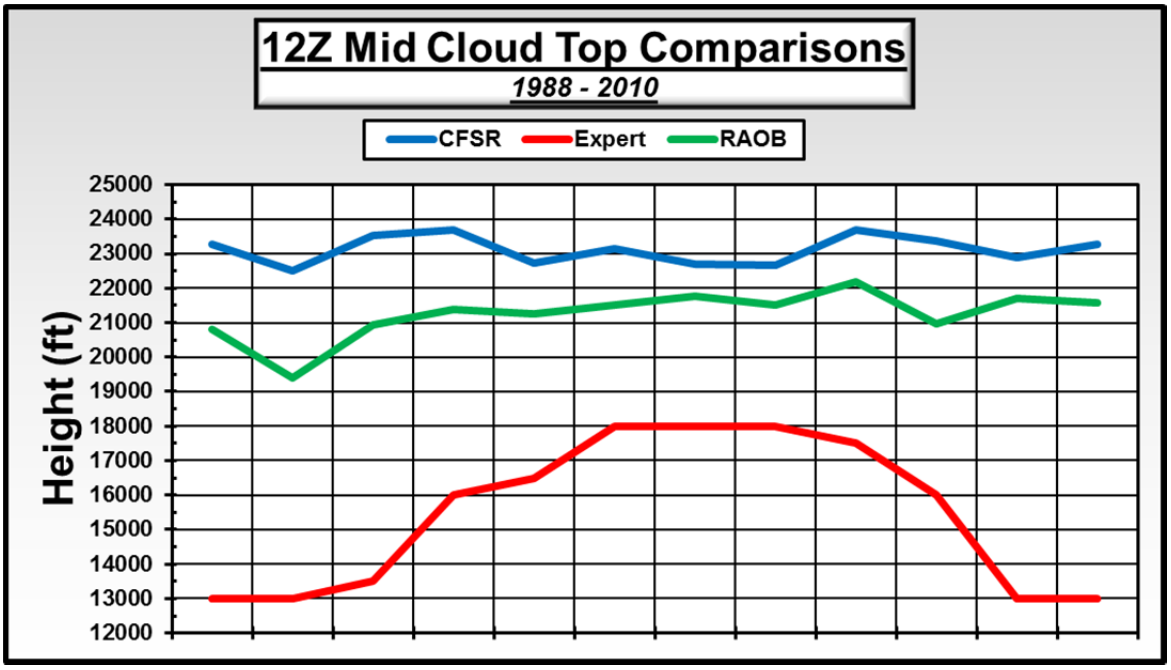

Figure 83. Monthly average mid cloud top heights for each data set from 1988–2010.

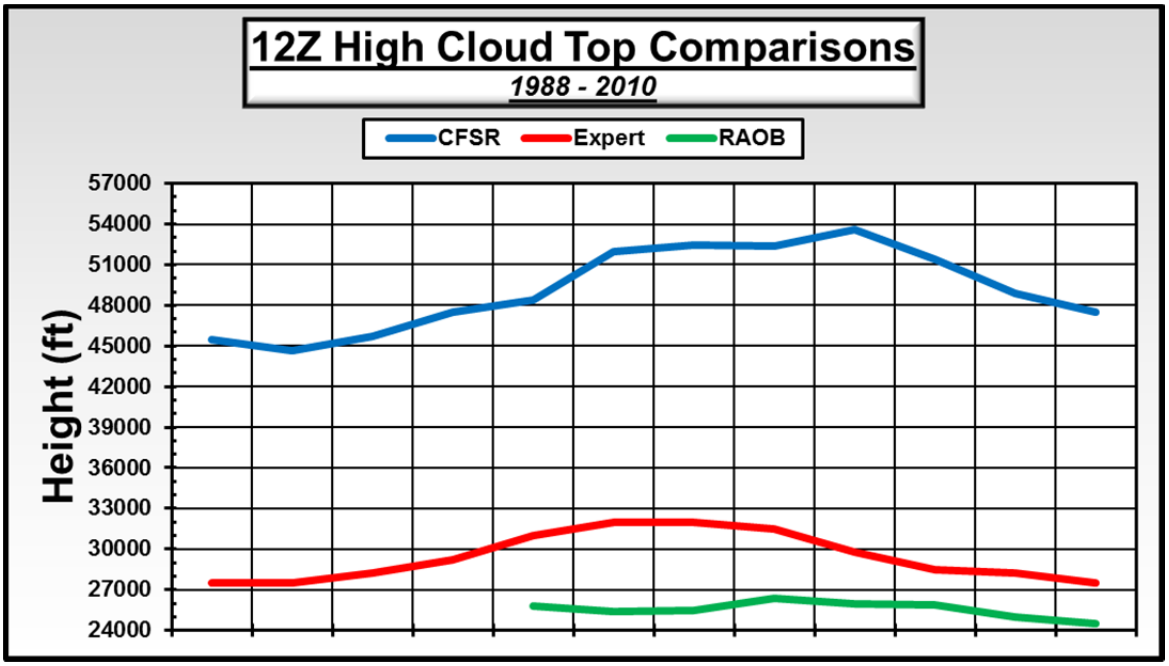

Figure 84. Monthly average low cloud top heights for each data set from 1988–2010.

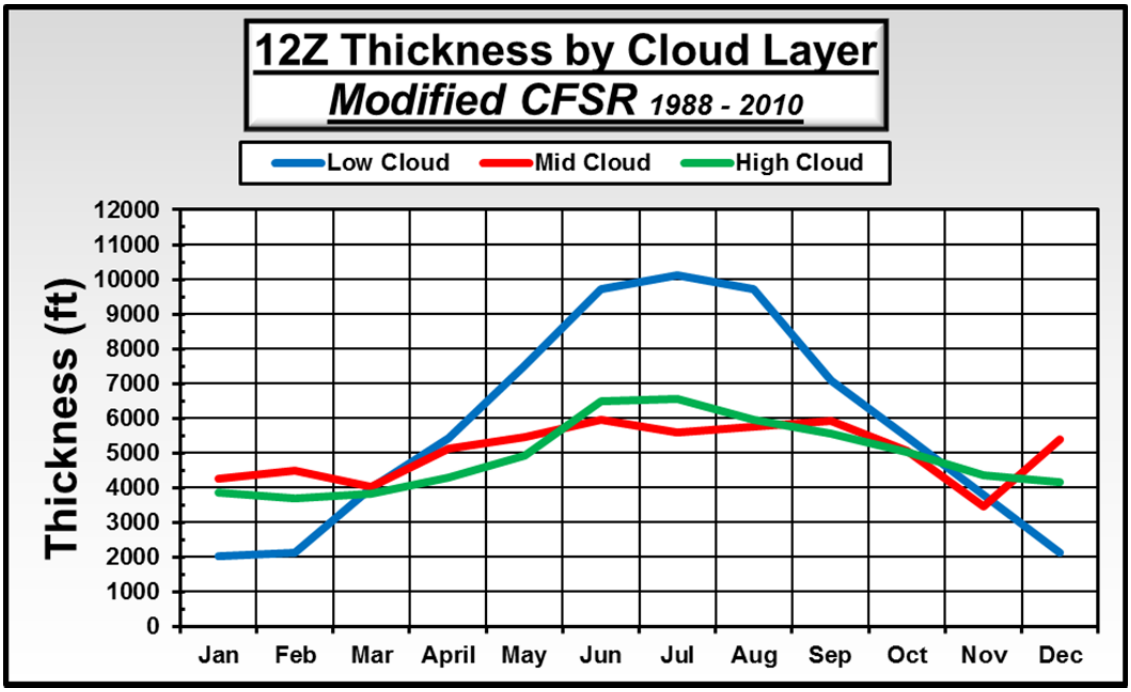

Figure 85. Monthly average cloud thicknesses by cloud layer based on the modified CFSR data set. The dashed black line represents the 4,500 ft thickness threshold in the thick cloud

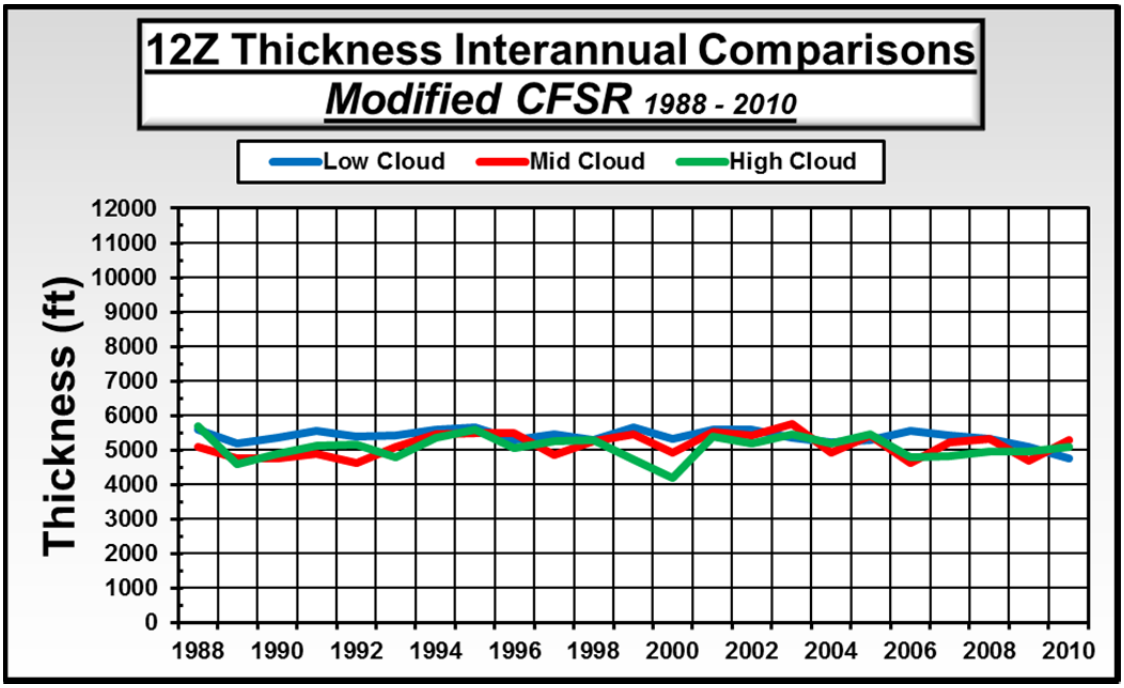

Figure 86. Interannual variation of cloud thickness separated by layer for 1988–2010 based on the modified CFSR data.

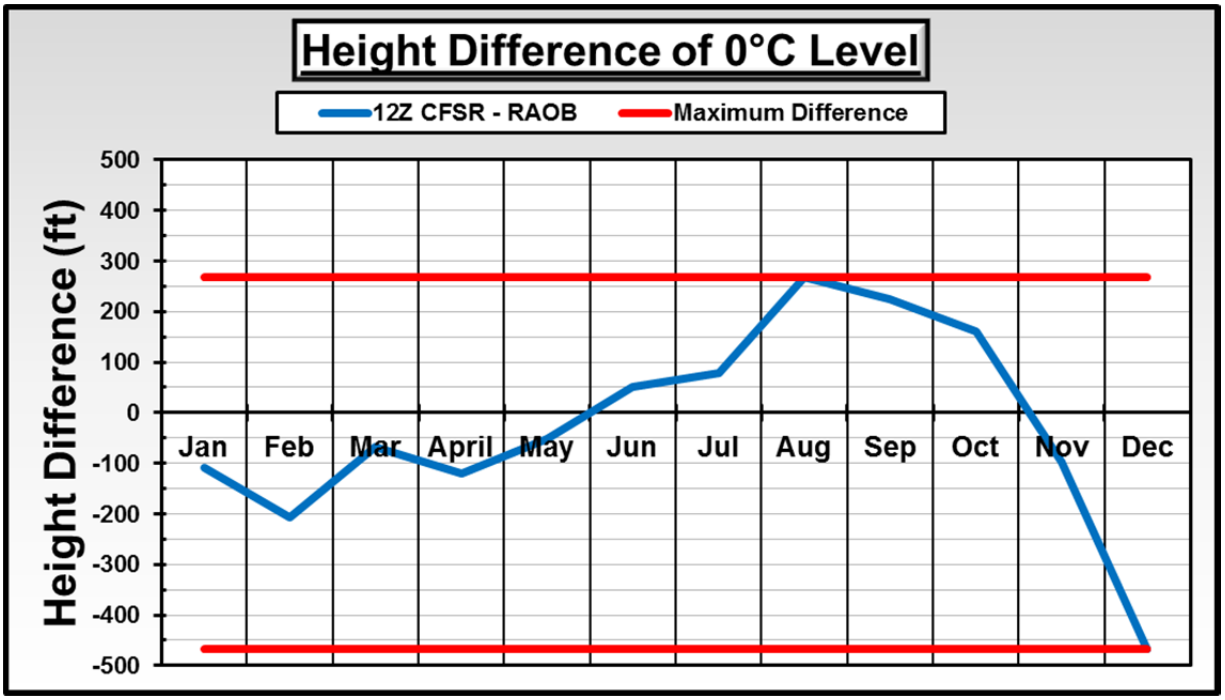

Figure 87. Monthly average difference between the CFSR 0° C height level and the RAOB 0° C height level (CFSR minus RAOB) in feet. Results based on 12Z values for all years in the study period. The red lines mark the largest differences. The average difference for all months was 28.

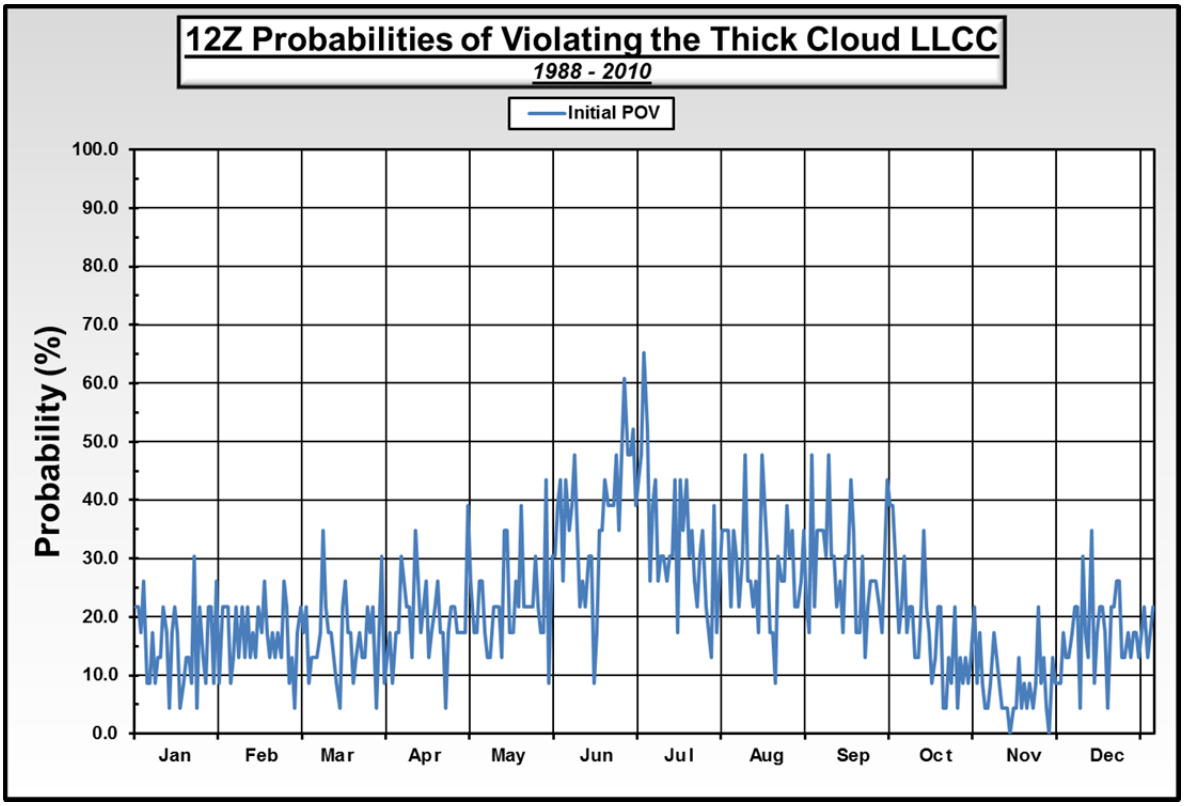

Figure 88. Daily probabilities of violating the thick cloud LLCC with no smoothing of the daily values. The probabilities are for each day of the year from 1 January through 31 December based on the modified CFSR data set for January 1988–December 2010. Note the large day-to-day variations in the absence of any temporal smoothing.

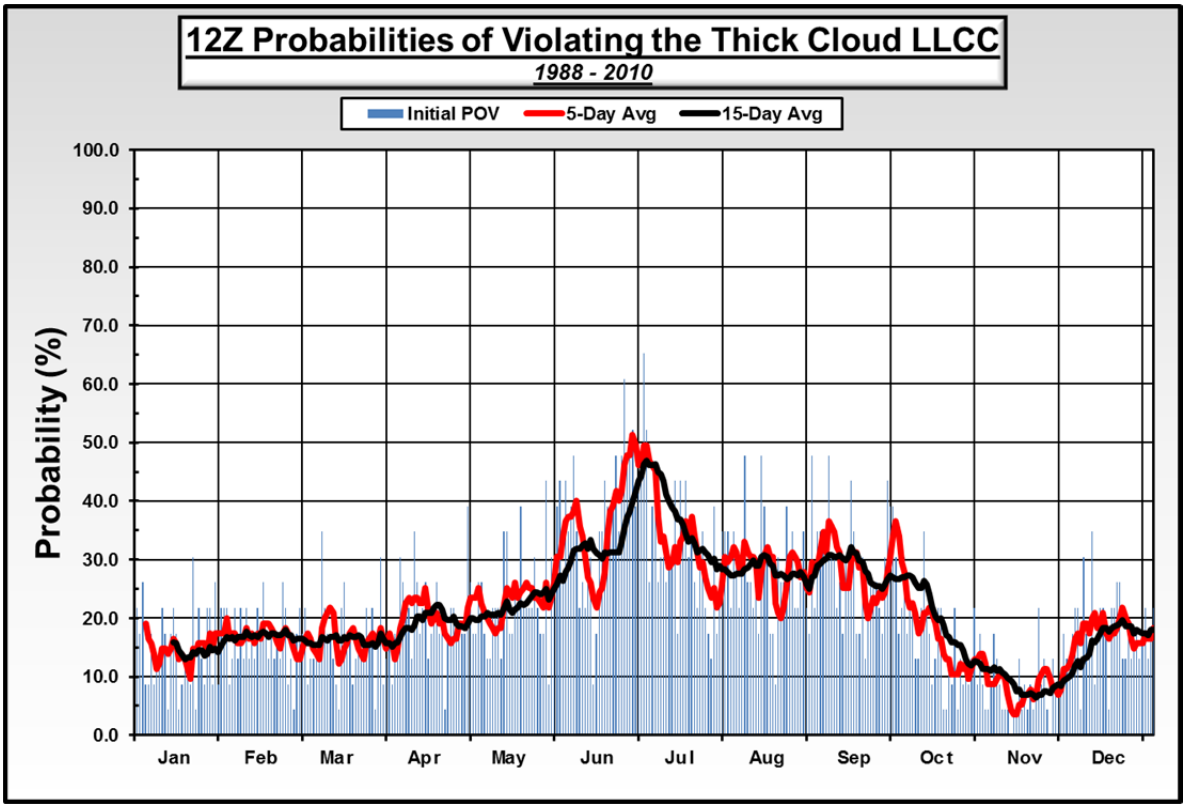

Figure 89. Daily probabilities of violating the thick cloud LLCC with no smoothing of the daily values (blue) with overlays of 5 and 15-day center weighted running means of the probabilities. The probabilities are for each day of the year from 1 January through 31 December based on the modified CFSR data set for January 1988–December 2010. Note the smaller day-to-day variations in the running mean probabilities, especially the 15-day running mean.

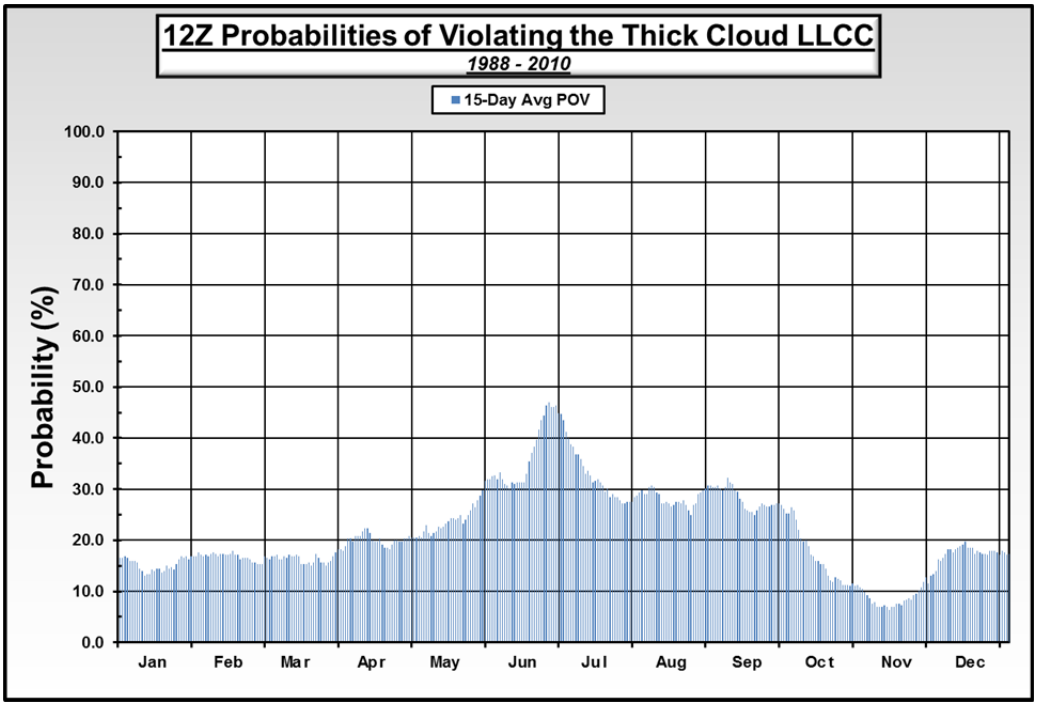

Figure 90. Daily probabilities of violating the thick cloud LLCC after applying a 15-day center weighted running mean smoothing of the initial probabilities (Figure 34). The probabilities are for each day of the year from 1 January through 31 December based on the modified CFSR data set for January 1988–December 2010.

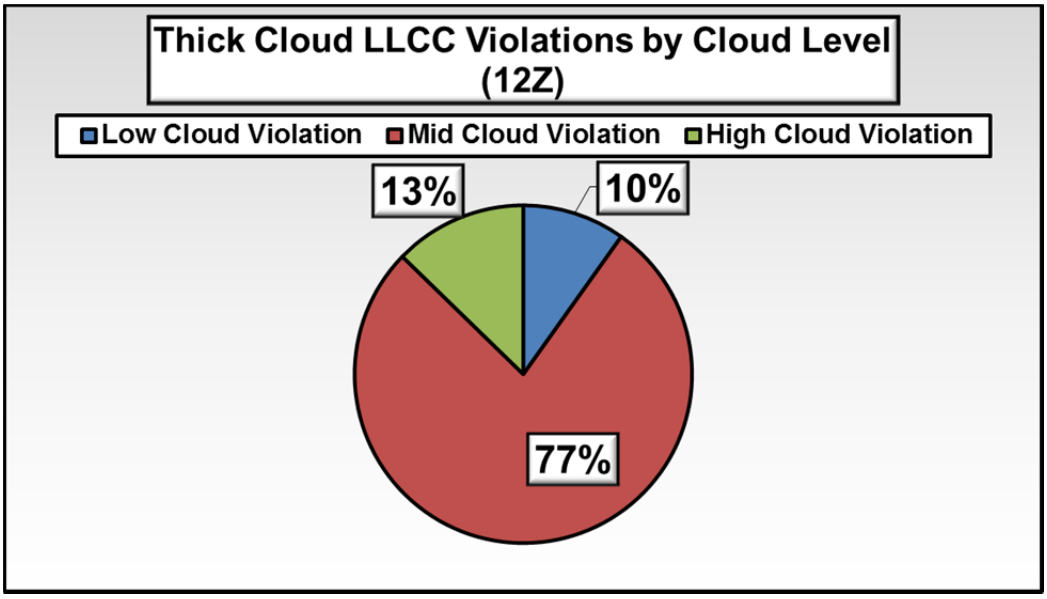

Figure 91. Percentage of 12Z thick cloud LLCC violations by cloud layer.

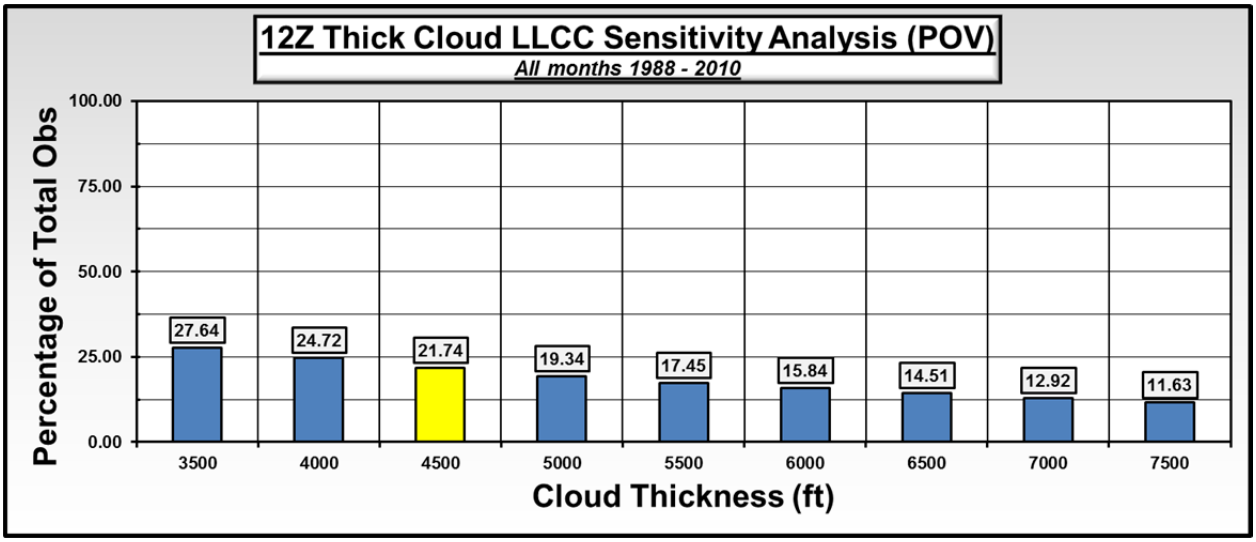

Figure 92. Daily mean climatological probabilities of violating the thick cloud LLCC based on using alternative thickness thresholds rather than the present threshold of 4,500 ft. The alternative thresholds are shown on the horizontal.

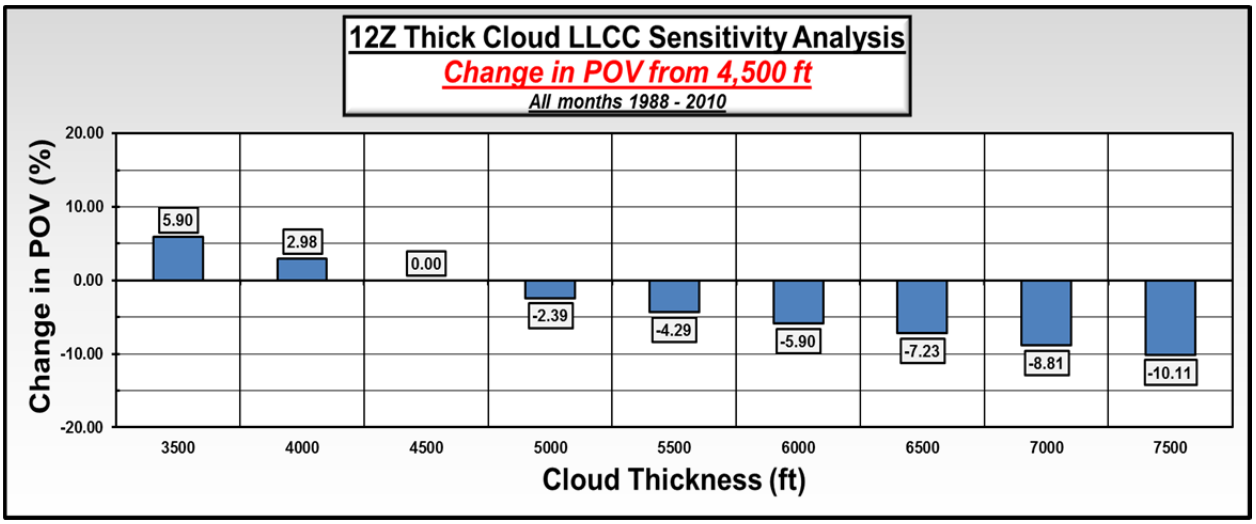

Figure 93. Daily mean change in the climatological probabilities of violating the thick cloud LLCC based on using alternative thickness thresholds rather than the present threshold of 4,500 ft. The alternative thresholds are shown on the horizontal.

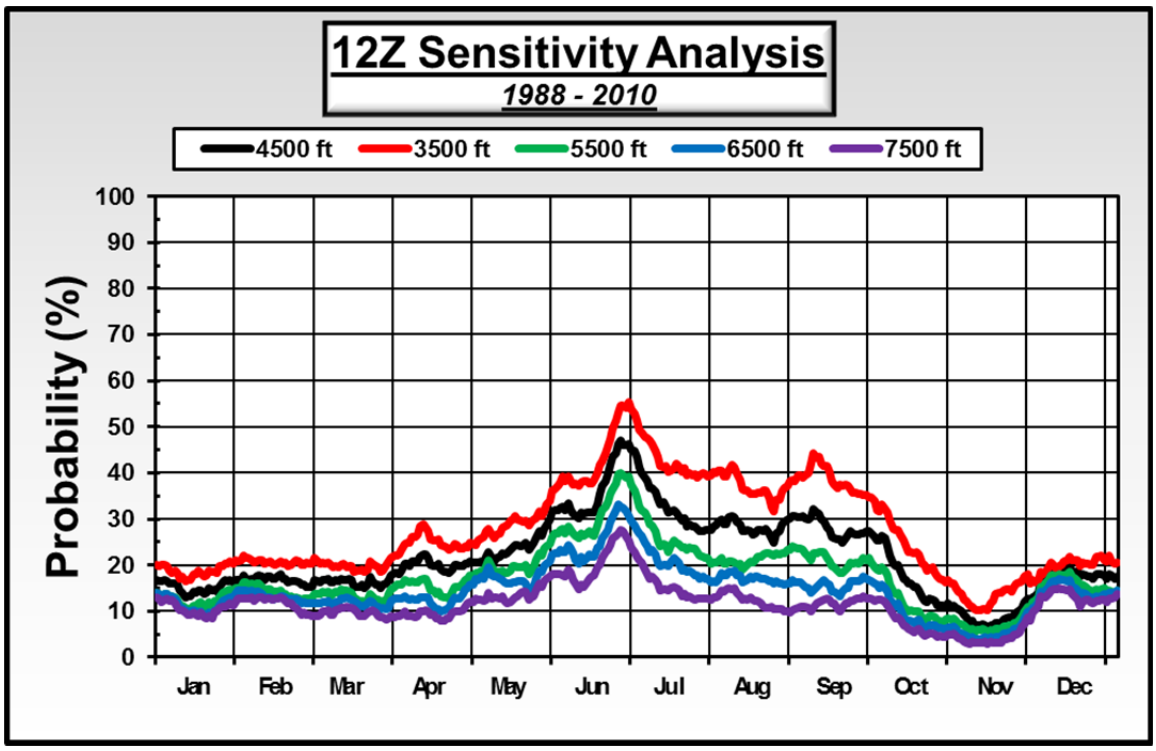

Figure 94. Daily probabilities of violating the thick cloud LLCC when using a thickness threshold of 3,500 ft (red), 4,500 ft (black), 5,500 ft (green), 6,500 ft (blue) and 7,500 ft (purple). The probabilities have been smoothed using a 15-day center weighted running mean smoother. The probabilities are for each day of the year from 1 January through 31 December based on the modified CFSR data set for January 1988–December.

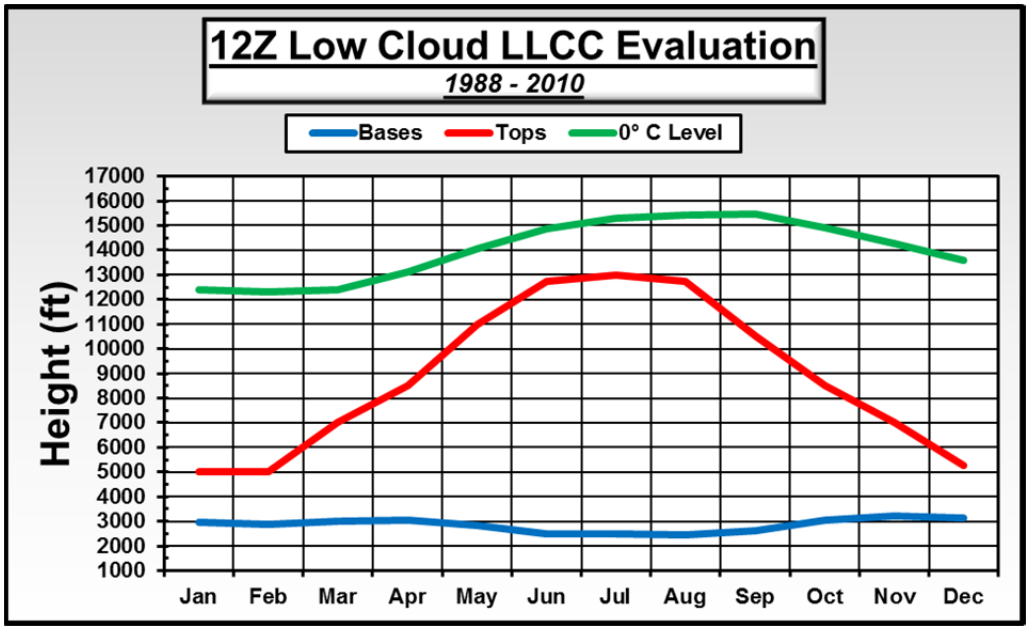

Figure 95. Monthly average low cloud base heights and top heights, and the height of the 0° C level. Note that monthly average height of the 0° C level was located above the monthly average mid cloud base height and top height in all.

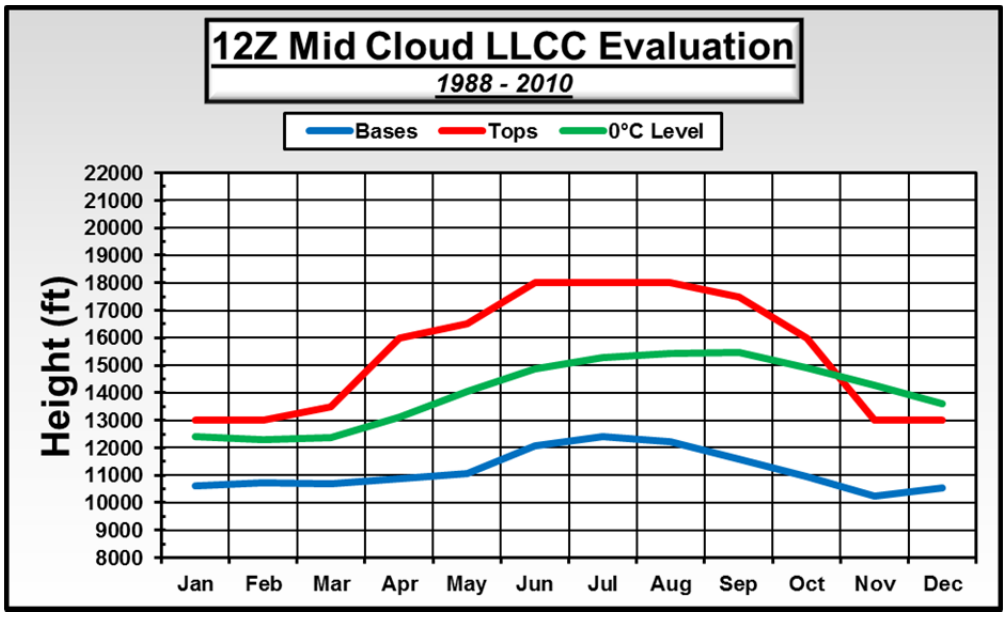

Figure 96. Monthly average mid cloud base heights and top heights, and the height of the 0° C level. Note that monthly average height of the 0° C level was located between the monthly average mid cloud base height and top height in all months except November and December. These results indicate that mid clouds tend to produce many of the violations of the thick cloud LLCC.

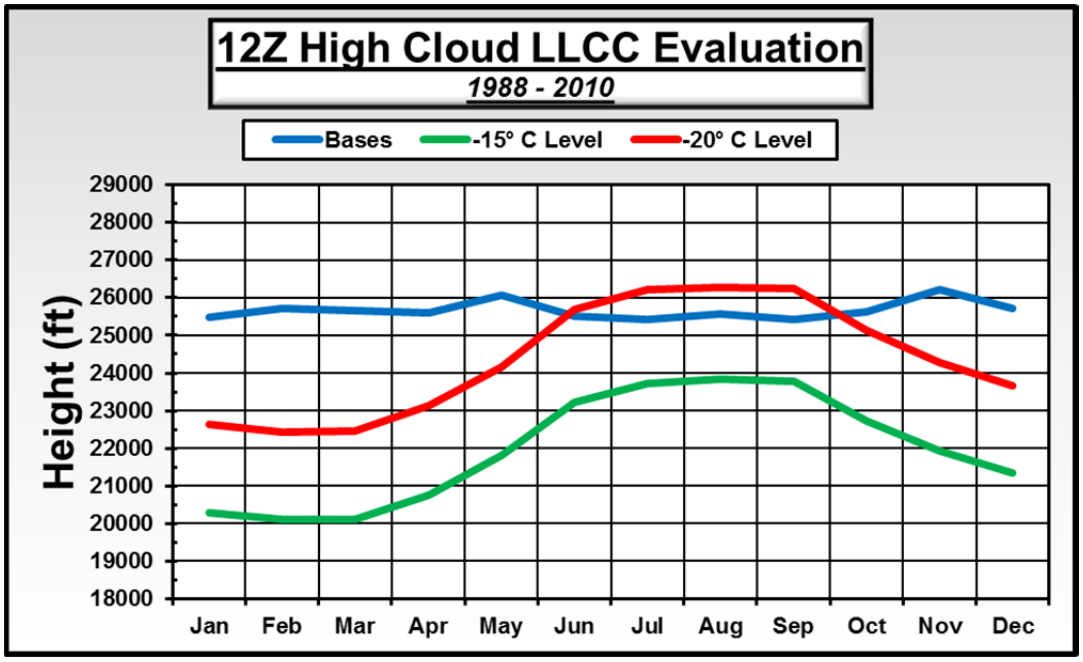

Figure 97. Monthly average high cloud base heights, and the heights of the -15° C and -20° C levels. High cloud top heights not shown because the high cloud base heights were the interacting cloud feature for determining thick cloud LLCC violations in this layer. Note that monthly average height of the -15° C level was located below the monthly average high cloud base height in all months

THIS PAGE INTENTIONALLY LEFT BLANK

LIST OF REFERENCES

Air Force Space Command (AFSPC), 2004: Range safety user requirements–Ground and launch personnel, equipment, systems, and material operations safety requirements, APSPC Manual 91-710 Volume 6, 143 pp.

Air Force Weather Agency (AFWA), 2006: Meteorological techniques, AFWA/TN-98/002 Revised, 243 pp.

Federal Aviation Administration (FAA): United States Department of Transportation, 2003: Commercial space transportation quarterly launch report. FAA 2nd Quarter Rep., 18 pp.

Goetz, E. C., 2001: Descriptive and conditional climatology for specific launch commit criteria for Cape Canaveral, Florida. M.S. thesis, Dept. of Engineering Physics, Air Force Institute of Technology, 110 pp.

GPS Visualizer, cited 2011: Radius around point map. [Available online at http://www.gpsvisualizer.com/calculators] Accessed September 2011.

Hazen D.S., and Co-authors, 1995: Weather impacts on launch operations at the eastern range and Kennedy Space Center. Sixth conference on aviation weather systems, Dallas, TX, 270-275.

Holton J.R., 2004: *An Introduction to Dynamic Meteorology*. Elselvier Inc, 535 pp.

Kalnay, E., and Coauthors, 1996: The NCEP/NCAR 40-year reanalysis project. *Bull. Amer. Meteor. Soc*, **77**, 437–471.

Krider, E. P., 1988: Spatial distribution of lightning strikes to ground during small thunderstorms in Florida. *Proc. 1988 Int. Aerospace and Ground Conf. on Lightning and Static Electricity*, Oklahoma City, OK, 318-323.

Merceret, F. J., and Coauthors, 2010: A history of the lightning launch commit criteria and the lightning advisory panel for America's space program, National Aeronautics and Space Administration (NASA), 234 pp.

McNamara,T. M., 2002: The horizontal extent of cloud-to-ground lightning over the Kennedy Space Center. M.S. thesis, Department of Engineering Physics, Air Force Institute of Technology, 100 pp.

Muller, E. C., 2010: Climate analysis of lightning launch commit criteria for Kennedy Space Center and Cape Canaveral Air Force Station. M.S. thesis, Department of Meteorology, Naval Postgraduate School, 147pp.

Mundhenk, B. D., 2009: A statistical-dynamical approach to intraseasonal prediction of tropical cyclogenesis in the western North Pacific. M.S. thesis, Dept of Meteorology, Naval Postgraduate School, 129 pp.

Murphree, T., 2008: *MR3610 Course Module 5: Introduction to Climate Science*. Dept. of Meteorology, Naval Postgraduate School, Monterey, California, 48 pp.

————, 2008b: *MR3610 Course Module 6: Smart Climatology*. Dept. of Meteorology, Naval Postgraduate School, Monterey, California, 52 pp.

National Atmospheric and Space Administration (NASA): NASA Facts, 1998: 12 pp.

National Oceanic Atmospheric Administration (NOAA): Federal Meteorological Handbook Number 1, United States Department of Commerce, 2005: 104 pp.

Poniatowski, K. S., 1987: Manned/Unmanned launch vehicle weather history at lift-off 1960 to present. Unpublished, NASA Headquarters, 55 pp. [Cited in Roeder and McNamara 2006.]

Roeder, W. P., J. E. Sardonia, S. C. Jacobs, M. S. Hinson, A. A. Guiffrida, and J. T. Madura, 1999: Avoiding triggered lightning threat to space launch from the Eastern Range/Kennedy Space Center. Preprints, *Eighth Conf. on Aviation, Range, and Aerospace Meteorology,* Dallas, TX, Amer. Meteor. Soc., 120–124.

————, and T. M. McNamara, 2006: A survey of the lightning launch commit criteria. Preprints, *Second Conf on Meteorological Applications of Lightning Data*, Atlanta, GA, Amer. Meteor. Soc., 18 pp.

Rogers R.R, Yau M.K, 1989: *A Short Course in Cloud Physics.* Rogers and Yau. 290 pp.

Saha, S., and Coauthors, 2010: The NCEP climate forecast system reanalysis. *Bull. Amer. Meteor. Soc.*, **91**, 1015-1057.

Sherwood, S. C., P. Minnis, and M. Gill, 2004: Deep convective cloud-top heights and their thermodynamic control during crystal-face, Journal of geophysical research, Vol 109, 11 pp.

Uman, M. A., and E. P. Krider, 1989: Natural and artificially initiated lightning. *Science*, **246**, 457–464.

Wallace J.M, Hobbs P.V, 1977: *Atmospheric Science, an Introductory Survey.* Elsevier Science, 467 pp.

Willet, J. C., and Coauthors, 2010: Rationales for the lightning flight-commit criteria, National Aeronautics and Space Administration (NASA), 251 pp.

World Meteorological Organization (WMO), 2008: Guide to Meteorological Instruments and Methods of Observation, 681 pp.

THIS PAGE INTENTIONALLY LEFT BLANK

INITIAL DISTRIBUTION LIST

1. Dudley Knox Library
   Naval Postgraduate School
   Monterey, California

2. Prof. Tom Murphree
   Naval Postgraduate School
   Monterey, California

3. Mr. Andrew P. Boerlage (*Col USAF ret*)
   Naval Postgraduate School
   Monterey, California

4. Mr. William Roeder
   45th Weather Squadron
   Patrick AFB, Florida

5. Mr. Todd McNamara
   45th Weather Squadron
   Patrick AFB, Florida

6. Mr. Frank Merceret
   Kennedy Space Center Weather Office
   Kennedy Space Center, Florida

7. Mr. Bob Dattore
   National Center for Atmospheric Research
   Boulder, Colorado

8. Air Force Weather Technical Library
   Asheville, North Carolina